ABSTRACT

Title of Thesis:	A REDESIGN OF THE FIRE PROPAGATION APPARATUS TO SIMPLIFY MANUFACTURING AND IMPROVE MEASURING CAPABILITIES
	Ryan T. Chaffer, Master of Science, 2021
Thesis Directed By:	Professor Stanislav Stoliarov, Fire Protection Engineering

The Fire Propagation apparatus (FPA) is an extremely powerful flammability test applicable to a wide range of materials. The material can be tested in a broad range of heating conditions in a controlled, customizable gaseous environment. Perhaps, the main drawback of the FPA is its complex design, which makes it difficult to manufacture and maintain. In this work, the main parts of the FPA, including the frame structure, combustion air distribution chamber, water cooled outer shield, load cell, and sample support assembly were redesigned and built to improve manufacturability, maintainability, and ease end user operations. It also demonstrated that the new design produces higher resolution sample mass evolution measurements than the original design. A comparative study between the FPA, Cone Calorimeter, and Controlled Atmosphere Pyrolysis Apparatus II was conducted at both flaming and non-flaming conditions using poly(methyl methacrylate). Some systematic differences in the

performance of these material flammability test methods were observed, which require further investigation.

A REDESIGN OF THE FIRE PROPAGATION APPARATUS TO SIMPLIFY MANUFACTURING AND INCREASE MEASURING CAPABILITIES

by

Ryan T. Chaffer

Thesis submitted to the Faculty of the Graduate School of the
University of Maryland, College Park, in partial fulfillment
of the requirements for the degree of
Masters if Science
2021

Advisory Committee:
Professor Stanislav Stoliarov, Chair
Dr. Fernando Raffan-Montoya
Professor James Milke

Acknowledgements

First, I would like to thank my family for their unhesitating support. The continuous words or encouragement has made the process easier and an enjoyable experience.

Next, I would like to thank Dr. Stanislav Stoliarov for his encouragement, guidance, and patience over the past two years. I am extremely appreciative of the opportunity given to me to conduct this research with you.

Next, I would like to thank Dr. Fernando Raffan-Montoya for his support during the process of the redesign. Whenever I had a question, no matter how obscure, you were always there to answer them and steer me in the right direction.

I would like to thank Dr. James Milke for accepting to be on my nomination committee. Thank you for giving your time to evaluate my work.

I would like to thank my research group for their support through the process. Whenever I needed help or had a question, it was always addressed without hesitation. You all have played an important role in my development as a researcher, and I am grateful for all your friendship.

Lastly, I would like to thank FM Global. Without their contribution and sponsorship of this project, it would not have been possible.

Table of Contents

List of Tables

List of Figures

List of Abbreviations

FPA: Fire Propagation Apparatus

CADS: Combustion Air Distribution System

CACC: Controlled Atmosphere Cone Calorimeter

ADC: Air Distribution Chamber

IAMS: Internal Attachment Mounting System

WCOS: Water Cooled Outer Shield

SSA: Sample Support Assembly

HSD: Horizontal Sample Dish

HF: Heat Flux

HF_{Ref}: Reference Heat Flux

CAPA II: Controlled Atmosphere Pyrolysis Apparatus II

MLR: Mass Loss Rate

PMMA: Poly (methyl methacrylate)

Chapter 1: Introduction

1.1 Motivation

Engineered polymer materials have become increasingly popular over the past several decades in the construction of buildings, automobiles, and other industries. Seen as a practical alternative to traditional materials, polymer materials' core features of controllable physical properties, raw material availability for production, and widespread processing methods have contributed to their universal use [1]. The most prominent disadvantage to the use of these materials is that the majority of polymers are based on organic compounds and are inherently flammable [2]. The widespread use of engineered polymer materials demands that the flammability properties and characteristics be understood and well documented, allowing the end user to make educated decisions for material selection.

The parameters typically used to determine the flammability properties and hazards of a material when exposed to fire are ignitability, surface flame spread, and heat release rate [3]. There are several bench scale flammability tests that can be used to determine a polymer's flammability properties'. Oxygen consumption calorimetry is the most widespread method for measurement of material flammability properties due to its ability to provide several flammability properties in a single test [14]. Under flaming conditions, the oxygen consumption calorimetry method has been widely validated and accepted by the research community to calculate material heat release

rate [15]. Bench scale flammability tests that utilize oxygen consumption calorimetry are the Cone Calorimeter [8] and the Fire Propagation Apparatus [9] [4]. Bench scale pyrolysis data of mass loss and mass loss rate are of interest to understand how a material reacts in an oxygen free/limited environment [16]. Bench scale tests capable of producing environments suitable for pyrolysis are the Fire Propagation Apparatus [9] and the Controlled Atmosphere Pyrolysis Apparatus II [5]. An understanding of each test method and its limitations is required to properly determine a materials flammability properties.

1.2 Flammability Testing Background

1.2.2 Fire Propagation Apparatus (FPA)

The Fire Propagation Apparatus is used to determine the flammability of materials and products, obtain transient response to prescribed heat fluxes in inert or oxidizing environments, and obtain measurements of generation rates of fire products [9]. The FPA is standardized by ASTM E2058 and ISO 12136 [9, 22]. The material flammability properties calculated by the FPA include time to ignition, convective heat release rate, chemical heat release rate, mass loss rate, effective heat of combustion, char yield, and generation rates of combustion products.

Unlike the cone calorimeter, heat is supplied via four infrared heating lamps, each outfitted with six tungsten core bulb elements. The lamps can produce a peak heat flux of 110 kW m^{-2} at the sample surface. Sample ignition is obtained by a stoichiometric ethylene/air mixture pilot flame with a 10 mm length. The flame is placed 10 mm above the sample face and 10 mm radially inward from the sample edge.

When experiments are conducted in the horizontal configuration, two sample geometries can be used. Samples may have a square geometry, 101.6 mm by 101.6 mm with a thickness range of 3 mm to 13 mm [10]. Samples may also have a circular geometry, with a diameter of 96.5 mm with the same thickness range as square geometry. Similar to the cone calorimeter, samples are wrapped in aluminum foil prior to heat exposure, leaving only the top sample face exposed. Samples are placed in a fully insulated sample dish, leaving only the top surface face exposed, unlike the cone calorimeter where insulation is only present on the back surface of the sample.

Combustion area gas flow is supplied through an air distribution box. The air supply is metered at 200 SLPM and blows upward from the bottom to collection hood, as depicted in the FPA experimental set up in Figure 1.1 [11]. Due to the controllability of the air entering the combustion zone, the volumetric oxygen concentration can be varied between 0 % to 40 %, mimicking conditions of an under ventilated or over ventilated fire [12]. This wider range of ventilation conditions offers greater versatility compared to the cone calorimeter, where all experiments are conducted in ambient air with no ability to control oxygen concentration.

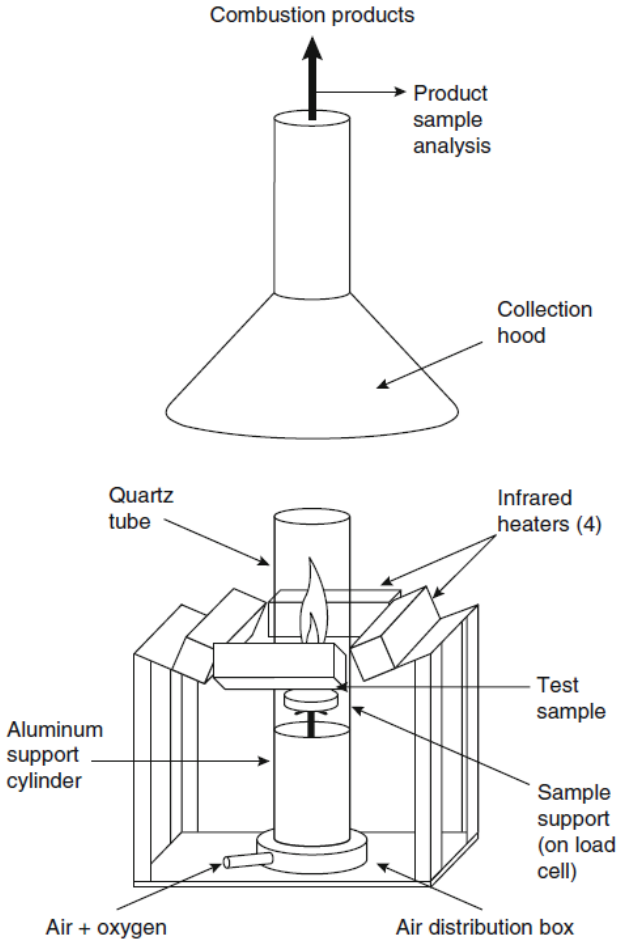

Figure 1.1: *FPA experimental set up* [6].

While the FPA can obtain measurements under a wider range of conditions than the cone calorimeter, the FPA has its limitations. The FPA has an inherently complex design which, in turn, presents several manufacturing challenges. The majority of parts used by the FPA are typically constructed from aluminum sheet metal with a thickness ranging from 2 mm to 3 mm. Additionally, the sheet metal needs to be welded together to create the final parts. There are many intricate geometric details inside the apparatus, such as the aluminum discharge tubes as seen in Figure 1.2. The discharge tubes have

tight angles that need to be fabricated and subsequently welded together. Figure 1.2 is also representative of the level of detail present in the apparatus drawing provided by the ASTM E2058 standard [9]. Figure 1.3 shows the end location of the discharge tubes. These tubes are welded to the inner wall of a cylindrical shape. As designed, there is minimal room to work and make proper welds to insure structural strength and proper location.

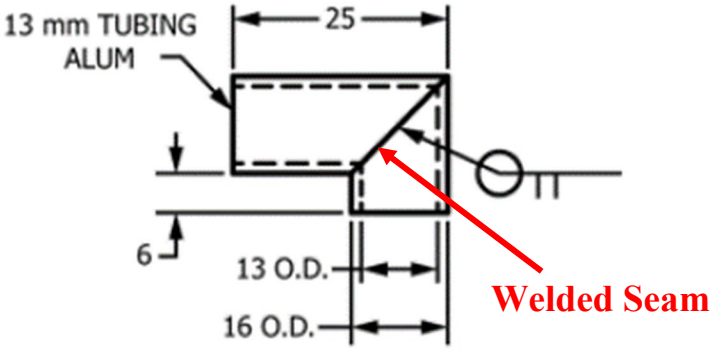

Figure 1.2: *FPA aluminum discharge tubes detailed view* [9].

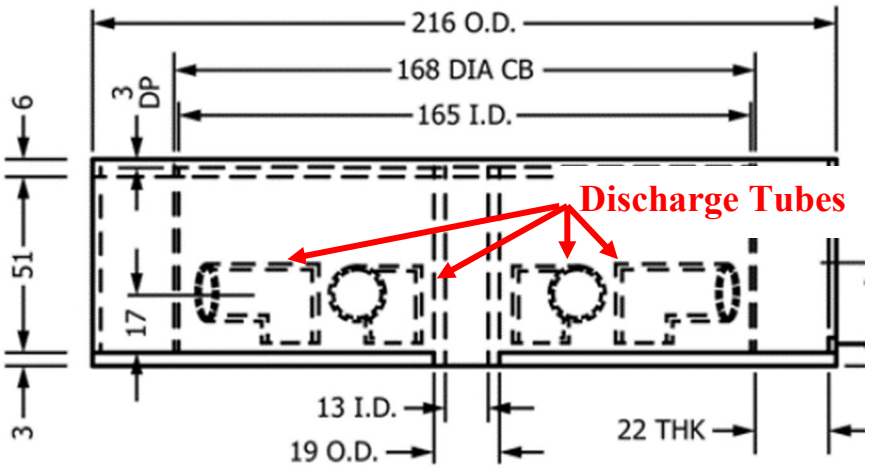

Figure 1.3: *FPA aluminum discharge tube installed location inside the air distribution chamber* [9].

These complex design challenges also lead to end user difficulty when performing calibrations and running tests. Operators must remove the sample holder and its supporting amenities in order to install the heat flux gauge and heat flux gauge mount. This process is time consuming as the heat flux must be determined daily prior to running a test. The difficulty associated with this process is not outlined in ASTM E2058, leaving operators to solve this problem on their own.

The FPA relies on a large array of fabricated primary parts and secondary support components for proper operation. These primary parts include a Frame Structure, Combustion Air Distribution System (CADS), Water Cooled Outer Shield (WCOS), Load Cell System, and Sample Support Assembly (SSA). The secondary support components consist of a quartz tube adapter, pneumatic cylinders, and horizontal sample dish (HSD).

A FPA frame structure build in accordance with ASTM E2058 has dimensions of 457 mm by 457 mm with a height of 864 mm. The frame is made from steel "U" channel, with dimensions of 50.8 mm x 50.8 mm x 50.8 mm. The steel "U" channel is welded together, creating the frame structure. Figure 1.6 shows a FPA frame structure, including infrared lamp mounting, pneumatic cylinder mounting, and load cell mounting.

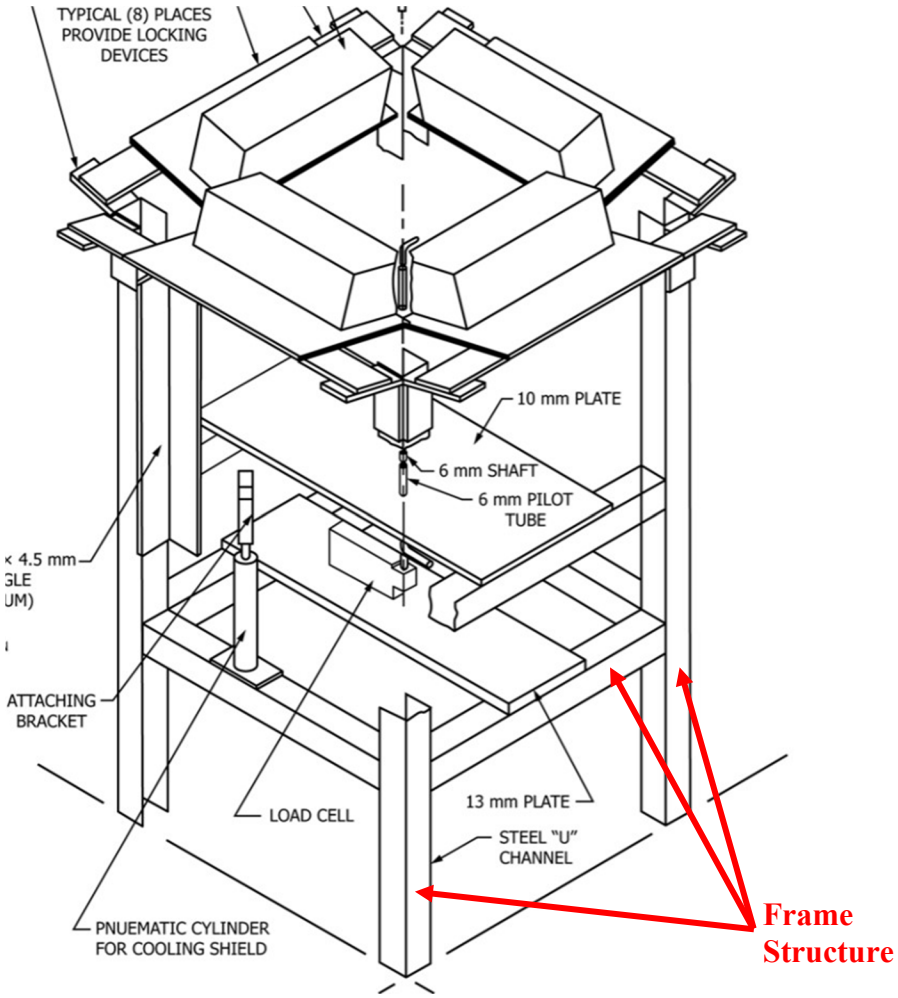

Figure 1.4: *FPA standard frame structure* [9].

A combustion air distribution system (CADS) built in accordance with ASTM E2058 section 6.7, shown in Figure 1.5, courtesy of FM Global, consists of two elements. The air distribution chamber and an aluminum support cylinder [9]. The air distribution chamber, constructed from aluminum, contains eight discharge tubes arranged in a circular pattern with a diameter of 165 mm. To produce uniform air flow, the eight discharge tubes, with an inner diameter of 13 mm, disperse onto the bottom plate. The discharge tubes and their mounting locations were previously shown in Figures 1.2 and 1.3. A gas mixture then rises through a set of three stainless steel wire meshes, of size 10, 20, and 30 from bottom to top [9], and up into the aluminum support cylinder. The wire mesh size refers to the diameter of the wire used and the size of the mesh opening. For example, size 20 wire mesh has an opening size of 1.041 mm and a wire diameter of 0.228 mm. The air distribution chamber is fabricated by welding 3 mm thick aluminum sheet metal together. The chamber also acts as a manifold, one primary feed line is used to provide the eight discharge tubes with air. The aluminum support cylinder is water cooled, supports quartz tubes, and aids in the control of air flow from the air distribution chamber through end of the quartz tubes. The aluminum support cylinder has an inside diameter of 154 mm and a height of 240 mm. This support cylinder is rigidly welded to the top of the air distribution chamber, producing the combustion air distribution system.

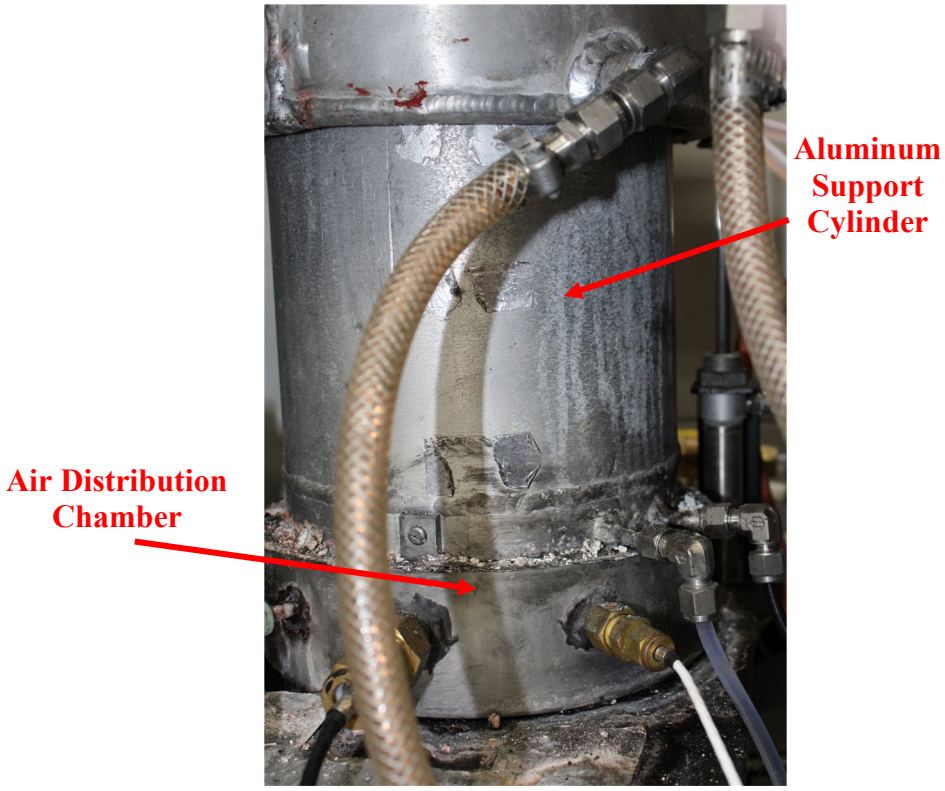

Figure 1.5: *FPA standard* combustion air distribution system.

A quartz tube adapter, shown in Figure 1.6, courtesy of FM global, is made from stainless-steel. The purpose of the adapter is to couple the lower quartz tube to the upper quartz tube. The adapter has an inside diameter of 154 mm and a height of 51 mm. The outer diameter of the adapter is 162 mm, which is designed to be inserted into the quartz tube.

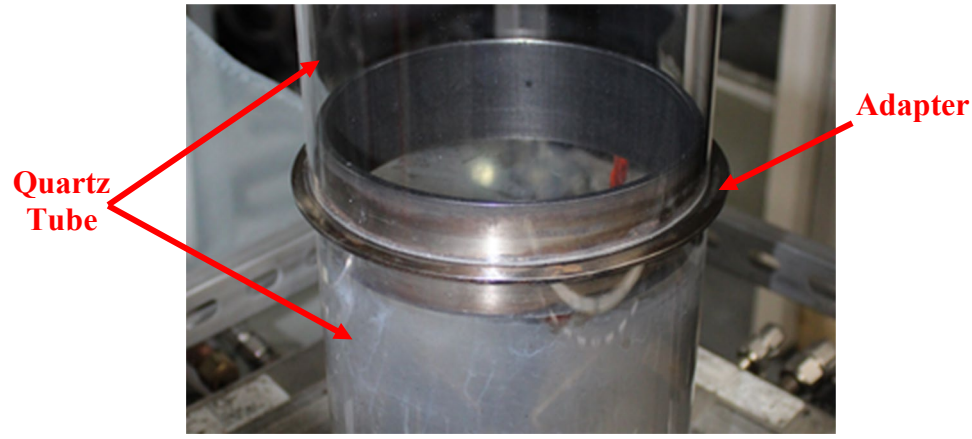

Figure 1.6: *FPA standard* quartz tube adapter.

A WCOS built in accordance with ASTM E2058 section 6.8, shown in Figure 1.7, courtesy of FM Global, is fabricated from aluminum sheet metal with a thickness of 2 mm. The WCOS has a height of 229 mm, an outer diameter of 225 mm and an inner diameter of 203 mm. The internal water jacket has a thickness of 11 mm. Water cooling ports are located and the bottom (inlet) and top (outlet). The WCOS is driven by a single pneumatic cylinder. When it is time for sample exposure to the lamps, the WCOS must drop within 1 second.

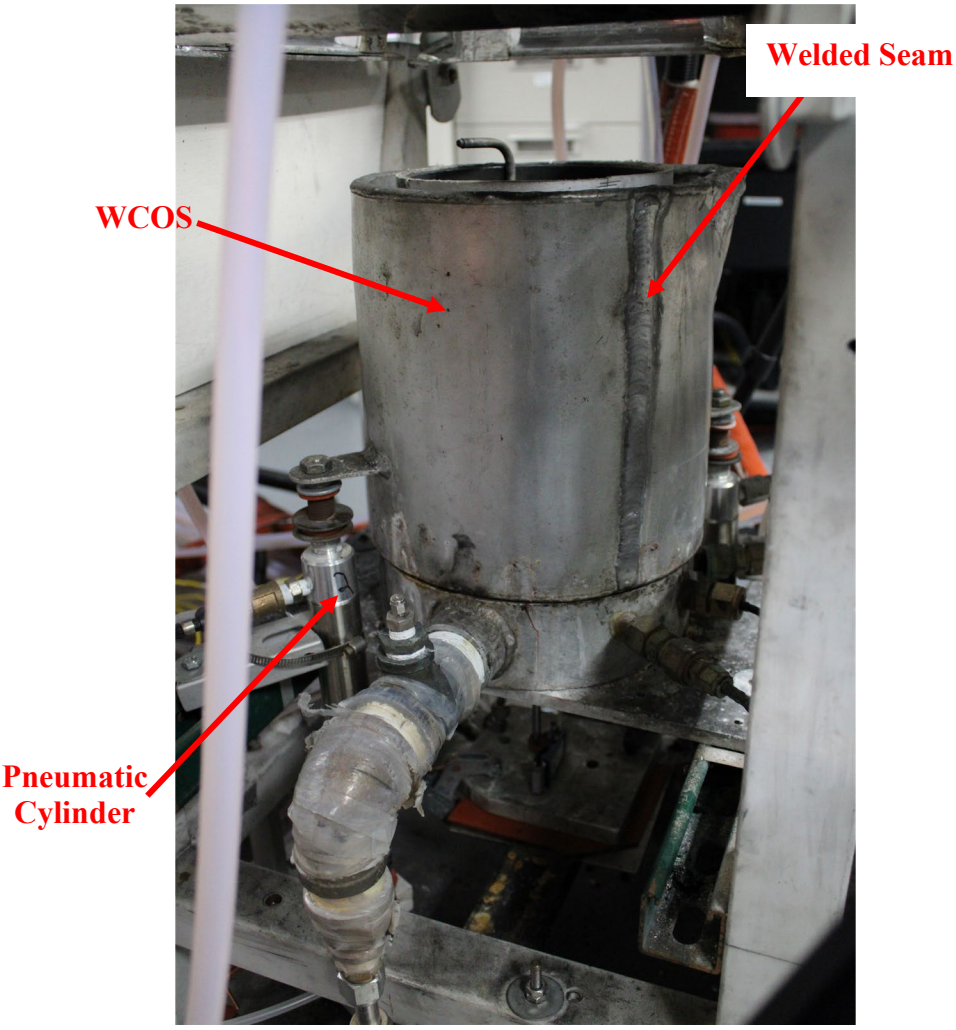

Figure 1.7: *FPA standard water-cooled outer shield.*

A load cell system and SSA build in accordance with ASTM E2058 section 6.3, consists of a load cell with a resolution of 0.1 g and a capacity of 1000 g. The SSA consists of a 6.35 mm diameter, 330 mm long stainless-steel rod, a 100 mm diameter load platform with a thickness of 1.5 mm, two low friction ball bearings, and an adjustable threaded rod to account for varying sample thicknesses. Figure 1.8, courtesy of FM Global, shows a load cell and SSA compliant with the standard.

(a)

(b)

Figure 1.8: *FPA standard load cell(a) and sample support assembly(b).*

A circular horizontal sample dish made in accordance with ASTM E2058 section 8.1, is constructed from aluminum. The dish has an outer diameter of 114 mm, an inner diameter of 96.5 mm, and a height of 25.4 mm. The sample dish interior sides are lined with three layers of 3 mm thick insulation. The bottom of the sample dish is lined with four layers of 3 mm thick insulation. Figure 1.9, courtesy of FM Global shows a sample dish with and without insulation.

Figure 1.9: *FPA standard sample dish.*

1.2.1 Cone Calorimeter

The cone calorimeter is a bench-scale testing apparatus used to carry out flammability studies of materials [6]. Adopted by both ASTM (E1354) and the ISO (5660-1), the cone calorimeter determines heat release rate by the oxygen consumption method [8, 21]. The material flammability properties calculated by the cone calorimeter include time to ignition, heat release rate, mass loss rate, effective heat of combustion, visible smoke development, and char yield.

Standard cone calorimeters operate in an exposed environment, with ample ambient air to support combustion. Samples are heated via an electrical conical heater, with heat fluxes ranging from 0 kW m^{-2} to 100 kW m^{-2} [8]. Experience has shown upper limits of 70 kW m^{-2} are typical for conical heaters. Higher values are possible at the expense of faster degradation and premature failure of heater components. The heater is made of a 5kW electric heating element, wrapped inside a conical shell, made from stainless steel. When tests are performed in the horizontal orientation, the sample face is located approximately 25 mm below the lower face of the heater. Products of combustion and flames rise through the circular opening in the heater. The experimental design layout is depicted in Figure 1.10.

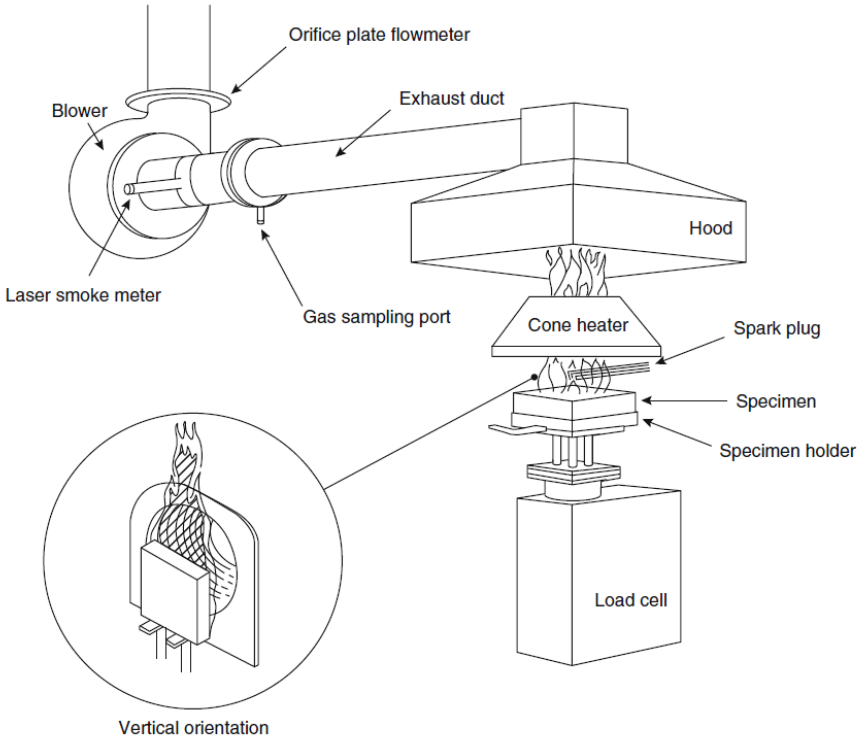

Figure 1.10: *Cone calorimeter experimental set up* [7].

Samples are ignited by an electrical spark ignition system. The igniter is placed over the center of the horizontal sample at an elevation of 13 ± 2 mm above the sample face. When ignition of the sample occurs, the igniter is removed. Samples have a size of 100 mm by 100 mm with a thickness of no more than 50 mm [8]. Samples are prepared with a single layer of aluminum foil, with a thickness of 0.025 mm to 0.04 mm, wrapped around the sides and bottom faces. This is done to prevent any spilling of liquid material [3]. The back side of the sample is placed on an insulation material with a thickness no less than 13 mm [8].

Although the cone calorimeter is an extremely versatile apparatus, its experimental design properties drive limitations in testing. Depending on material type

and properties, swelling of the sample prior to ignition can interfere with the spark ignition system. Substantial sample swelling through the duration of a test can lead to variations of heat flux along the height of the sample as well as the sample contacting the conical heater. Adequate, uncontrolled ventilation is required to promote flaming behavior. Nevertheless, the cone calorimeter's design allows for it to be easily manufactured and produced commercially for research use.

A controlled atmosphere cone calorimeter (CACC) has been developed to assess material flammability properties and gaseous emissions with varying levels of oxidation [19]. The CACC combustion chamber design and layout can be seen in Figure 1.11. The CACC consists of a plenum where a nitrogen air mixture is injected. The gas mixture is injected into a sealed chamber. The sealed chamber houses the sample, conical heater, and load cell. The flow of gas through the CACC is different than the cone calorimeter. In the standard cone calorimeter, gas is pulled through the system by an exhaust fan. The CACC requires that gas be injected under pressure into the system. This does not eliminate the need for an exhaust fan [17]. The CACC design leads to the creation of a pressure differential inside the combustion chamber. Because of the pressure differential, a truly hermetic seal is difficult to accomplish [17]. The primary disadvantage to the CACC design is maintaining airtight seals throughout the plenum and combustion chamber areas while not over pressurizing the system.

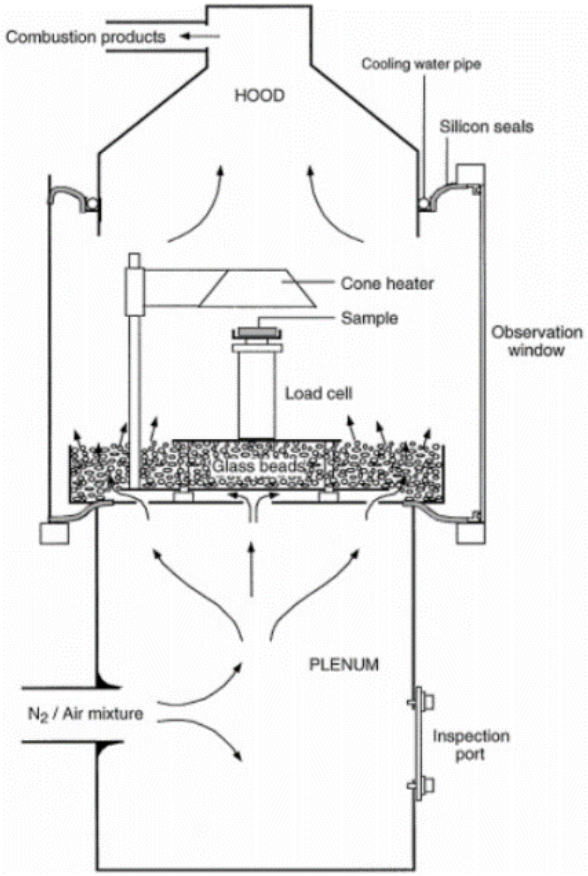

Figure 1.11: *Controlled atmosphere cone calorimeter combustion chamber design* [18].

The CACC extends the capability of a standard cone calorimeter to have similar combustion/ gasification zone atmosphere characteristics as the FPA. The CACC requires more maintenance when compared to the FPA. The FPA is designed to switch between flaming and non-flaming testing scenarios almost instantaneously, making less work for end user operators. The ability to quickly switch a CACC back to a standard cone calorimeter is not as straight forward as the FPA. The CACC primary flaw compared to the FPA is that it requires a fully sealed, pressurized enclosure to

operate properly [18]. Whereas the FPA has sufficient gas flow distribution properties that allows for an anerobic gasification environment, while maintaining standard atmospheric pressure.

1.2.3 Controlled Atmosphere Pyrolysis Apparatus II (CAPA II)

The Controlled Atmosphere Pyrolysis Apparatus is a custom engineered experimental apparatus that provides well defined boundary layers and highly resolved measurements of mass, thickness profile, and temperature for non-thermally thin materials exposed to radiant heat [5]. Figure 1.12 shows the experimental apparatus design. The oxygen concentration in the pyrolysis zone can be reduced to below 1 vol%.

The CAPA II consists of four major parts. An open-to-the-atmosphere gasification chamber, infrared camera, a load cell system, and a conical heater. The gasification chamber, constructed from two round aluminum tubes, both with a thickness of 6.4 mm, houses a stainless-steel sample holder, 82 mm in diameter. The sides of the sample holder are lined with four layers of 6.35 mm thick insulation. The bottom side of the sample holder is left open, which allows for sample back surface temperature to be taken via an infrared camera. Gasification chamber cooling is provided through copper tubing, 6.35 mm in diameter, wrapped around exterior walls, shown in Figure 1.13. The load cell system has a resolution of 1 mg and a sampling rate of 2 Hz. The conical heater, capable of providing up to 100 kW m^{-2} heat flux, is positioned on a moving track for rapid placement and removal above the sample.

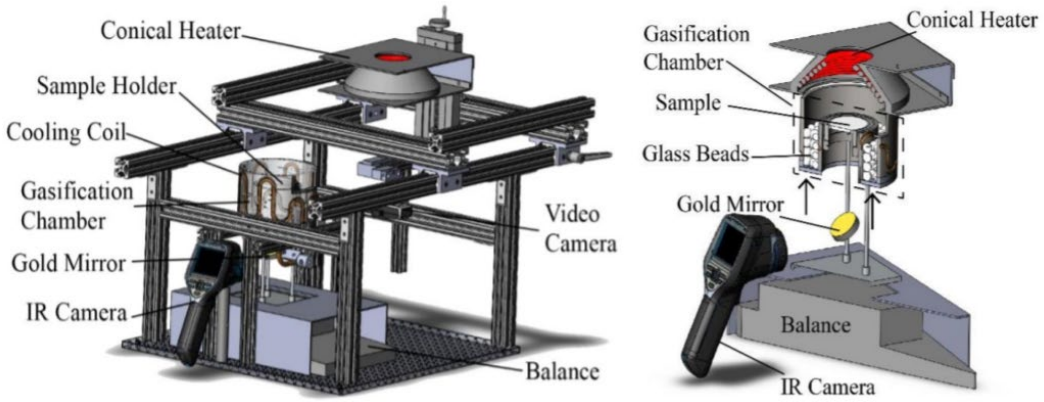

Figure 1.12: *CAPA II experimental set up [5].*

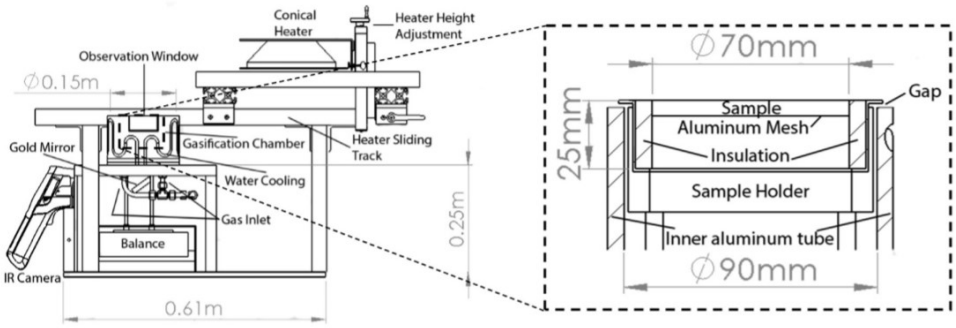

Figure 1.13: *CAPA II experimental schematic [5].*

The CAPA II is limited by its ability to produce accurate data for highly thermally stable and highly intumescent solids [5]. Sample swelling and unsteady temperatures in the gasification chamber make it difficult to accurately define thermal boundary conditions. Compared to the FPA, the CAPA II provides sample mass data of pyrolysis in an anerobic environment. The CAPA II does not have the ability to collect and analyze products of pyrolysis. The CAPA II is strictly used for controlled atmosphere non-flaming combustion tests, compared to the FPA where both flaming and non-flaming test are possible.

1.4 Project Plan

Through the beginning stages of this project, it became increasingly evident that the engineering drawings provided in the standard were not sufficient for production in modern day machine shops. The level of detail required for current machining practices is not adequately represented.

In order to use modern day machinists, a complete comprehensive set of new engineering schematics needed to be produced. The work performed focused only on mass loss data acquisition. The objective of this work was to redesign FPA parts and components to address three points of interest. Manufacturability is the first point of interest. By simplifying the design, changing material types, and minimizing the amount of welding needed, the FPA can be manufactured more universally as fewer special skills are required. The second point of interest is maintainability. This addresses the difficulty associated with replacing worn out parts. By incorporating off the shelf parts, if a failure occurs, the apparatus can be back up and running in a few days as opposed to weeks or even months, minimizing down time and allowing for more experiments to be run. The last point of interest is ease of use and operation. As outlined above, some manual processes required by the FPA are time consuming and cumbersome. Additionally, improvements in measurement data noise reduction were addressed through vibration minimization.

The redesigned parts include the combustion air distribution system, upper quartz tube adapter, water cooled outer shield, load cell system, sample support

assembly, and horizontal sample dish. Additional improvements were made to the pilot flame system, heat flux gauge mounting, and apparatus diagnostic equipment.

A comparative mass loss rate study between the FPA, cone calorimeter, and CAPA II was performed. The study provided a base line understanding of the FPA, which identified some systematic differences that require further investigation.

Chapter 2: Apparatus Design Changes

2.1 Frame Structure

The redesigned FPA frame structure maintains the dimensions listed in the standard, 457 mm by 457 mm with a heigh of 864 mm. The material type and construction was changed. The redesigned frame is made from t-slot aluminum framing, shown in Figure 2.1. This material was chosen over the steel u-channel described in the standard [9]. The t-slot framing allows for easier assembly and adjustability. The modularity of the t-slot framing promotes further expansion of the apparatus in the future. Additionally, the t-slot framing does not require welding, every connection point is made with screws, nuts, and plate brackets. The new frame structure improves manufacturability, maintainability, and ease of use. All parts can be purchased and assembled within a day. In the case of failure, replacements are readily available. Refer to appendix A.1 for detail CAD drawings of the frame structure.

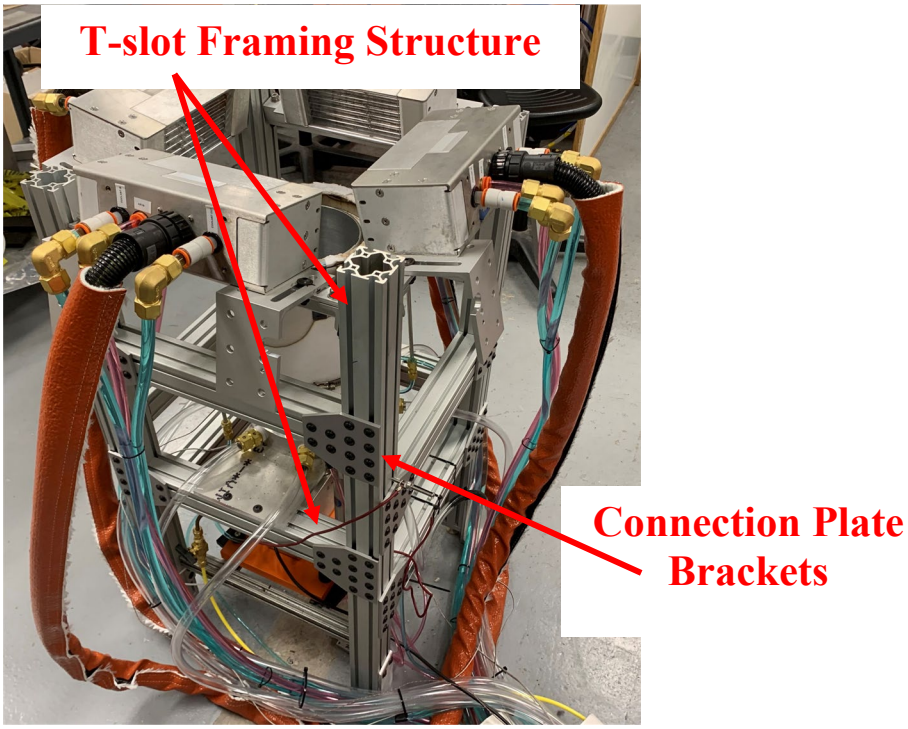

Figure 2.1: *FPA redesigned aluminum frame structure.*

In order to mount the infrared lamps to the frame structure, a multipart bracket was designed. Figure 2.2 depicts the mounting system. The lower cross bar is designed to allow for rotational movement of the infrared lamps, setting the angle to the proper setting. The current angle is set to 12° for the horizontal axis as specified in the standard ASTM E2058 [9]. The upper infrared lamp mounting brackets, two per lamp, allows for horizontal movement in and out of the sample plane. Appendix A.2 provides detailed drawing of both the lower cross bar and upper infrared lamp mounting brackets.

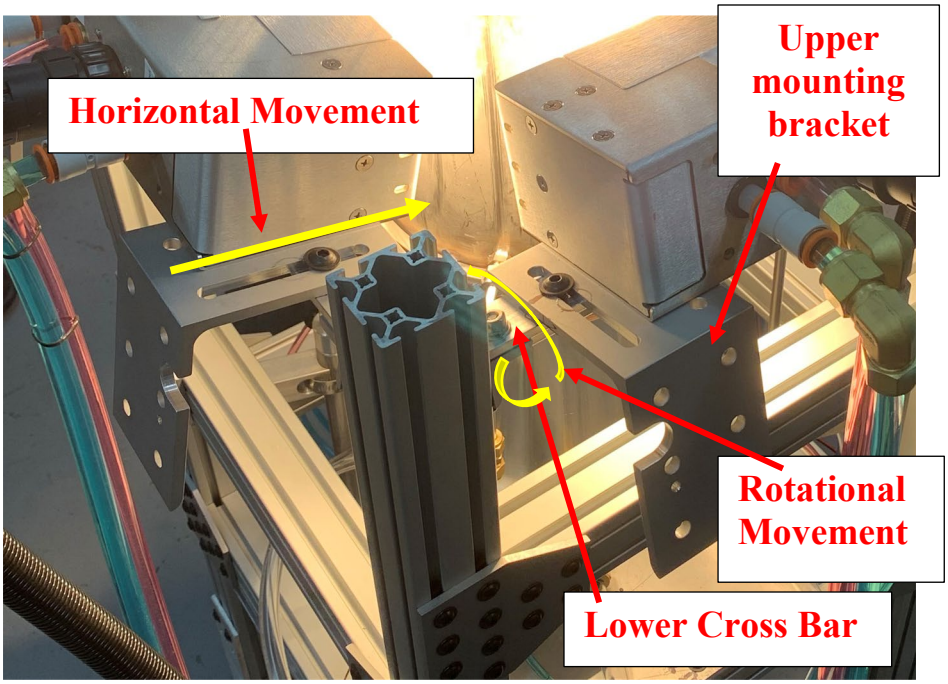

Figure 2.2: *FPA infrared lamp mounting brackets*.

2.2 Combustion Air Distribution System (CADS)

2.2.1 Air Distribution Chamber and Support Cylinder

When using the drawings provided by the standard, it proved difficult to locate a machine shop willing to use these drawings, manufacture some of the small intricate parts, and weld aluminum. The solution to this problem was to create a new combustion air distribution system, with more complete drawings, requiring no welding to be done. The redesigned CADS, seen in Figure 2.3, maintains critical dimensions set by ASTM E2058 section 6.7 [9]. Figure 2.4 is a cross sectional view of the redesigned CADS. It is also constructed of aluminum but machined from a single piece of aluminum (billet aluminum). The final product is seen in Figure 2.5. This new design does not require welding or any intricate parts to be attached. Instead, everything is easily accessible if

repairs are needed, or damage occurs. Small parts that required machining and welding have been replaced with mass-produced tube fittings.

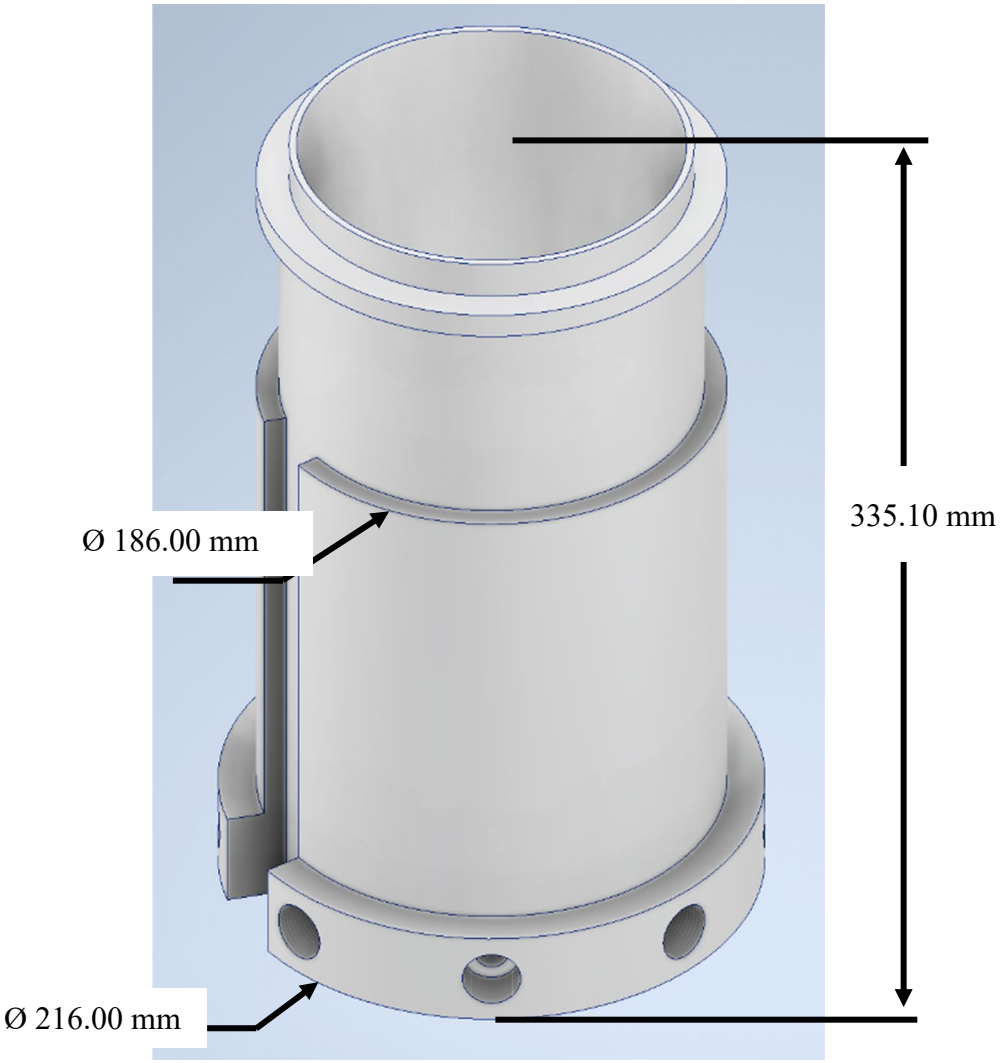

Figure 2.3: *Redesigned Combustion Air Distribution Chamber System.*

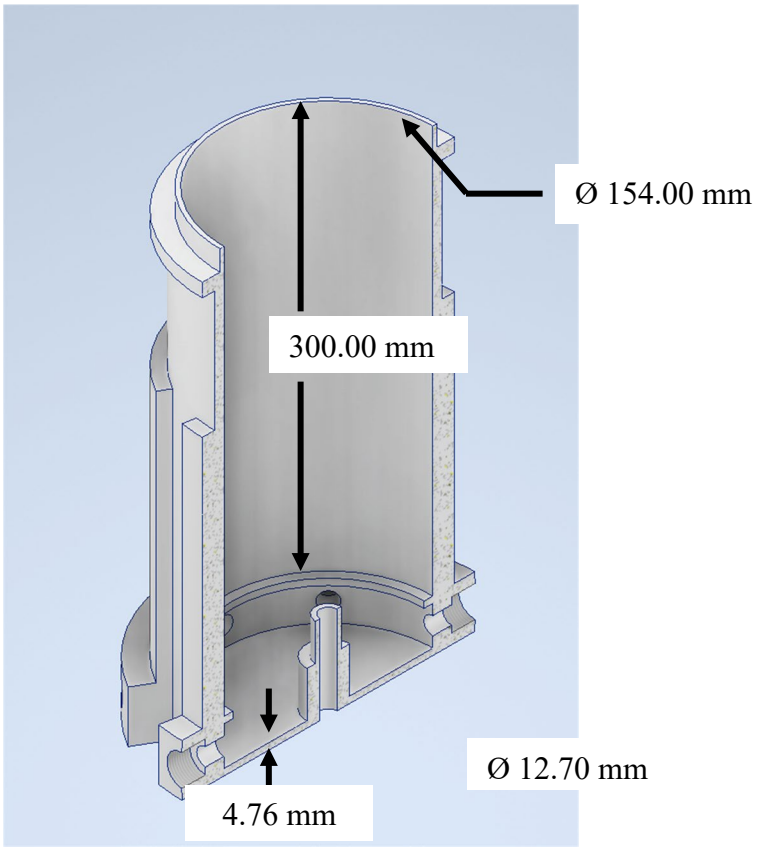

Figure 2.4: *Redesigned Combustion Air Distribution Chamber System cross sectional view.*

Figure 2.5: *Final aluminum machined CADS.*

The aluminum support cylinder maintains the same height and inner diameter as the standard. The main difference lies in the cylinder cooling system. Cooling is now provided through a copper coil, wrapped around the upper portion of the cylinder in the indentation depicted in Figure 2.6. The copper coil has an outer diameter of 6.35 mm, inner diameter of 3.86 mm and a total length of 3.35 m.

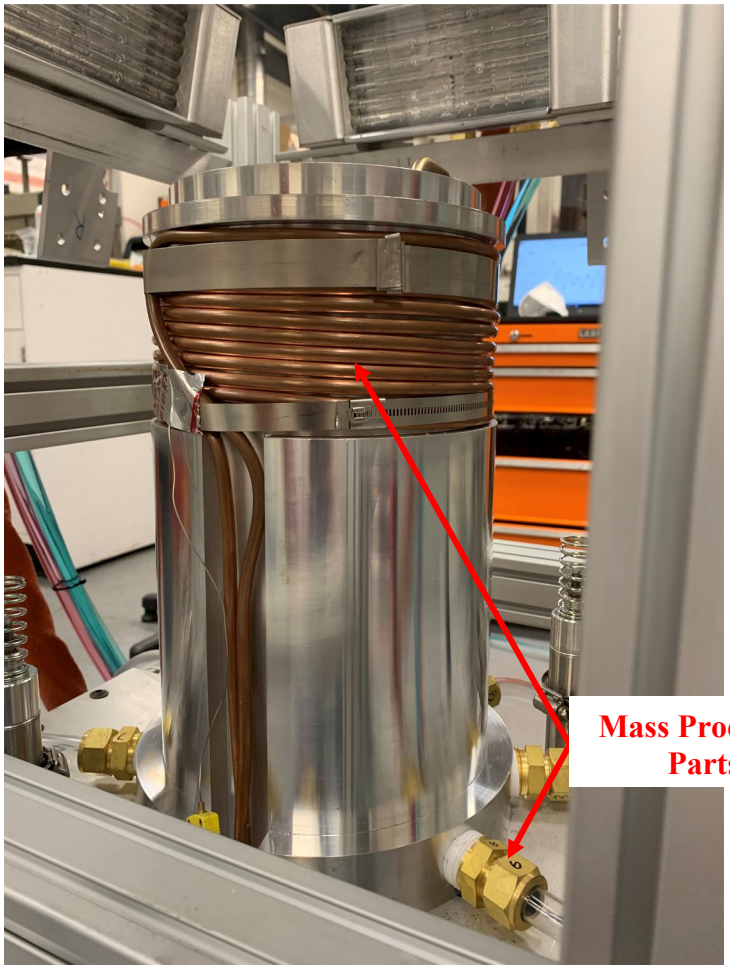

Figure 2.6: *Cooper cooling coil wrapped around ADC.*

The air distribution chamber has also been changed. The eight discharge tubes have been removed. Air enters the mixing chamber, 154.0 mm in diameter and 28.5 mm in height, through eight evenly spaced 13.0 mm injection ports. The air is supplied to each port individually via a tube, with 13.0 mm ID, from a manifold upstream. The upstream manifold, seen in Figure 2.7(a), takes a single inlet feed and splits it into eight. Figure 2.7(b) shows the final design external implementation; Figure 2.7(c) shows the computer-generated cross-sectional view of the ADC lower mixing chamber internals. Brass fittings used in the upstream manifold consists of eight Swagelok B-1010-1-8 and one Swagelok B-1010-1-12. The eight brass fittings used in the air distribution chamber are Swagelok B-1010-1-12. After the air enters the mixing chamber, it passes upwards through three layers of size 20 stainless steel mesh and a layer of 3.00 mm glass beads, 24.5 mm in height shown in Figure 2.8. This is used to promote uniform mixing and flow from the lower chamber into the upper combustion chamber.

Figure 2.7(a): *Upstream distribution manifold.*

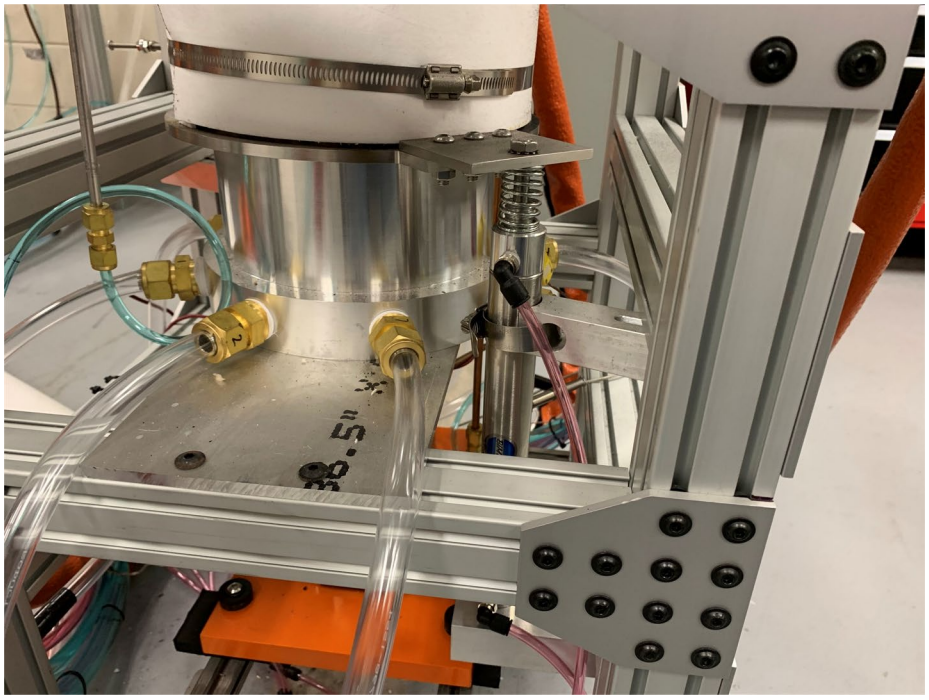

Figure 2.7(b): *Exterior portion of ADC with air supply tubes and fittings.*

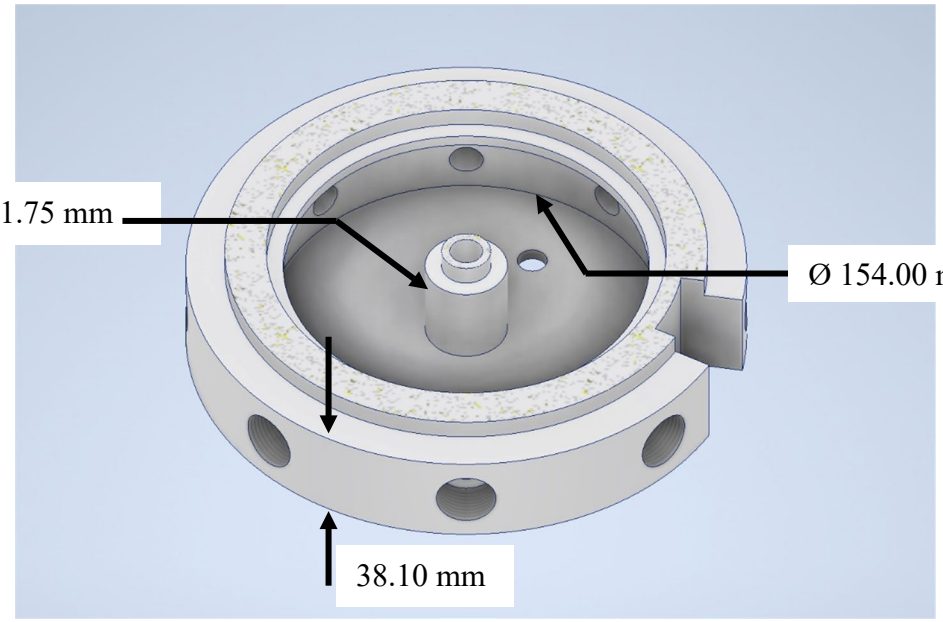

Figure 2.7(c): *Interior portion of redesigned ADC, lower mixing chamber cross sectional view.*

Figure 2.8: *Top view of glass bead layer.*

The overall height of the CADS was increased from 300.00 mm to 338.10 mm. This change in height was caused by the addition of the lower mixing chamber, 38.10 mm depth, where the eight injection ports are located. Because the air is not directed towards the bottom plate, additional space was added to promote mixing before the flow enters the section containing the stainless-steel meshes and glass beads. Refer to Appendix A.4 for detailed CAD drawings as well as additional views of the CADS. Appendix A.3 provides drawings for the CADS base mounting plate, used to couple the CADS to the frame structure.

2.2.2 Internal Attachment Mounting System (IAMS)

To promote a modular mounting system to switch between the sample bearing holder and heat flux gauge mount, a 19.05 mm diameter hollow stud was incorporated into the design. Attachments can be changed out quickly and with ease through the use of a stainless-steel compression union fitting with reusable noninvasive PTFE (Teflon) ferrules. Figure 2.9(a) shows the mounting of the bearing holder used for the sample support assembly. Figure 2.9(b) shows the mounting of the heat flux gauge mount in the same location as the sample support assembly bearing. This design allows for additional attachments in the future.

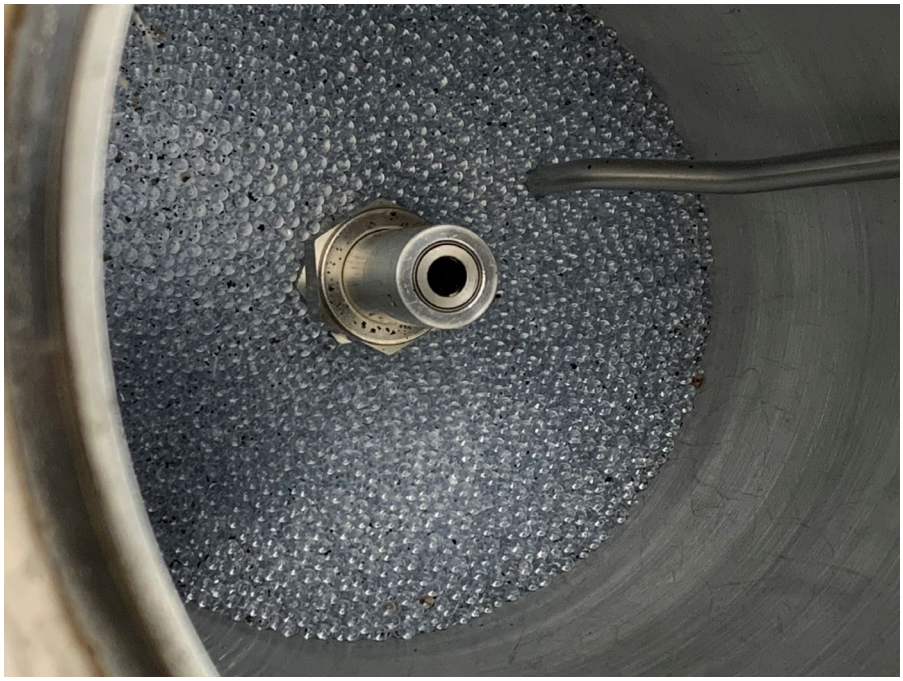

Figure 2.9(a): *IAMS with sample bearing holder installed.*

Figure 2.9(b): *Heat flux gauge mount in IAMS.*

2.2.3 Upper Quartz Tube Adapter

The quartz tube adapter specified in the standard, made from stainless steel has also been redesigned. The new design utilizes an external coupling mechanism opposed to an internal one as used in the standard and shown in Figure 2.10. The new design is made to minimize direct exposure to exhaust gases, allowing the adapter to be constructed out of aluminum. Additionally, the new design minimizes exhaust gas flow disturbances by creating a continuous surface inside the quartz tubes. The original design created a step inside the quartz tubes, which had the potential to alter exhaust gas mixing. By using 3.00 mm thick high temperature ceramic paper insulation, a gasket is produced, decreasing potential combustion product exhaust losses. Refer to Appendix A.5 for detailed CAD drawings of the upper quartz tube adapter.

(a)

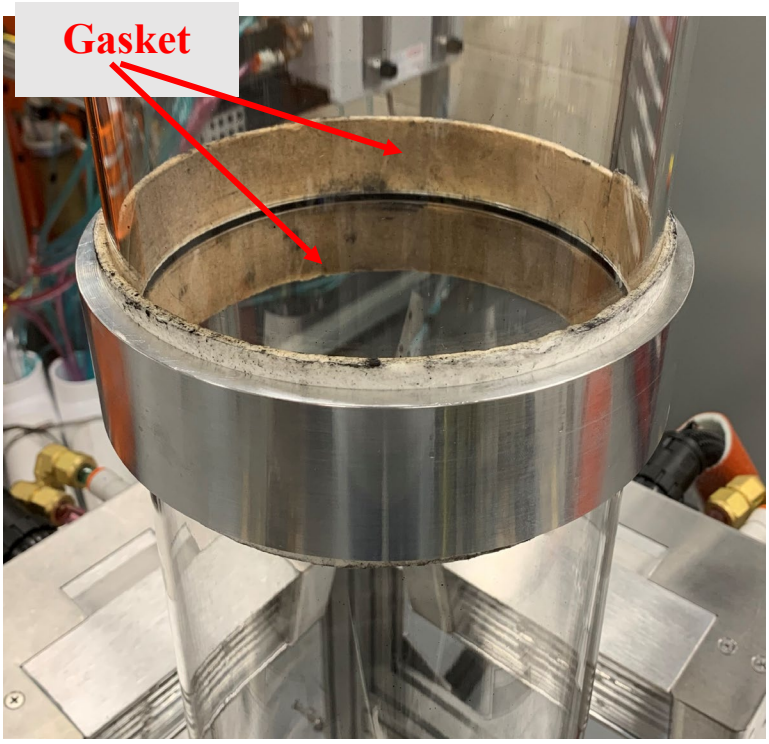

(b)

Figure 2.10: *Standard specified (a) vs redesigned (b) quartz tube pipe connector.*

The design changes made to the CADS have improved manufacturability by reducing welded parts, improved stock material availability, and allowed for the production of a comprehensive drawing set. Maintainability was improved by replacing complex machined parts with mass-produced parts, such as material base stock and tube fittings, available at any industrial supplier company. Ease of use was improved by implementation of design changes that allow for simpler manual operations to be conducted.

2.3 Water Cooled Outer Shield (WCOS)

To prevent test sample exposure to infrared heaters (see Figure 2.11) during the warmup period, a water-cooled outer shield (WCOS) is placed between the lamps and the sample. The WCOS is driven by two pneumatic cylinders that raise and lower the shield via an electronic actuation switch. The WCOS consists of two stainless steel tubes, welded together with caps on each end. The process of welding stainless steel is less difficult than aluminum. Compared to the standard where aluminum is used, the new design has an outer diameter of 215.90 mm, an inner diameter of 197.10 mm, and a height of 228.60 mm. The water jacket between the two tubes is 3.30 mm wide. Both inner and outer cylinder walls have a thickness of 3.175 mm. To aid in heat control at higher heat fluxes, COTRONICS CORP. Ultra Temp 300 Ceramic Paper insulation, with a thickness of 3.175 mm, is added to the exterior walls and top surface of the shield. This is used to aid in the prevention of water vaporization inside the cooling channel.

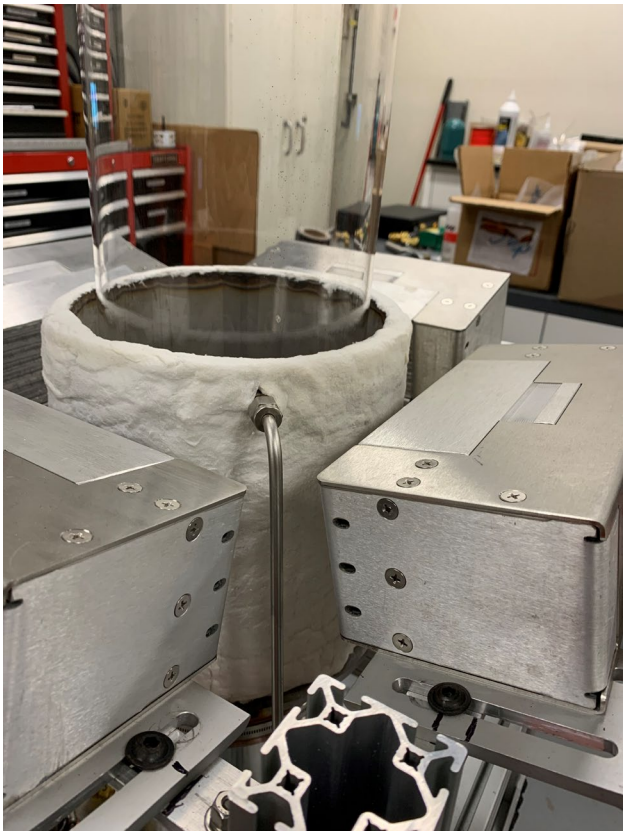

Figure 2.11: *WCOS in raised position ready to perform a test.*

Water inlet and outlet ports are welded into the exterior wall of the shield at the bottom and top respectively. The ports are offset by 180 degrees to allow water to flow through the channel and minimize air pockets from being formed. Figure 2.12 shows the computer-generated drawing of the WCOS, its mounting system, and the pneumatic cylinders.

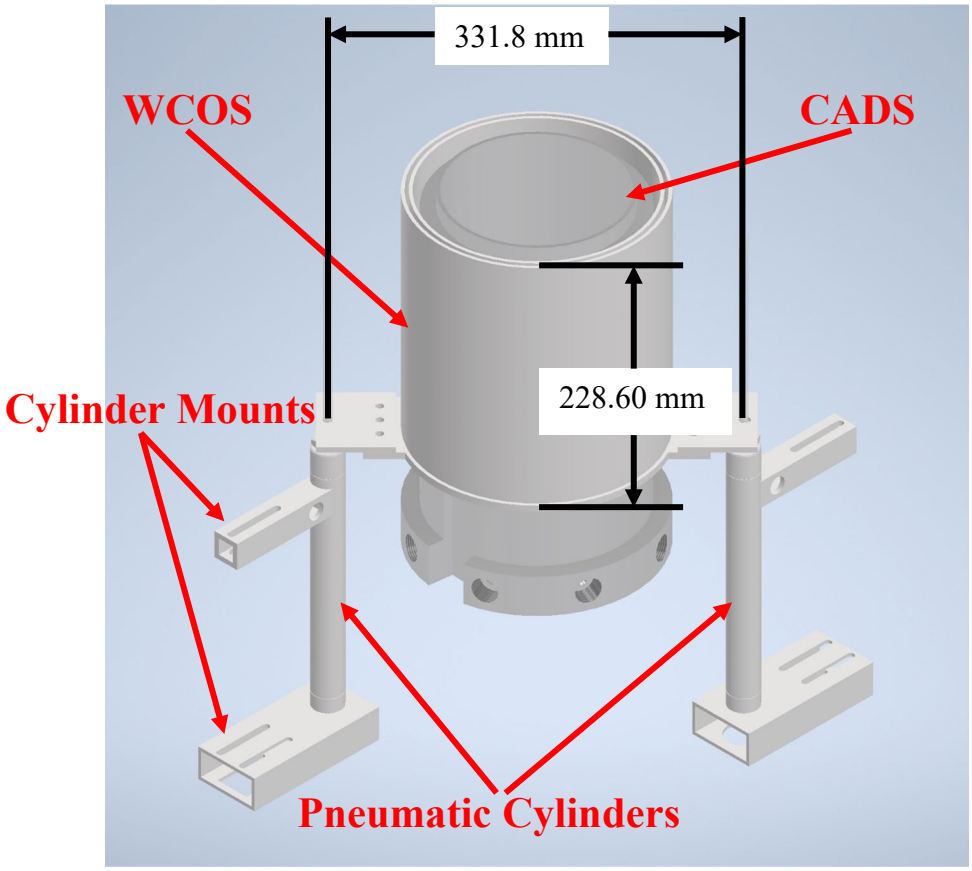

Figure 2.12: *Computer generated drawing of the WCOS and its supporting parts around the CADS.*

The WCOS pneumatic cylinders, each have a bore of 26.98 mm and a stroke of 177.8 mm. The cylinders are double-acting, meaning air controls both upwards and downwards movement. When filled with water, the WCOS has a mass of 9.5 kg. The air cylinders operate under 40 PSI and utilize a speed controller to adjust the speed and force when raising and lowering the WCOS. When the WCOS is turned to the dropping position, it has a response time of 0.84 seconds. As seen in Figure 2.13, springs are used on the air cylinders to minimize vibration transfer from the dropping of the WCOS to the rest of the apparatus.

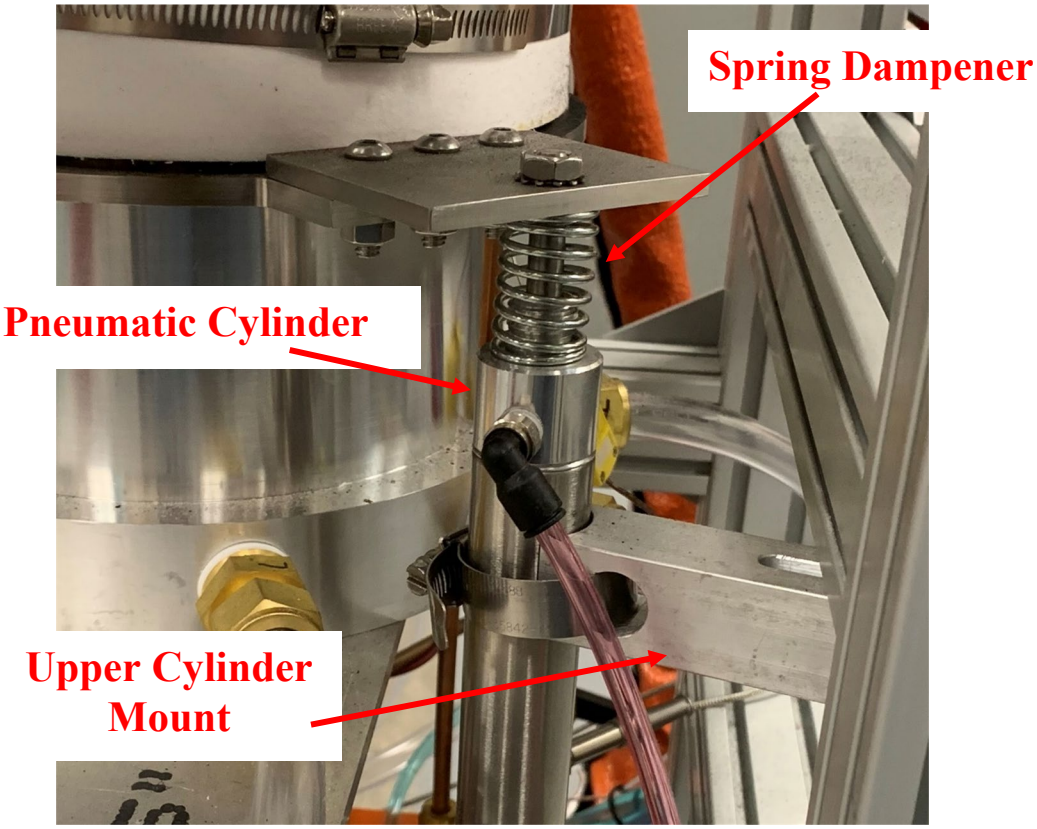

Figure 2.13: *WCOS Cylinder Mounts with Spring Dampeners.*

The WCOS mounting system that couples the shield to the pneumatic cylinders is depicted in Figure 2.14. This mounting system is designed to be modular in nature and can be redesigned at any time. The bracket is 76.2 mm by 63.5 mm, with a thickness of 4.76 mm. The WCOS mounting holes are 6.35 mm in diameter with a center-to-center offset of 19.05 mm. Refer to appendix A.6 and A.7 for detailed CAD drawings of the WCOS and its supporting mount system.

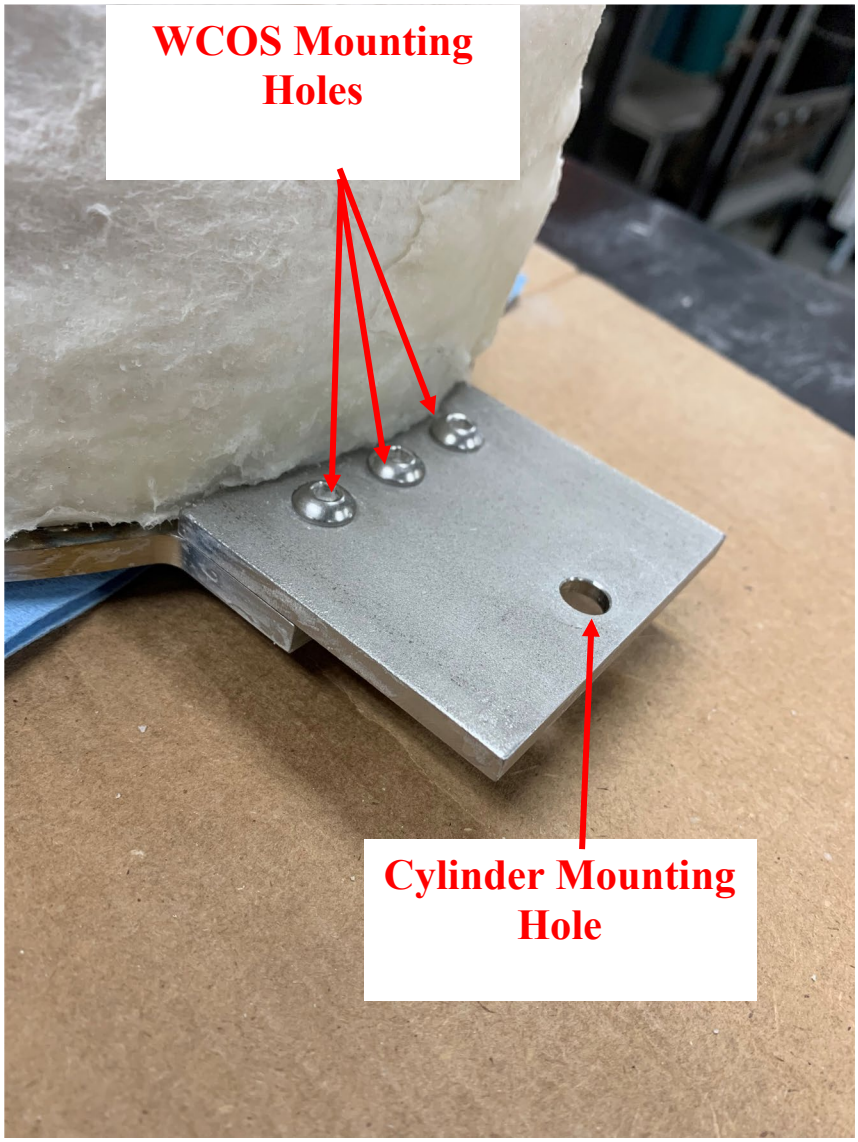

Figure 2.14: *WCOS to pneumatic cylinder mounting bracket.*

The material change from aluminum to stainless steel provided increased manufacturability. Stainless steel is more corrosion resistant than aluminum, improving the maintainability. By implementing two pneumatic cylinders, the WCOS moves smoothly and quickly, allowing the operator to maintain focus during a test.

2.4 Load Cell System and Sample Support Assembly

2.4.1 Load Cell

The load cell used is a Sartorius WZA8202-N. This unit has a weighing capacity of 8200 g and an accuracy of ±0.01 g. Data acquisition samples at a rate of 5 Hz. In accordance with the standard, section 6.3, the load cell should have an accuracy of ±0.1 g and a weighing capacity of 1000 g. The selected Sartorius load cell was chosen to improve data accuracy and weighing capabilities to allow for an increased range of sample masses.

The load cell was mounted to the FPA frame through a 203.20 mm x 304.80 mm x 19.05 mm thick steel plate (load cell base plate) and four 50.80 mm x 50.80 mm x 13.00 mm thick Neoprene rubber blocks with a Durometer rating of 30A, as illustrated in Figure 2.15. The steel plate has a mass of 9.21 kg. Refer to appendix A.9 for detailed CAD drawings of the load cell base plate. The Neoprene rubber blocks are used to decouple and isolate the load cell base plate from the FPA frame to reduce vibration exposure to the load cell and minimize noise in the output signals. Mass data was sampled at a rate of 5 Hz and recorded by the Simple Data Logger program developed by Smart Lux.

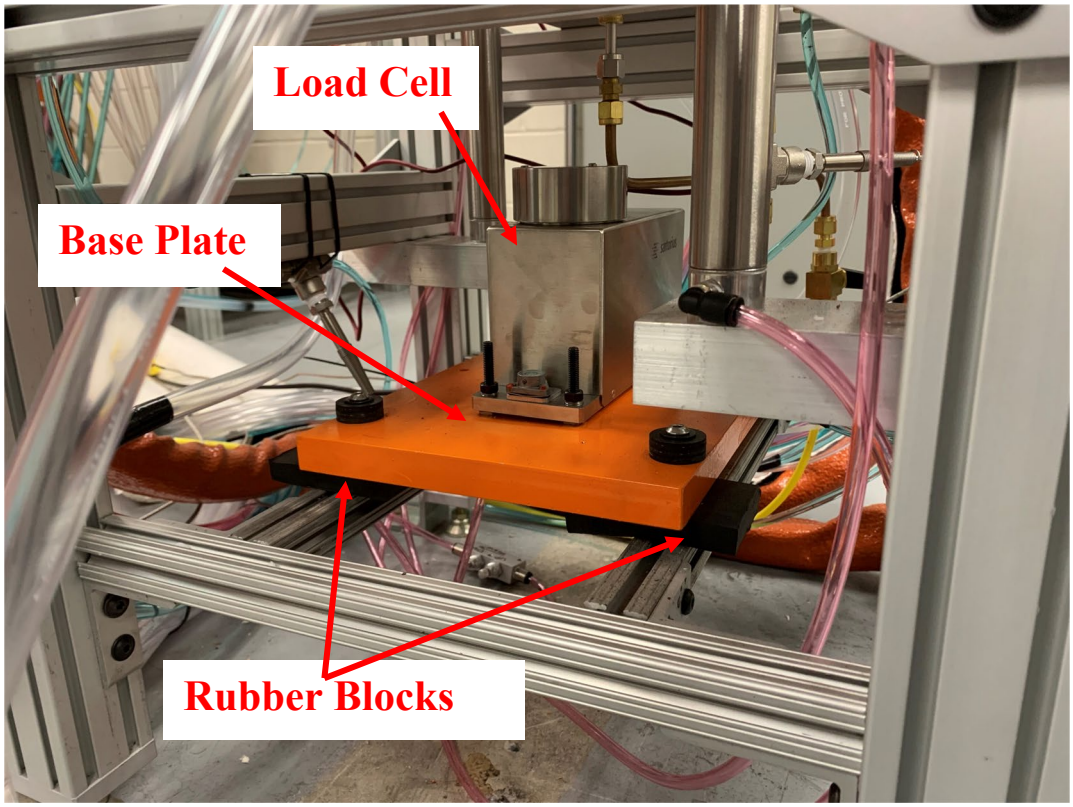

Figure 2.15: *Upgraded load cell mounded to base plate in FPA Frame.*

2.4.2 Sample Support Assembly (SSA)

The sample support assembly (SSA), shown in Figure 2.16, consists of a bearing holder, center shaft, adjustable foot, and an upper platform. The bearing holder, which is removable from the assembly, is designed to support the center shaft of the SSA. The bearings used are Thomson Industries model #A4812. This linear motion bearing has a length of 19.05 mm, an outer diameter of 12.70 mm, and is designed to be used with a 6.35 mm diameter rod. The holder is constructed from aluminum. It has a length of 76.20 mm, an outer diameter of 19.05 mm and an inner diameter of 7.94 mm. The holder is machined on both sides to accommodate the size of the bearing. The bearings are held in place with six set screws, three per bearing. Due to the length of

the bearing holder, a larger center shaft to bearing interface is present when compared to ASTM E2058.

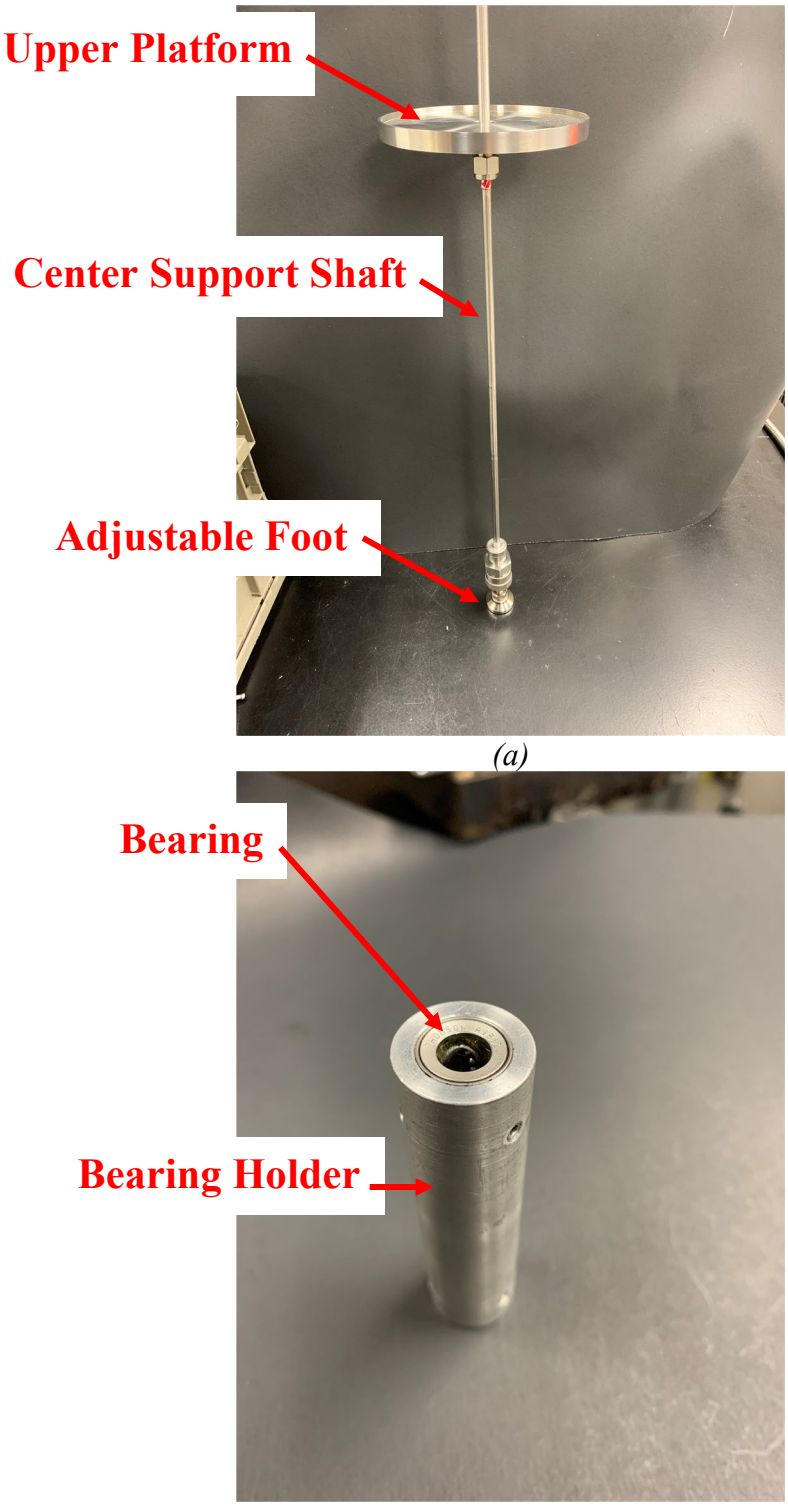

Figure 2.16: *Sample support assembly (a) and bearing holder(b).*

The center shaft has a length of 332.00 mm and a diameter of 5.56 mm. The shaft size was chosen to be undersized when compared to the bearing inner diameter and to the standard. Refer to appendix A.9 for detailed CAD drawings of the SSA. During initial apparatus construction, it was found that when using a 6.35 mm diameter shaft, the mass reading of the sample was incorrect and deviated by about 16% from the true sample mass. This difference was caused by the friction between the shaft surface and bearing. Through the use of an undersized shaft diameter, 0.79 mm smaller, the difference in mass is reduced to 0.04%. The sample mass was taken before each test with a stand-alone bench top mass balance.

2.4.3 Horizontal Sample Dish (HSD)

The horizontal sample dish (HSD), shown in Figure 2.17, was constructed from stainless-steel. The HSD has an outside diameter of 111.13 mm, an inside diameter of 108.59 mm and a height of 28.58 mm. Appendix A.9 has detailed CAD drawings of the HSD. The HSD was designed to be compatible with various sample thicknesses ranging from 6.35 mm to 12.70 mm. The HSD is lined with 3 layers of 6.35 mm thick ceramic fiber board insulation. Samples are insulated on all sides except for the face exposed to the heaters. By removing one layer of insulation, the sample thickness can increase. The design changes made to the HSD make it easier on users because less adjustment time is required when sample thicknesses are changed. The HSD was designed to sit inside the recessed area of the upper platform of the SSA. This recessed area aids in the centering of the sample inside the CADS, ensuring repeatable in-plane sample location from test to test.

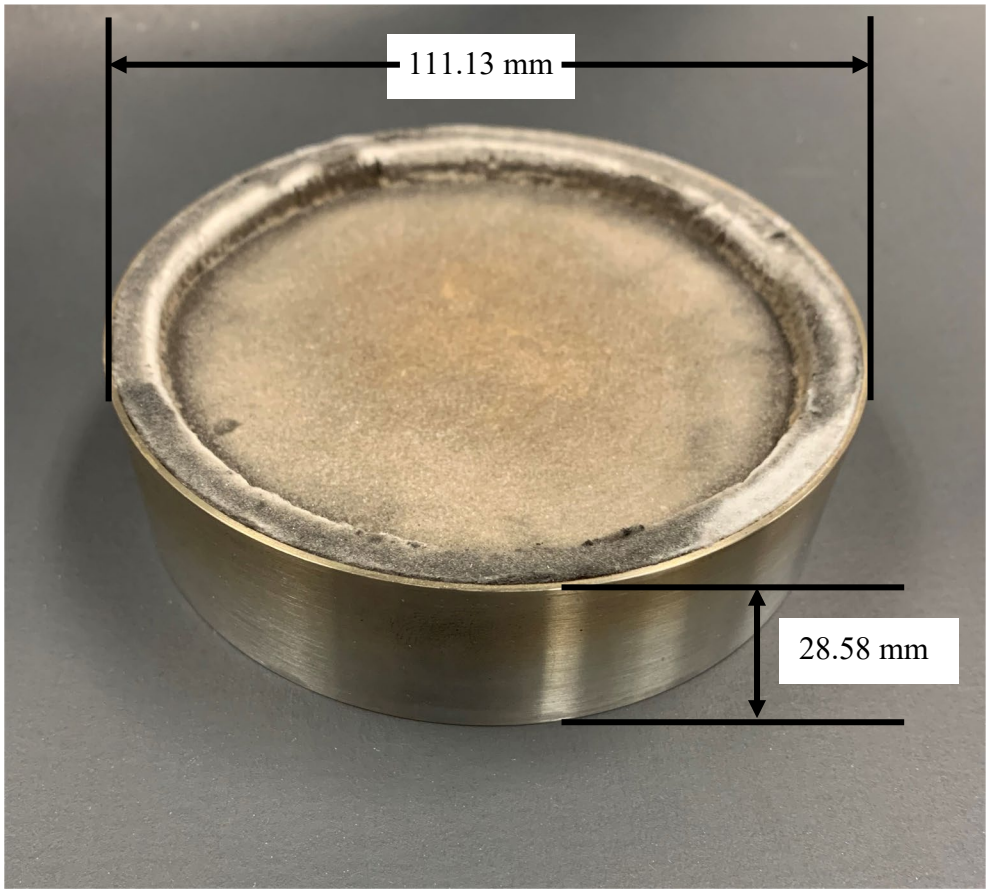

Figure 2.17: *Redesigned horizontal sample dish with ceramic fiber insulation liner.*

Due to the stainless-steel construction, the sample dish can withstand higher heat fluxes for a longer period when compared to the aluminum horizontal sample dish as specified in ASTM E2058 section 8.1[9]. This material choice in turn leads to an increased sample dish life span while reducing the overhead associated with aluminum dishes.

The redesigning and upgrading of the SSA and load cell systems, contribute to increase operator ability. With an increased resolution and capacity, large samples can be tested. Sample dishes are easily manufacturable and have a prolonged life span. The sample support assembly allows for easy installation and removal. Figure 2.18 shows a computer-generated section view of the FPA fully assembled including the load cell, SSA, WCOS, and CADC.

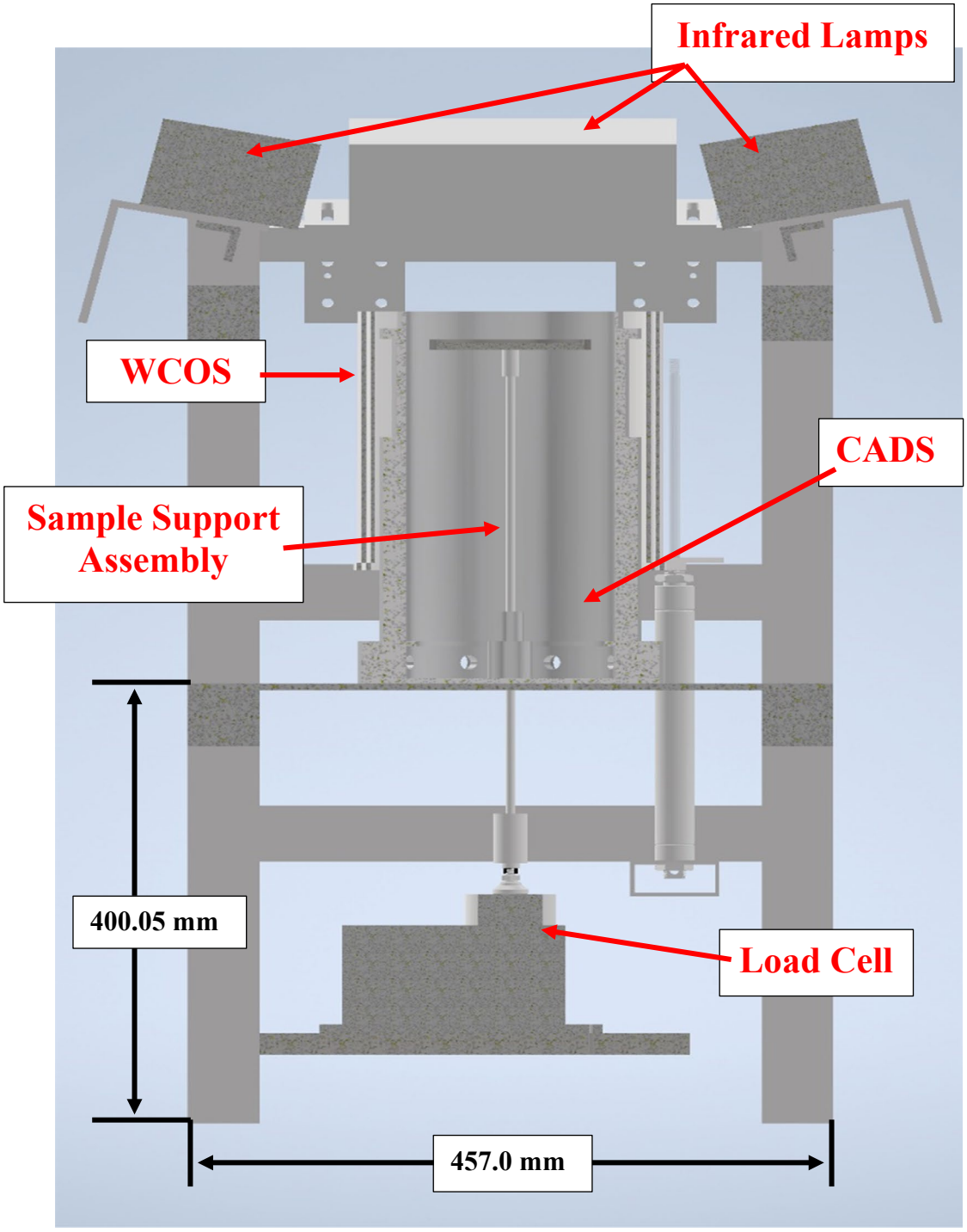

Figure 2.18: *FPA section view.*

2.5 Pilot Flame

The pilot flame for the FPA is a stoichiometric ethylene-air flame with a length of 10 mm as presented in the standard. The addition of two Dwyer flow meters allows for accurate control of the flame, ensuring it remains stoichiometric. Ethylene utilizes a Dwyer Model VA1043 flow meter, and the compressed air utilizes a Model VA1048 flow meter. The flow rates necessary for a 10 mm stoichiometric flame are 20.75 mL min^{-1} and 297.5 mL min^{-1} (as measured at the standard atmospheric pressure and temperature) for ethylene and air respectively. The flow rates were determined through the use of the global combustion equation and trial and error. The global combustion equation was used to determine the stoichiometric volume ratio of ethylene to air, under the assumption of ideal gas behavior. The volume ratio was found to be 1:0.07. Using the volume ratio, the ethylene and compressed air flow rates were adjusted until the flame had a length of 10 mm while maintaining stoichiometry. The flow meters were initially calibrated for use with air. Subsequently, the following correction factor equation is used for ethylene

$$Q_2 = Q_1 \div \sqrt{\frac{1}{S.G.}} \quad (1)$$

Where Q_2 is the corrected flow rate, Q_1 is the observed flow rate, 1 is the specific gravity of air, and S.G. is the specific gravity of the gas being used in the flow meter. The value used for the specific gravity of ethylene was 0.992. The above flow rate for ethylene is the corrected flow rate (Q_2).

Both flowmeters use a scaled reading for flow measurements. When set correctly, as seen in Figure 2.19, ethylene is set to 37 and air to 38. Figure 2.20(a) shows the scale to flow rate values of the ethylene flow meter, Figure 2.20(b) is for air.

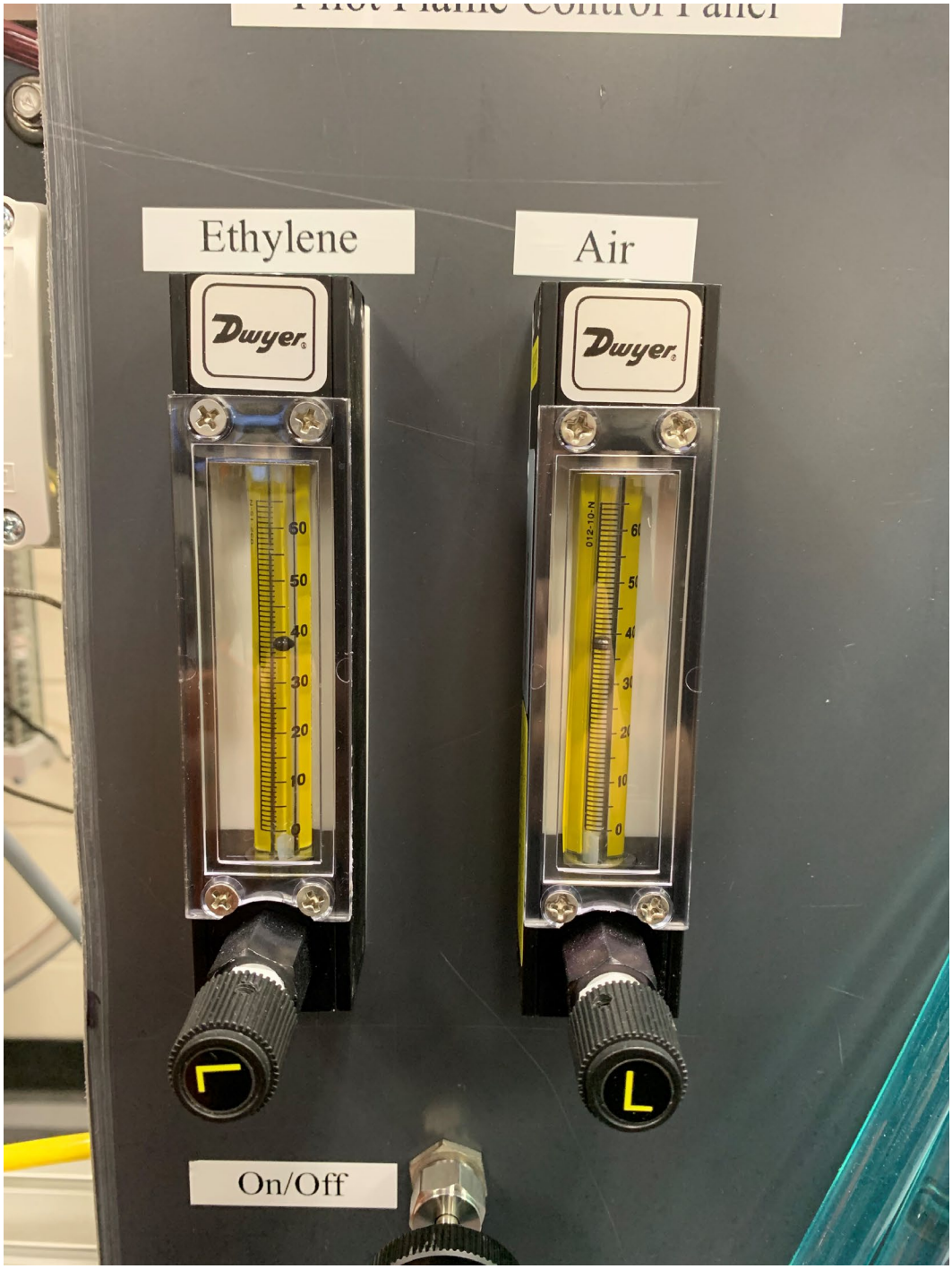

Figure 2.19: *Ethylene and air pilot flame flow meters.*

Scale Readings	Flow [ml/min]
65	48.7
60	43.8
55	38.1
50	32.7
45	27.9
40	22.9
35	19.0
30	15.5
25	12.6
20	9.9
15	7.3
10	5.4
5	3.7

Figure 2.20(a): *Ethylene flow meter scale reading.*

Scale Readings	Flow [ml/min]
65	518
60	478
55	439
50	399
45	359
40	318
35	277
30	237
25	197
20	158
15	123
10	91
5	63

Figure 2.20(b): *Compressed air flow meter scale reading.*

2.6 Heat Flux Gauge Mount

For proper heat flux measurements, a mount was designed to allow for rapid installation and removal of a heat flux gauge. The heat flux gauge mount base design was provided by FM global, shown in Figure 2.21, slight modifications were made for convenience. Figure 2.22 shows the modified heat flux gauge mount. The adjustability of the mount allows for heat flux mapping of the sample top surface face both in plane and vertically. The mount is part of the IAMS. It is easily replaced with the sample bearing holder when tests are conducted. The heat flux gauge mount is constructed from 3.175 mm thick stainless steel. The center pass through of the mount makes connecting water lines and electrical connection straight forward. Figure 2.23 shows the heat flux gauge mounted in the CADS. Refer to appendix A.10 for detailed CAD drawings of the heat flux gauge mount.

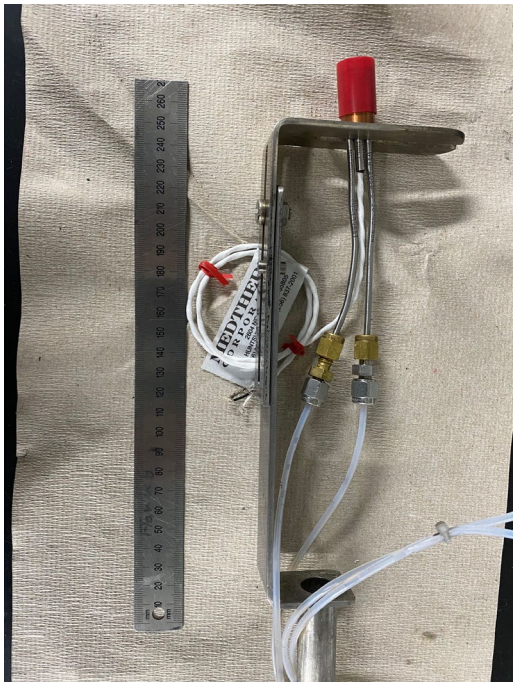

Figure 2.21: *FM Global Heat Flux Gauge Design.*

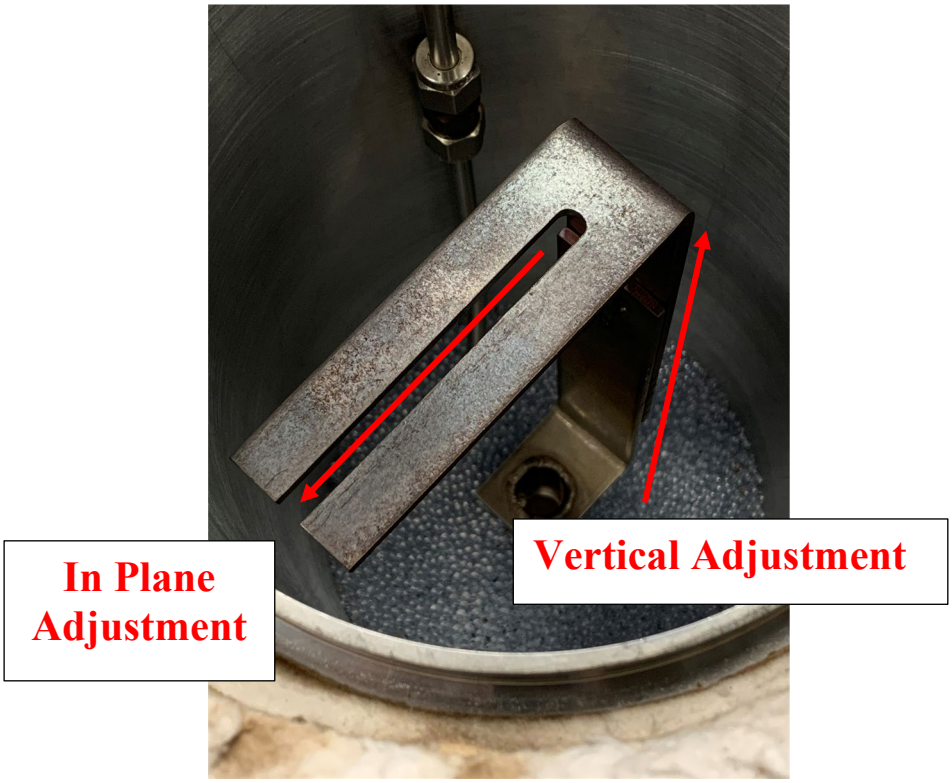

Figure 2.22: *Heat Flux Gauge Mount.*

Figure 2.23: *Heat Flux Gauge Mount with Heat flux gauge installed.*

2.7 Apparatus Diagnostic Equipment

2.7.1 Temperature Sensors

The FPA was outfitted with additional temperature sensors to detect potential issues in water-cooled parts. The temperature sensors used were Omega ungrounded K-type thermocouples, model TC-K-NPT-U-72. Five temperature measurements were taken, inlet water temperature, heating lamp outlet temperature, WCOS outlet temperature, ADC copper coil outlet temperature, and aluminum surface temperature of the CADS. Temperature data was sampled at a rate of 3 Hz using a National Instruments CompactDAQ chassis and LabVIEW software. When performing tests at high heat fluxes, on the order of 90 kW m^{-2}, the peak temperature observed in a water-cooling circuit was 35°C from the WCOS during lamp preheat time.

Through the use of this diagnostic equipment, operators can easily identify a cooling issue prior to part failure. The system is also expandable for future addition of diagnostic equipment.

Chapter 3: Apparatus Characterization

Three different types of measurements were taken to form a base line characterization of the redesigned FPA. The heat flux observed by a sample was taken to determine the relationship between heat flux and power output settings. Additionally, the heat flux was taken to determine the time dependent drift of radiation a sample would experience. The air flow uniformity around a sample was determined to ensure a flaming sample would have sufficient air for combustion. The temperatures of key apparatus components were taken to ensure sufficient cooling was present.

3.1 Heat Flux to Power Setting

Lamp output power is controlled as a function of percent from 0% up to 100%. As a first order approximations of heat flux at each power level, Figure 3.1 shows heat flux to power setting curve. The trend follows an exponential growth curve with the equation

$$HF = 0.060317 * {P_{set}}^{1.6648} \quad (3)$$

where HF is the desired heat flux setting, and P_{set} is the power level input for the lamp controller, in percent. The heat flux gauge was positioned to be in the identical to where the sample top surface is usually located. The reproducibility of the heat flux to power curve was found to be P_{set} ± 0.30 %. The uncertainty was calculated by taking the standard deviation of power input percentage from day-to-day operations.

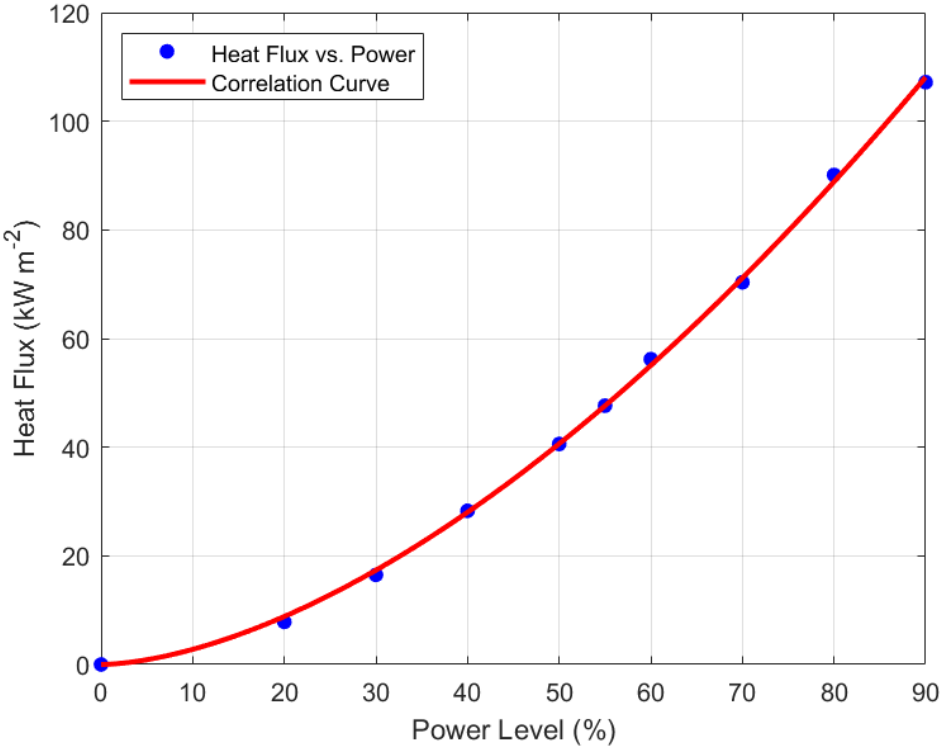

Figure 3.1: *Heat flux to power curve.*

3.2 Heat Flux Variation

The variation in heat flux vertically was determined in accordance with ASTM E2058. Figure 3.2 shows the variation in the vertical direction both 10 mm and 20mm above and below the sample top surface. The vertical elevation center of the top sample face was taken to be the same elevation as the uppermost edge of the CADS. The distance from the infrared lamps bottommost edge to the CADS upper most edge and sample top surface is 74.295 mm. The heat flux gauge was located in the center of the CADS, shown by the red center line in Figure 3.2. This center location is equivalent to the center of a circular sample. The maximum deviation from the sample top surface was 1.09%. This is within the range of 5% set by the standard.

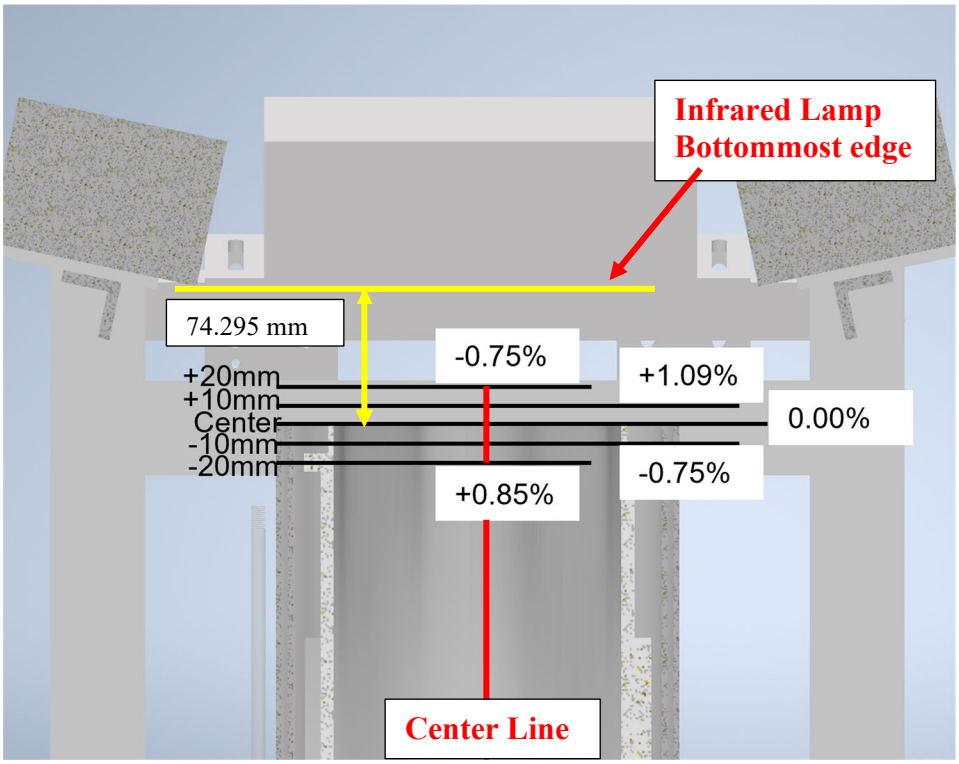

Figure 3.2: *Vertical heat flux variation.*

Figure 3.3 shows the variation within the surface plane of the sample, located at a vertical elevation equivalent to the uppermost edge of the CADS as previously stated. Measurements were taken radially at the sample edge (R_1 = 48.2 mm), and halfway to the sample edge (R_2 = 24.1 mm). Figure 3.4 shows the location of the heat flux gauge for each surface plane measurement, represented by the red dots. For each radial distance, the heat flux was taken at 8 spots, corresponding to locations directly in front of each lamp and halfway between lamps. The mean deviation from the sample center to the sample edge is 4.2%. From the sample center to halfway to the edge, the mean deviation is 0.35%. The mean deviation was calculated using the following equation

$$MD = \sum_{i=1}^{n} \frac{100}{n} * abs(\frac{HF_c - HF_i}{HF_i}) \quad (2)$$

Where *MD* is the mean deviation given in percent, *abs* is the absolute value, HF_c is the heat flux at the center, HF_i is the heat flux at the point of interest, *i* represents the point of interest, and *n* is the total number of points of interest. In the mean deviation calculations at both R_1 and R_2, *n* was equal to 8.

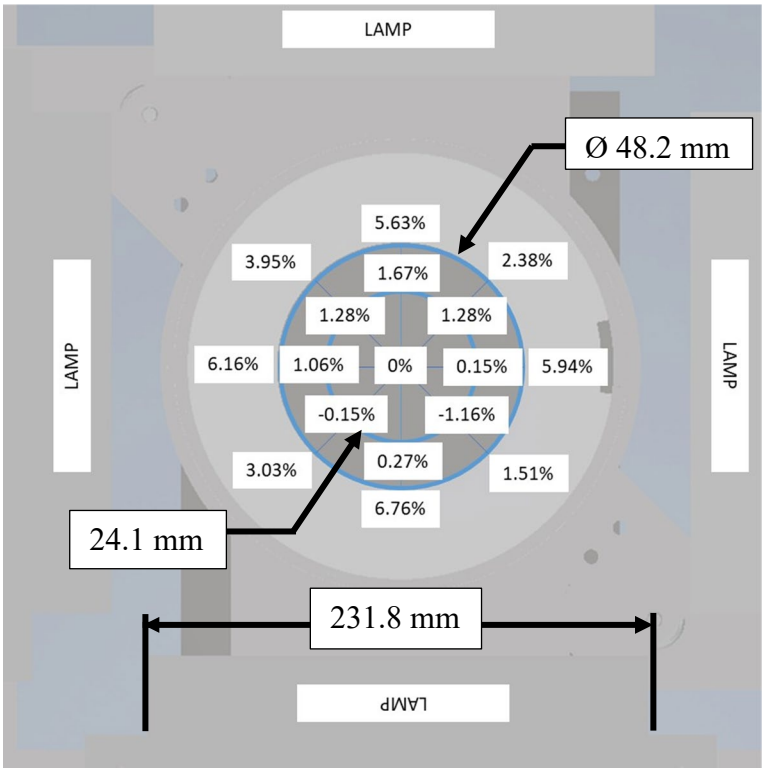

Figure 3.3: *In plane heat flux variation.*

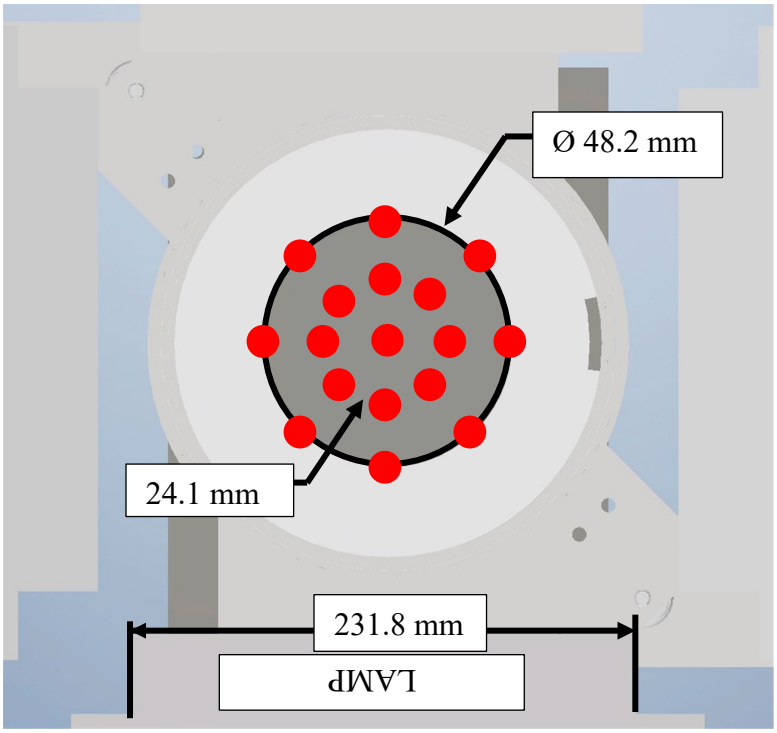

Figure 3.4: *In plane heat flux variation heat flux gauge locations.*

The heat flux was observed to slightly drift with time. Figure 3.5 shows the non-dimensionalized heat flux, taken from a point equivalent to the center of a sample, at four power settings of the infrared lamps, run for a total of 900 seconds each. The non-dimensionalized heat flux equation used was

$$HF_{nd} = \frac{HF}{HF_{Ref}} \tag{3}$$

Where HF_{nd} is the non-dimensionalized heat flux, HF is the Heat Flux value at any time, and HF_{Ref} is the average heat flux value from 45 seconds to 75 seconds after the WCOS drops, exposing the heat flux gauge to the radiation from the infrared lamps. When running tests, the heat flux is taken to be the value of HF_{Ref}.

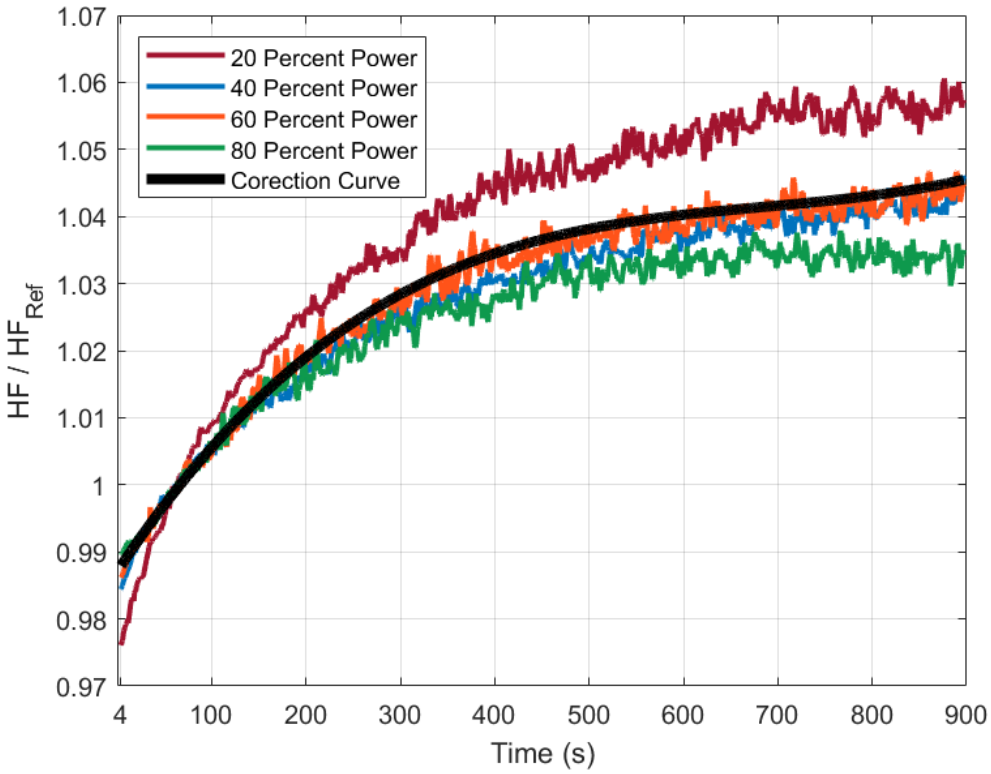

Figure 3.5: *Non-dimensionalized heat flux vs time.*

The heat flux drift characterization equation depicted by the correction curve in Figure 3.5 is a third-degree polynomial. The equation was developed by first non-dimensionalizing the heat flux data at each power setting, then taking the average of the non-dimensionalized heat flux data to generate a correction curve. The correction curve and equation was created using the MATLAB Curve Fitting application. The heat flux drift characterization equation is

$$HF = HF_{Ref} * (1.415 \times 10^{-10} * t^3 - 2.893 \times 10^{-7} * t^2 + 2.099 \times 10^{-4} * t + 0.9879) \quad (4)$$

Where *HF* is the heat flux at the desired time throughout the experiment, HF_{Ref} is the average heat flux from 45 to 75 seconds, and *t* is the time in seconds since the WCOS was dropped.

The cause of the observed heat flux drift may be caused by a few factors. The quartz tubes could cause the heat flux drift. Over time, the quartz tubes may start to reradiate. Since the infrared lamps rely on a power level input, output will remain constant. Without cooling of the quartz tubes, reradiation will continue. Further investigation is needed to determine the cause and better understand the heat flux drift.

3.3 Air Flow Uniformity

The air flow uniformity inside the CADS was determined using an OmegaHHF-SD1 hot wire anemometer. The air flow rate was set at 200 SLPM, with a reference temperature and pressure of 25°C and 1 atm respectively. The measurement was taken at the uppermost open cross section of the CADS, identical to where the sample top surface is usually located, with three size 20 stainless steel mesh and 24.50 mm layer

of 3.00 mm diameter glass beads to promote air flow uniformity. The SSA, and horizontal sample dish were both present when these measurements were taken. The quartz tubes were not present, as they would inhibit the ability to measure the air flow around the sample. A representative quartz tube was made from cardboard, allowing the hot wire anemometer to be used through a small slot in the side of the cardboard cylinder. Measurements were taken radially around the sample plane at random point. The air flow velocity uniformity was found to be 0.18 m s^{-1} ± 0.02 m s^{-1}. The uncertainty was calculated using standard deviation of all measured points.

3.4 Apparatus Temperature Profiles

The temperature profiles of the FPA were found as previously discussed in section 2.7.1. Figure 3.6 shows the temperature profiles for a 15-minute run at a power setting of 80%, equivalent to 92 kW m^{-2}. The peak temperature observed was 73°C by the aluminum surface temperature. This aluminum surface has minimal water cooling, as it is the support for the quartz tubes to sit on. The inlet water temperature remained constant throughout the run at 26°C. The WCOS observed a peak temperature of 37°C by the end of the 120 second lamp warm up period. Both the infrared lamps and copper cooling coil observed a peak temperature of 35°C at the end of the run.

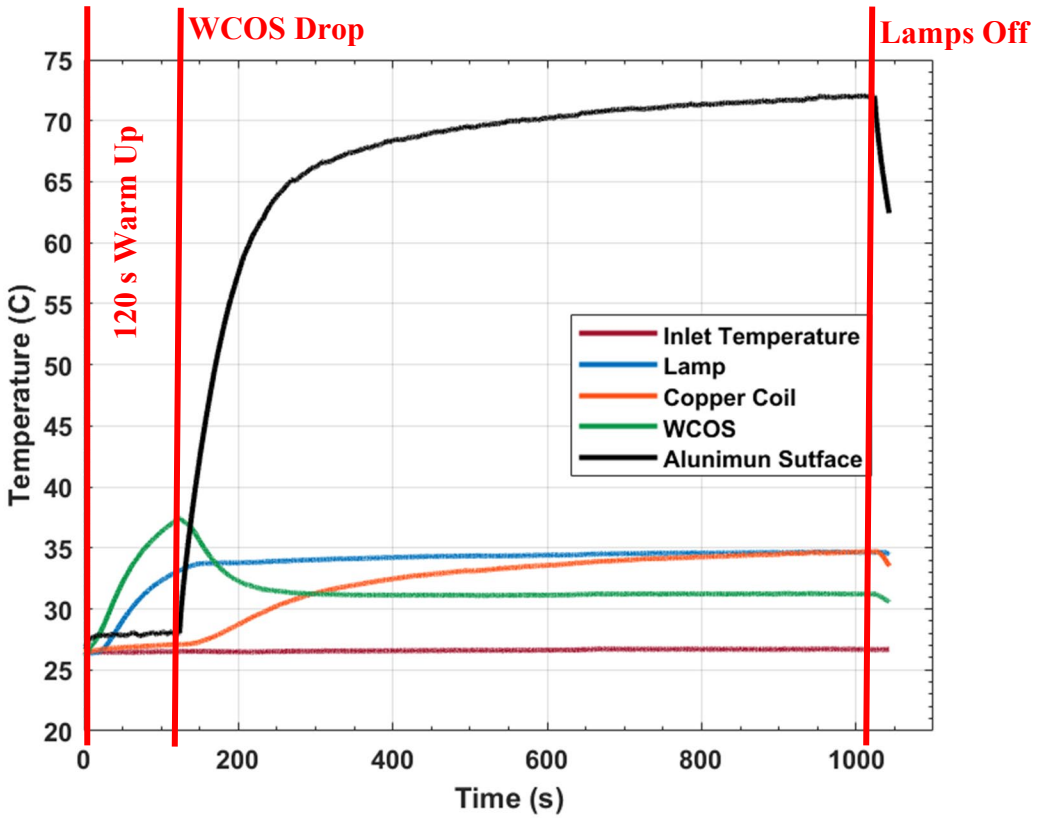

Figure 3.6: *Apparatus temperature profiles at 80% power for 15-minutes.*

Chapter 4: Performance Comparison with Cone Calorimeter and CAPA

A comparative series of test were conducted between the Fire Propagation Apparatus, cone calorimeter, and Controlled Atmosphere Pyrolysis Apparatus II to determine the mass loss rate. The material used throughout the study was poly(methyl methacrylate). The FPA and cone calorimeter tests were run at two heat fluxes, 25 kW m^{-2} and 50 kW m^{-2}. CAPA II tests were run at 52 kW m^{-2}. This heat flux differs from the FPA and cone calorimeter tests because it better represents the heat flux observed by a sample in the FPA. This heat flux is the spatially averaged heat flux across the FPA sample halfway through an experiment. The CAPA II is nearly perfectly spatially uniform in the heater heat flux (less than 5% drop at the sample edge); the CAPA heat flux does not drift in time [5]. Samples were tested with both coated and uncoated top sample faces.

4.1 Material Specifications

The material used during this study was chose to be poly(methyl methacrylate) (PMMA), Acrylite GP Black 9H01. This material is commonly used for testing and has well characterized material properties. This allows for better comparisons to validate the new design of the FPA. Samples were run in two fashions, coated and uncoated at the top sample surface face. The paint coating used, Medtherm Corporation HT2000, has an emissivity of 0.92. The paint coating used is shown to have the same optical properties over a wide range of wavelengths, including the FPA and cone calorimeter.

The samples prepared for the FPA experiments were each 96.40 mm ± 1.0 mm with a thickness of 6.00 mm ± 0.30 mm. Samples were cut from bulk material using a 102.00 mm hole saw, Milwaukee #49-56-9685. The average mass of each sample was 50.36 g ± 1.50 g. Prior to testing, samples were conditioned in a desiccator for at least 48 hours. For coated samples, a layer of high temperature, high emissivity flat black paint was used to promote even heating across the sample surface. Prior to coating, the sample face surface was scuffed with 600 grit sandpaper to allow better adhesion between the paint and sample surface, as seen in Figure 4.1. For uncoated sample, no sanding was done, and the sample face was left in its natural form. Figure 4.2 shows a coated sample.

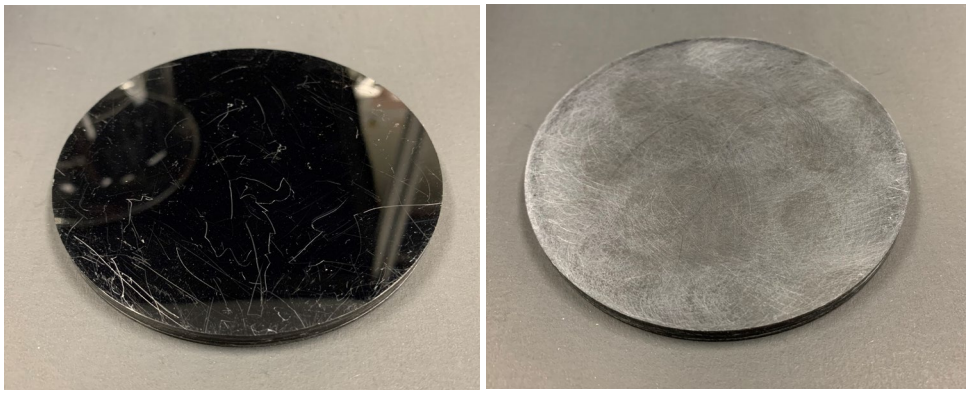

Figure 4.1: *FPA natural sample surface to scuffed surface.*

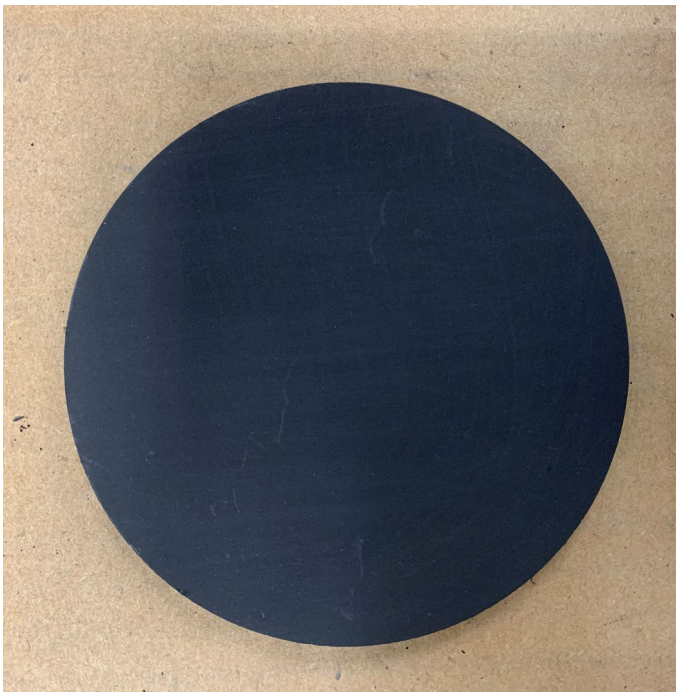

Figure 4.2: *FPA Coated sample surface.*

The samples prepared for cone calorimetry experiments were each 100.00 mm ± 2.00 mm squares with a thickness of 6.00 mm ± 0.30 mm. The average mass of each sample was 69.01 g ± 1.50 g. Prior to testing, samples were conditioned in a desiccator for at least 48 hours. Coated samples were prepared in a similar fashion to the FPA. Figure 4.3 shows a cone calorimeter sample pre and post sanding. For uncoated sample, no sanding was done, and the sample face was left in its natural form. Figure 4.4 shows a coated sample.

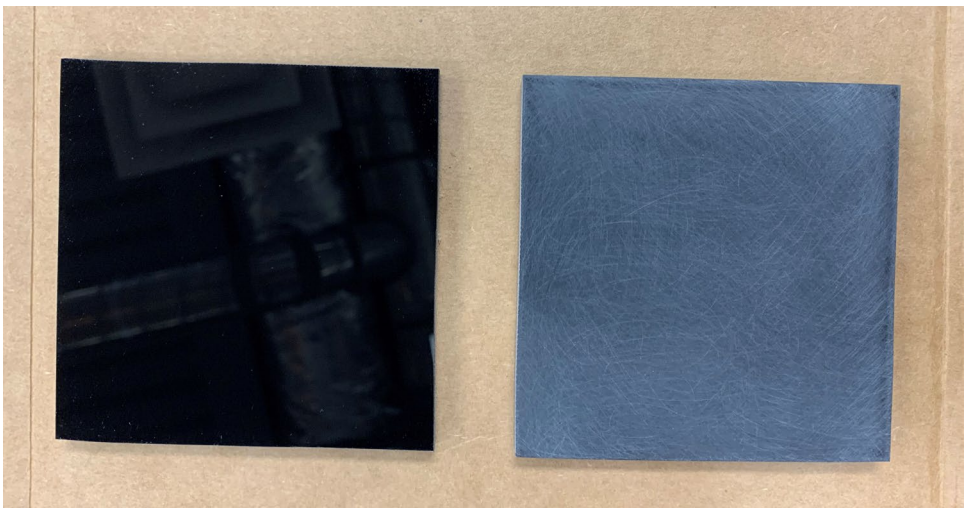

Figure 4.3: *Cone natural sample surface to scuffed surface.*

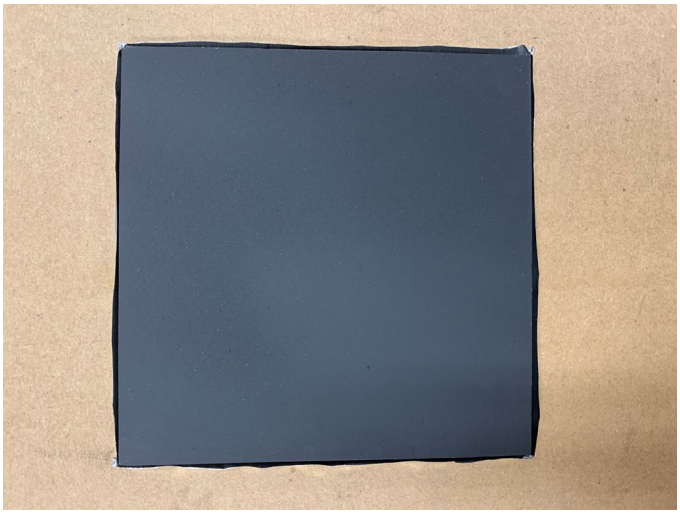

Figure 4.4: *Cone coated sample.*

The samples prepared for the CAPA II experiments were each 68.80 mm ± 1.0 mm with a thickness of 6.00 mm ± 0.30 mm. Samples were cut from bulk material by a machine shop. The average mass of each sample was 27.3 g ± 0.50 g. Prior to testing, samples were conditioned in a desiccator for at least 48 hours. All samples run were uncoated, the sample face was left in its natural form Figure 4.5 shows an uncoated sample.

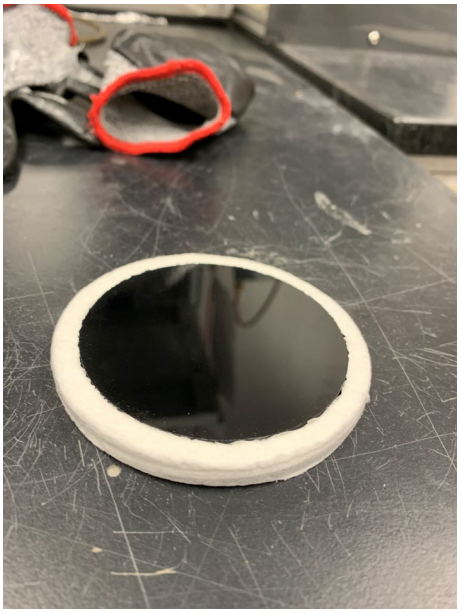

Figure 4.5: *CAPA II uncoated sample.*

4.2 Testing Procedures

The test matrix in Table 4.1 shows the array of tests conducted using the FPA, Cone Calorimeter, and CAPA II.

Table 4.1: Test Matrix for PMMA in the FPA, Cone Calorimeter, and CAPA II.

Heat Flux (kW m^{-2}) / **Sample Finish**	**Fire Propagation Apparatus**		**Cone Calorimeter**		**CAPA II**
	Coated	Uncoated	Coated	Uncoated	Uncoated
25	3	3	2	2	0
50	0	3	0	2	0
50 (Anaerobic Environment)	0	3	0	0	2

4.2.1 FPA Testing Procedure

Experiments using the FPA were conducted to collect data pertaining to mass loss rate (MLR). The heat fluxes used for testing was 25 kW m^{-2} and 50 kW m^{-2}. The sample was mounted to the sample support assembly on top of the Sartorius load cell. Experiment air for the ADC was set to 200 SLPM with reference temperature and pressure of 25°C and 1 atm.

Flaming ignition was obtained using a pilot flame ignitor, placed 10 mm above the sample face 60 seconds before exposure to the infrared lamps. The standard ASTM E2058 does not specify a length of time for pilot flame engagement before exposure to the infrared lamps [9]. The pilot flame was removed from this position after self-sustained flaming was verified. Samples were left to burn to extinction, which was verified by the absence of a visible flame. The times documented during the tests are

as follows: lamps power on, WCOS dropping exposing sample to heat, time to first visible ignition, time to full ignition of sample, extinguishment of sample.

For experiments in anaerobic environments, the pilot flame was not used. The heat flux used was 50 ± 0.20 kW m^{-2}. The experiment air was replaced with nitrogen and delivered at a flow rate of 185 SLPM with a reference temperature and pressure of 25 °C and 1.00 atm respectively. The times documented during the tests are as follows: lamps power on, WCOS dropping exposing sample to heat, and time to extinction when no material was visibly left in the sample holder.

The prepared samples were weighed, and a layer of 0.025 mm thick heavy duty aluminum foil was wrapped around the sample, leaving only the top surface face exposed. The sample was then placed into the sample dish and set onto the Sample support assembly for testing. Refer to appendix B for detail operating procedures outlining how to start up and run the FPA.

4.2.2 Cone Calorimeter Testing Procedure

Experiments using the cone calorimeter were conducted to collect data pertaining to MLR. Mass data collection and heat flux ranges used for testing were identical to the FPA.

Flaming ignition was obtained using an electric spark ignitor, placed in between the heater and sample face. The electric spark ignition was located 13 mm above the sample face vertically and in the center horizontally. The ignitor was put in place and turned on directly after the sample was mounted. The ignitor was removed from this position after self-sustained flaming was verified. Samples were left to burn to

extinction, which was verified by the absence of a visible flame. The times documented during the tests are as follows: sample mounted on load cell, time to ignition, time to extinguishment.

The prepared cone calorimeter samples were weighed, and a layer of 0.025 mm thick heavy duty aluminum foil was wrapped around the sample, leaving only the top surface face exposed. The sample was the placed-on top of its sample holder for testing.

4.2.3 CAPA II Testing Procedure

Experiments using the CAPA II were conducted to collect data pertaining to mass loss rate. The data pertaining to MLR was collected using a Sartorius Cubis load cell with a resolution of 0.001 g. Mass data was sampled at a frequency of 5Hz.

The heat flux used for testing was 52 ± 0.20 kW m^{-2}. The sample was mounted to the sample support assembly on top the Sartorius load cell. Experiment nitrogen for the gasification chamber was set to 185 SLPM with reference temperature and pressure of 25°C and 1 atm for the duration of the experiment.

The prepared CAPA II samples were weighed, and a layer of 0.025 mm thick heavy duty aluminum foil was wrapped around the sample, leaving only the top surface face exposed. The sample dish was lined with two layer of 6.35 mm thick ceramic insulation board on the back side of the sample. The sample was then placed into the sample dish and set onto the Sample support assembly for testing. Figure 4.6 shows the sample preparation for the CAPA II. For all FPA, cone calorimeter, and CAPA II test, the same ceramic fiber insulation board was used for sample back surface insulation.

Figure 4.6: *CAPA II Sample preparation.*

4.3 Results

Figure 4.7 shows the mass loss rate curves for the FPA and cone calorimeter at both 25 kW m^{-2} (a) and 50 kW m^{-2} (b). Both FPA test curves are an average of three tests. Both cone calorimeter curves are an average of two tests. MLR curves were constructed using the time derivative of the raw sample mass over 2.6 seconds. The uncertainty was calculated using the following equation

$$\sigma = \frac{2 \times MLRSD}{\sqrt{N}} \tag{5}$$

where MLRSD it the standard deviation of the mass loss rate, and N is the number of data points collected. The standard deviation was calculated by binning over 2.6 seconds for all tests run in each segment, before the average MLR was taken. The integral mass loss rate was calculated for each curve. The maximum percent error from measured initial sample mass to integral sample mass was 0.92 %.

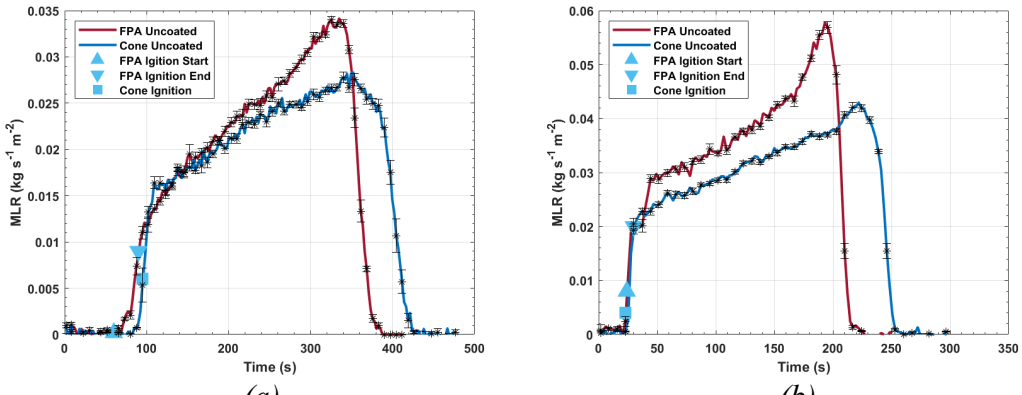

Figure 4.7: *FPA vs Cone Calorimeter, uncoated at 25 kW m^{-2} (a) and 50 kW m^{-2} (b) exposure.*

Despite the fact that the FPA and cone calorimeter tests were run at the same set incident heat flux, the MLR curves are not the same. There are inherent differences between the FPA and cone calorimeter tests that could lead to this discrepancy. It is estimated that the air flow around the sample in the FPA is 0.18 m s^{-1} based on combustion chamber air flow rate and cross-sectional area. In the cone calorimeter it is estimated at 0.17 m s^{-1} based on exhaust duct flow rate (0.035 m s^{-3}) and combustion zone cross-sectional area (458 mm x 458 mm).

The radiation spatial distribution from the heaters onto the sample is different between the FPA and cone calorimeter. In general, the heat flux is on average 4% greater at the edges of the circular FPA sample when compared to the center as discussed in Chapter 3. In addition, the heat flux will drift over the duration of a test. This means that a test run where the initial center heat flux is 50 kW m^{-2} will have an average initial heat flux across the sample surface of 52 kW m^{-2}. By the end of an experiment, the heat flux will have drifted upwards to an average of 53 kW m^{-2} across the sample surface. In the cone calorimeter, the heat flux is on average 5% lower at the edges of the square sample when compared to the center [13]. This means that a test run with the initial center heat flux at 50 kW m^{-2} will have an average heat flux of 47.5 kW m^{-2} across the sample surface.

The radiation spectral makeup of the FPA infrared lamps and cone calorimeter conical heater are different. Both the FPA and cone calorimeter heating sources can be considered gray bodies. On average, the cone calorimeter conical heater is 750°C and the FPA infrared lamp temperature is 2200°C [20]. The mean radiation wavelength in the FPA infrared lamps is significantly shorter than that of the cone calorimeter.

The FPA has a flaming ignitor for sample ignition, while the cone uses an electric spark ignitor. The FPA ignitor is located closer to the sample vertically than the cone, and it is possible the heat from the ignitor contributes to heat flux seen by the sample surface. With an electrical spark ignitor, this is not seen in the cone calorimeter.

Sample geometry is also different between the FPA and cone calorimeter. The FPA maintains a circular sample with a diameter of 96.40 mm where the cone calorimeter has a square sample with a size of 100 mm by 100 mm. The flame shape between the two geometries are somewhat different, which may lead to variations in flame heat feed back to the sample.

In the FPA a gradual ignition is observed at 25 kW m^{-2}. This first ignition point originates at the pilot flame location and spreads to the surrounding sample. In the FPA, the first ignition event happens at 60 seconds after exposure with complete sample ignition occurring at 90 seconds after exposure. Ignition originates at the edges of the sample and propagates inward to the center. In the cone calorimeter, ignition occurred 95 seconds after exposure. Cone calorimeter sample ignition happens almost instantaneously without time delays or noticeable flame spread. The FPA complete ignition occurs 5 seconds earlier than the cone calorimeter. This can be attributed to the nonuniformity of the heat flux seen by the FPA and cone calorimeter, as well as the contribution of the FPA pilot flame located near the sample edge. At 50 kW m^{-2}, the difference in sample ignition times between the FPA and cone calorimeter becomes less significant. In the FPA, the first ignition event happens at 23 seconds post exposure, with complete sample ignition occurring 6 seconds later. In the cone calorimeter, ignition occurred 23 seconds after exposure.

During the burning phase of the test, the observed MLR is systematically higher in the FPA than the cone calorimeter for both 25 kW m^{-2} and 50 kW m^{-2}. The MLR disagreement is larger at 50 kW m^{-2} than 25 kW m^{-2}. The primary reasons for the disagreement at 50 kW m^{-2} are thought to be the spatial non-uniformity of the heat flux at the sample surface and the spectral differences of the radiation sources. On average, the FPA heat flux is 10% higher than the cone calorimeter when accounting for both FPA and cone calorimeter spatial differences. In addition, the spectral makeup of the FPA promotes more in-depth absorption thus increasing the fraction of radiation absorbed by the sample with respect to the sample in the cone.

The faster time to ignition of the FPA to cone calorimeter at 25 kW m^{-2} is not believed to be caused by the differences in the spectral makeup of the heater radiation, but rather by the spatial non-uniformity of the incident heat flux. To check this hypothesis, samples were coated using high emissivity paint as discussed in section 4.1. Experiments were repeated with three tests run for the FPA and two for the cone calorimeter. Under these conditions, up to the point of ignition, the paint will maintain its optical properties, meaning the sample surface in both the FPA and cone calorimeter will have identical surface optical properties up to the point of ignition. Figure 4.8 shows FPA and cone calorimeter MLR curves for both coated and uncoated samples. As seen in the figure, the ignition points for coated samples did not converge closer to each other, rather the FPA was advanced, and the cone calorimeter was delayed. This supports the hypothesis that radiation spectral makeup is not the driving cause of the difference in ignition times, rather the differences in spatial nonuniformity of the heat flux across the sample surface and the additional heat flux of the FPA pilot flame are

likely responsible for the earlier ignition of uncoated samples in the FPA when compared to the cone calorimeter at 25 kW m^{-2}.

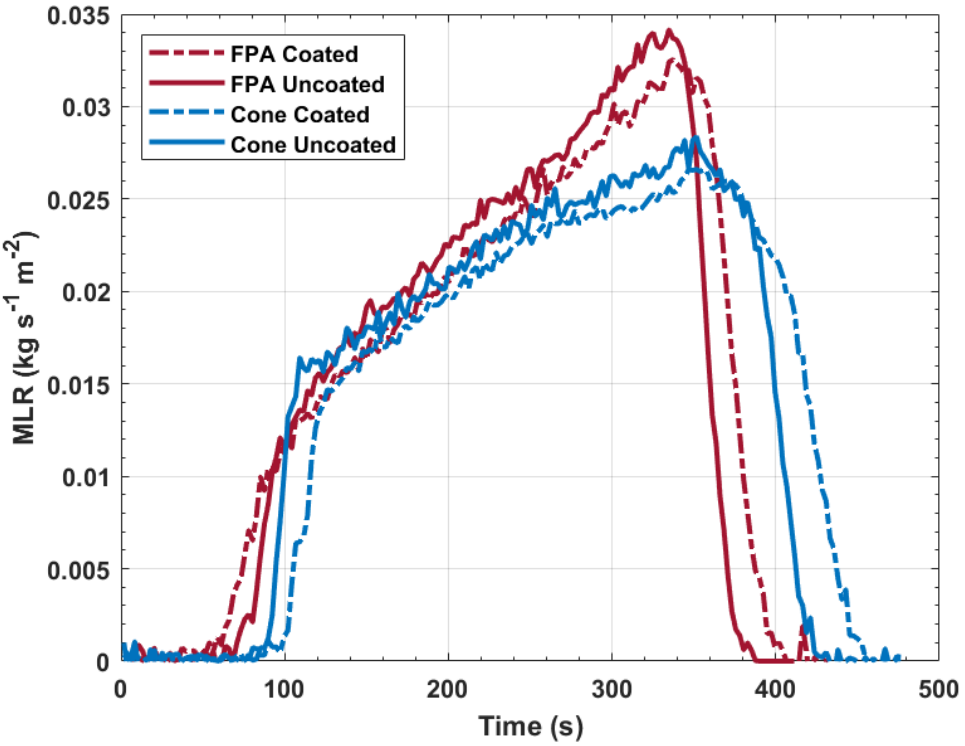

Figure 4.8: *FPA vs Cone Calorimeter, uncoated vs coated at 25 kW m^{-2} exposure.*

To further investigate the possible impact of the spectral radiation make up on the observed MLR, tests were run in an anerobic environment in both the FPA and CAPA II. Nitrogen was delivered at a flow rate of 185 SLPM in both setups. To account for heat flux drift and nonuniformity in the FPA, the heat flux in the CAPA II was set to 52 kW m^{-2}. The FPA remained at an initial center heat flux reading of 50 kW m^{-2}. Three tests were run in the FPA with nitrogen, and two tests were run in the CAPA II. The MLR curves and error bars are calculated in the same manner as previously discussed.

Figure 4.9 shows the FPA and CAPA II test results. The MLR curves are similar in nature, but systematic differences are still present. CAPA II onset of mass loss rate is systematically earlier than the FPA. The average MLR during steady gasification is systematically lower in the CAPA II than the FPA. Both of these differences can be explained by the differences in the spectral makeup of the radiation sources. The FPA's lower average wavelength radiation is thought to penetrate deeper into the sample and cause delayed mass loss onset and higher average MLR.

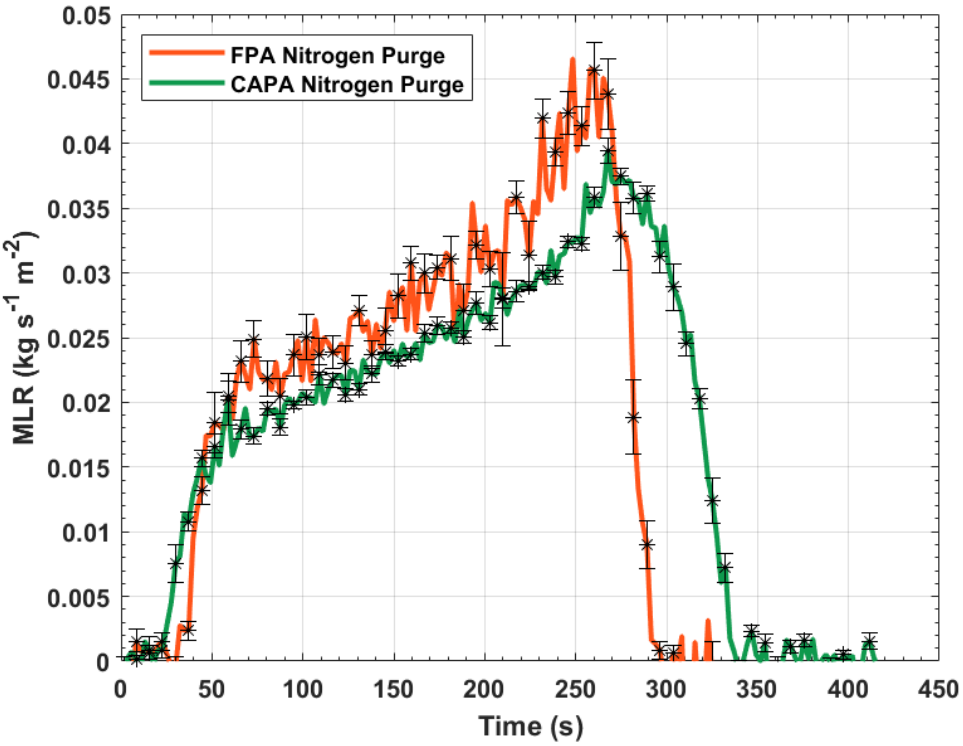

Figure 4.9: *FPA vs CAPA II, uncoated 50 kW m^{-2} exposure.*

Chapter 5: Conclusions and Future Work

This study presented the redesign of the Fire Propagation Apparatus. The redesigned parts include the Frame Structure, Combustion Air Distribution System, Upper Quartz Tube Adapter, Water Cooled Outer Shield, Load Cell System, Sample Support Assembly, and Heat Flux Gauge Mount. New systems, such as the Internal Attachment Mounting System, pilot flame controls, and Diagnostic Equipment were developed and added to the apparatus. The redesigned parts and newly developed systems have improved manufacturability, maintainability, and end user operations. The Combustion Air Distribution System is manufacturable on a more universal basis due to its one-piece aluminum construction. Supporting amenities of the sample holder and heat flux gauge mount are quickly exchangeable for one another due to the addition of the Internal Attachment Mounting System. The Water-Cooled Outer Shield can withstand higher heat fluxes for prolonged durations due to it stainless steel construction and insulation wrapping. The measurement resolution was increased with an upgraded load cell and improved vibration isolation. The Fire Propagation Apparatus redesign was conducted to allow for future growth of the apparatus, while maintaining robustness to prevent operational failure.

A comparative study of flaming and non-flaming poly(methyl methacrylate) was performed using the Fire Propagation Apparatus in oxidized and anerobic environments. The Fire Propagation Apparatus produced systematically higher mass loss rates when compared to the come calorimeter and Controlled Atmosphere Pyrolysis Apparatus II. Additionally, the Fire Propagation Apparatus produced sample

ignition propagation from the sample outer edge to the center. A more detailed comparative analysis of the Fire Propagation Apparatus, cone calorimeter, and Controlled Atmosphere Pyrolysis Apparatus II tests using multiple materials and modeling is necessary to fully understand and explain observed discrepancies between the results of these test methods.

The future work will be focused on designing and installing the fire effluent analysis system similar to the setup described in ASTM E2058. Additionally, an expanded test matrix, including additional polymers, will be used to further characterize the FPA and allow for a better understanding of the apparatus and how it compares to the cone calorimeter and CAPA II.

Appendices

A: FPA CAD Drawing

Note: Dimensions are provided in both standard and metric units in the following format:

inches
[millimeters]

A.1 Frame Structure

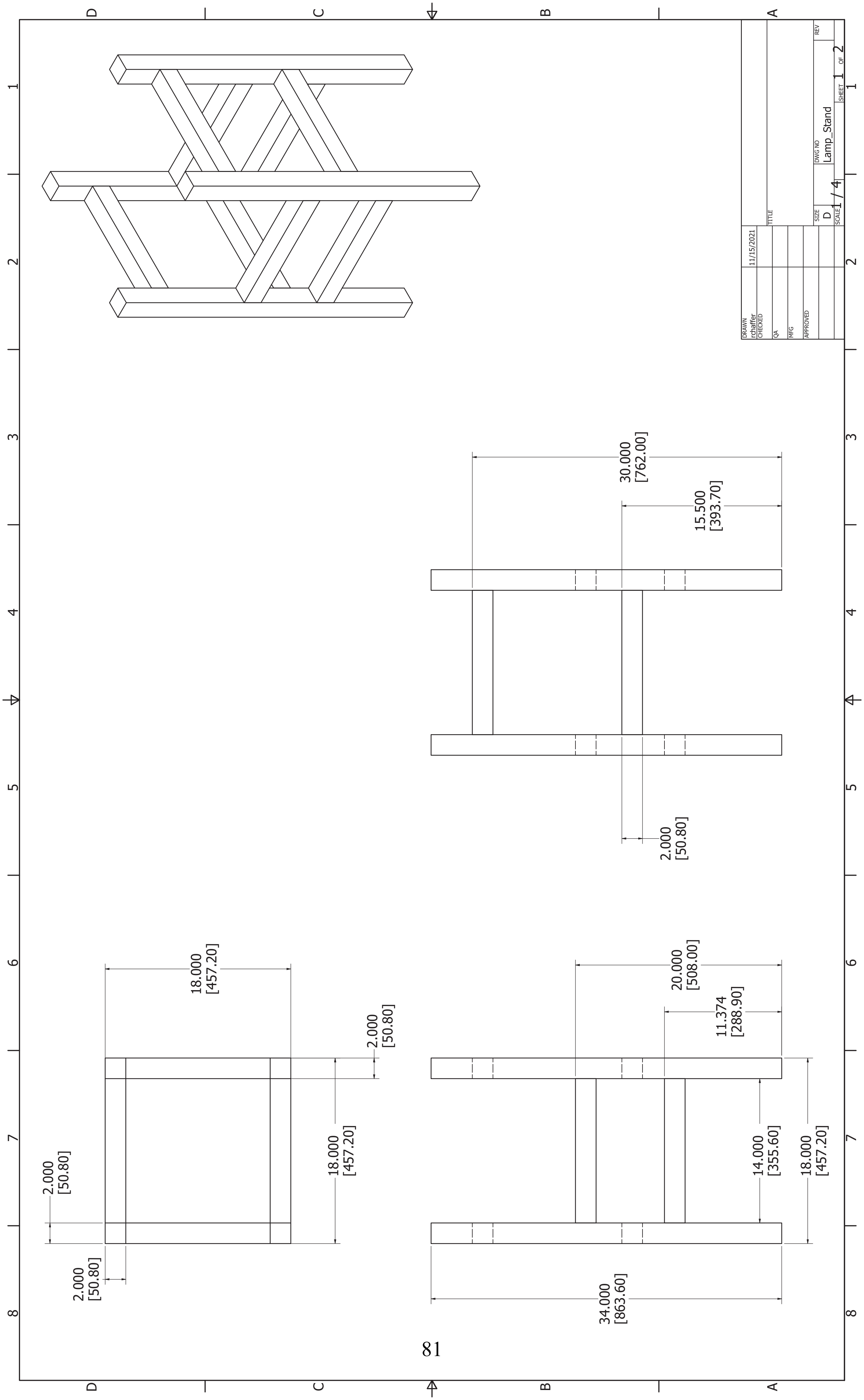
DRAWN
rchaffer
11/15/2021
CHECKED
QA
MFG
APPROVED
TITLE
SIZE
D
DWG NO
Lamp_Stand
REV
SCALE 1 / 4
SHEET 1 OF 2
30.000 [762.00]
15.500 [393.70]
2.000 [50.80]
20.000 [508.00]
11.374 [288.90]
14.000 [355.60]
18.000 [457.20]
34.000 [863.60]
18.000 [457.20]
2.000 [50.80]
18.000 [457.20]
2.000 [50.80]
2.000 [50.80]
A B C D
1 2 3 4 5 6 7 8

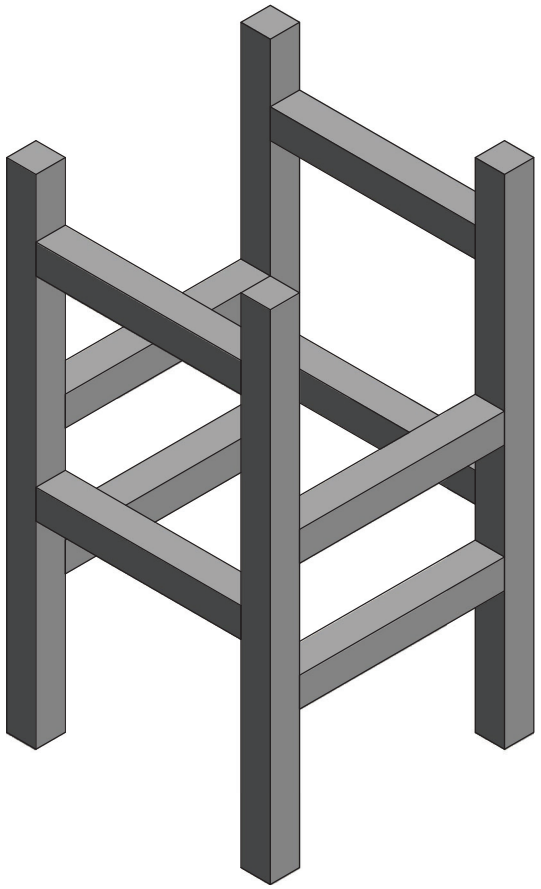

DRAWN	rchaffer	11/15/2021
CHECKED		
QA		
MFG		
APPROVED		

TITLE

SIZE D | DWG NO Lamp_Stand | REV

SCALE 1/3 | SHEET 2 OF 2

82

A.2 Infrared Lamp Mounting Brackets

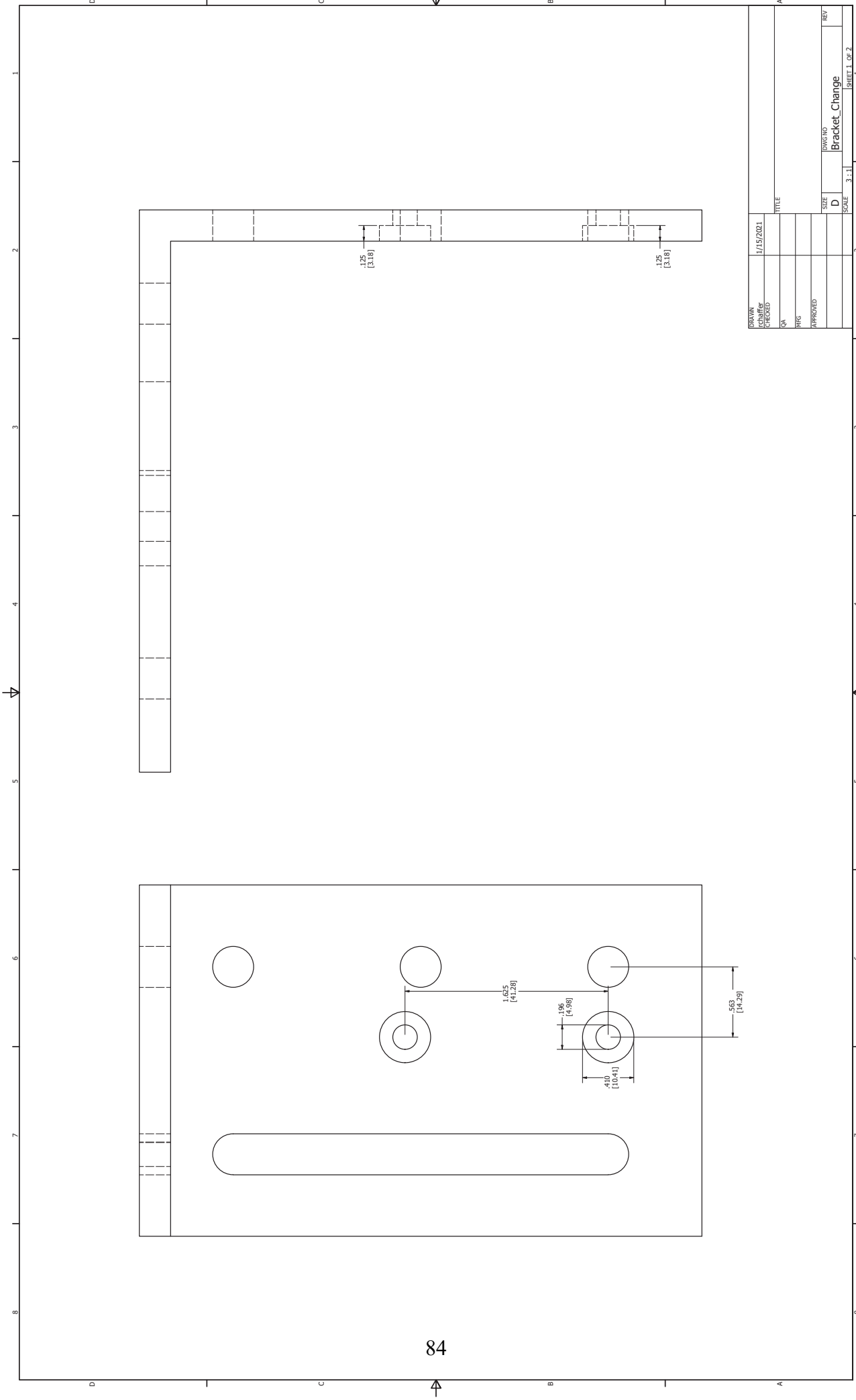
.125
[3.18]
.125
[3.18]
1.625
[41.28]
.196
[4.98]
.563
[14.29]
.410
[10.41]
DRAWN
rchaffer
1/15/2021
CHECKED
QA
MFG
APPROVED
TITLE
SIZE
D
DWG NO
Bracket_Change
REV
SCALE
3 : 1
SHEET 1 OF 2

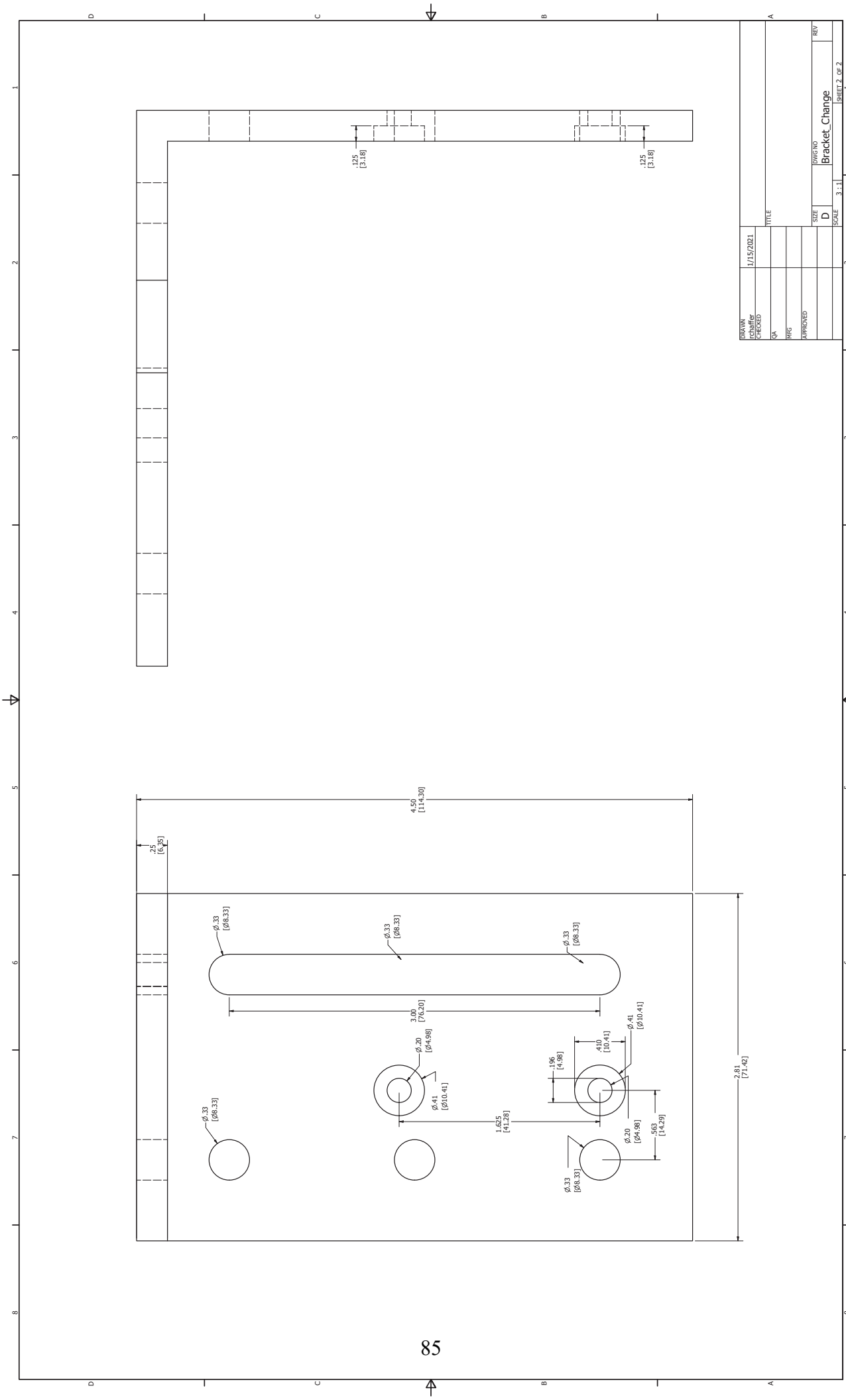
.125
[3.18]
.125
[3.18]
4.50
[114.30]
.25
[6.35]
Ø.33
[Ø8.33]
Ø.33
[Ø8.33]
Ø.33
[Ø8.33]
3.00
[76.20]
Ø.20
[Ø4.98]
Ø.41
[Ø10.41]
.410
[10.41]
Ø.41
[Ø10.41]
.196
[4.98]
Ø.33
[Ø8.33]
1.625
[41.28]
Ø.20
[Ø4.98]
.563
[14.29]
Ø.33
[Ø8.33]
2.81
[71.42]
DRAWN
rchaffer
1/15/2021
CHECKED
QA
MFG
APPROVED
TITLE
SIZE
D
DWG NO
Bracket_Change
REV
SCALE
3 : 1
SHEET 2 OF 2

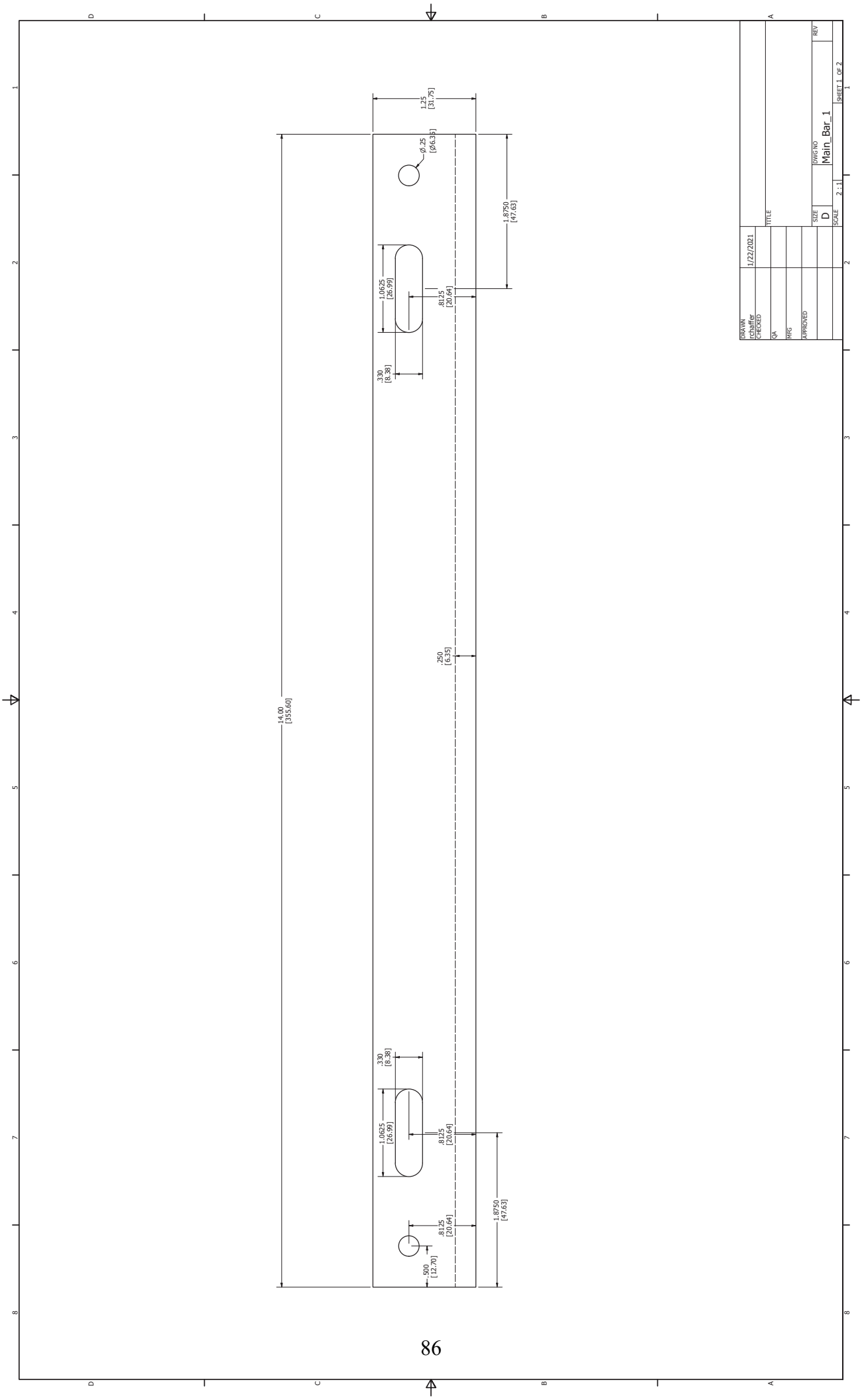
1.25
[31.75]
Ø.25
[Ø6.35]
1.8750
[47.63]
1.0625
[26.99]
.8125
[20.64]
.330
[8.38]
.250
[6.35]
14.00
[355.60]
.330
[8.38]
1.0625
[26.99]
.8125
[20.64]
1.8750
[47.63]
.8125
[20.64]
.500
[12.70]
DRAWN
rchaffer
1/22/2021
CHECKED
QA
MFG
APPROVED
TITLE
SIZE
D
DWG NO
Main_Bar_1
REV
SCALE
2 : 1
SHEET 1 OF 2

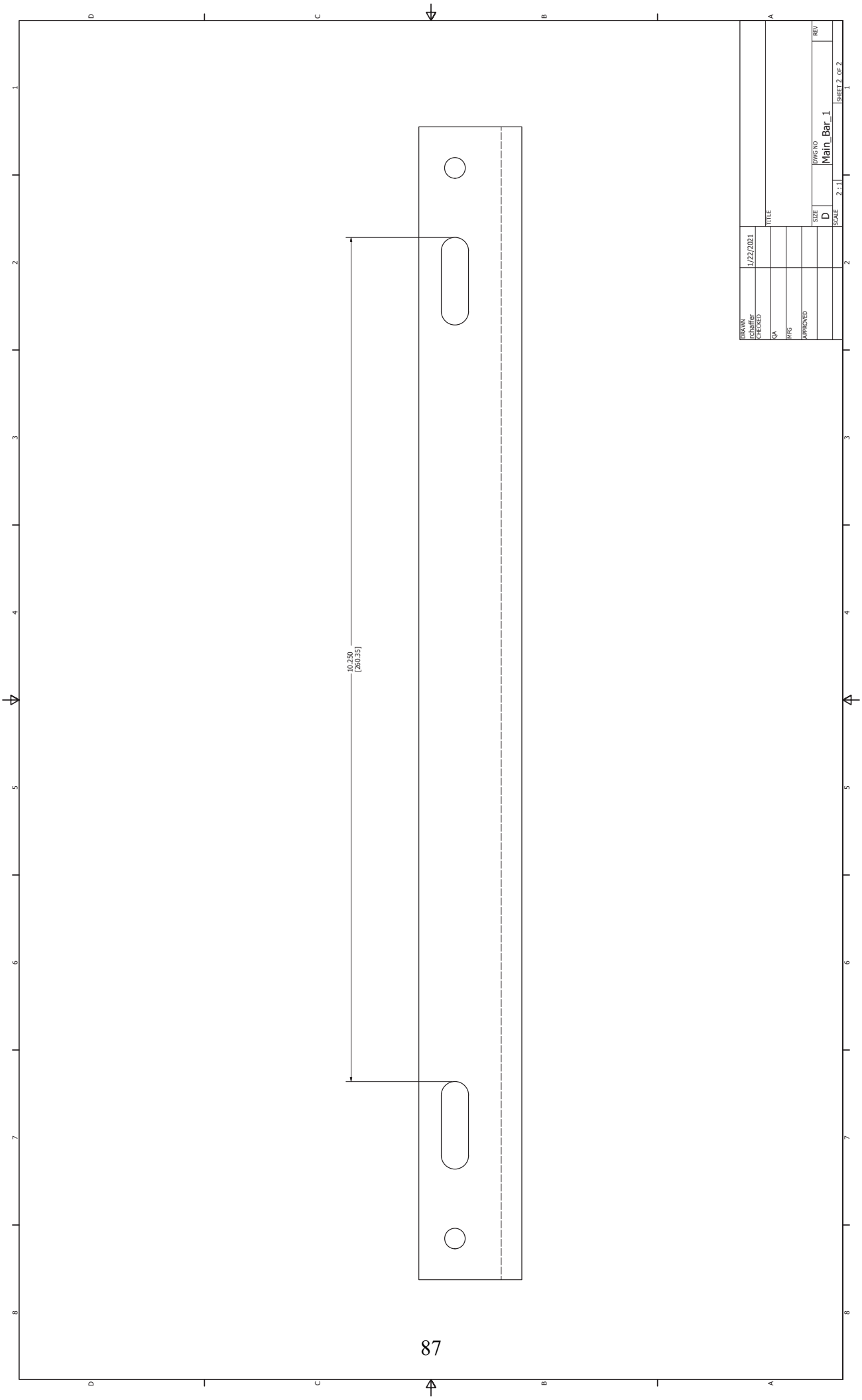
10.250
[260.35]
DRAWN
rchaffer
1/22/2021
CHECKED
QA
MFG
APPROVED
TITLE
SIZE
D
DWG NO
Main_Bar_1
REV
SCALE
2 : 11
SHEET 2 OF 2

A.3 Combustion Air Distribution System Base Mounting Plate

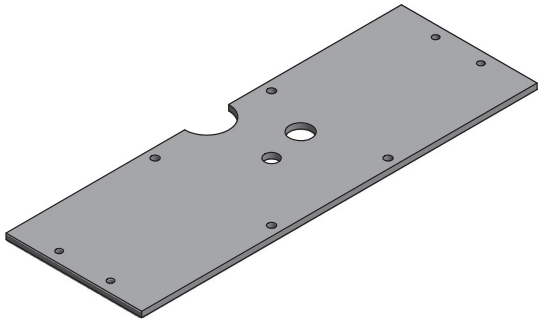

DRAWN rchaffer	1/13/2021		
CHECKED		TITLE	
QA			
MFG			
APPROVED			
		SIZE D	DWG NO Base Plate REV
		SCALE 1 / 2	SHEET 1 OF 4

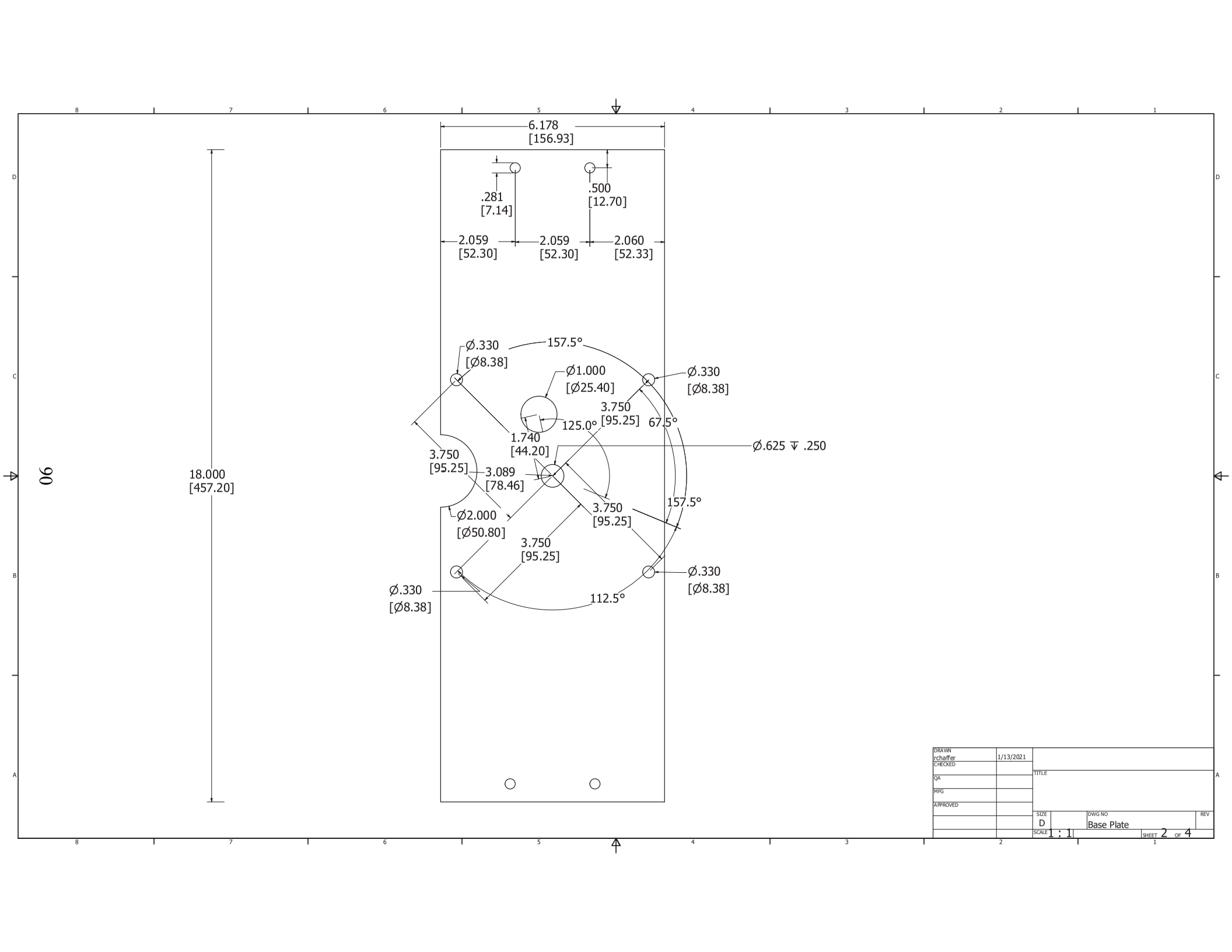
6.178
[156.93]
.281
[7.14]
.500
[12.70]
2.059
[52.30]
2.059
[52.30]
2.060
[52.33]
18.000
[457.20]
Ø.330
[Ø8.38]
157.5°
Ø1.000
[Ø25.40]
Ø.330
[Ø8.38]
3.750
[95.25]
67.5°
125.0°
1.740
[44.20]
Ø.625 ↧ .250
3.750
[95.25]
3.089
[78.46]
3.750
[95.25]
157.5°
Ø2.000
[Ø50.80]
3.750
[95.25]
Ø.330
[Ø8.38]
Ø.330
[Ø8.38]
112.5°
90
DRAWN
rchaffer
1/13/2021
CHECKED
QA
MFG
APPROVED
TITLE
SIZE
D
DWG NO
Base Plate
REV
SCALE 1 : 1
SHEET 2 OF 4

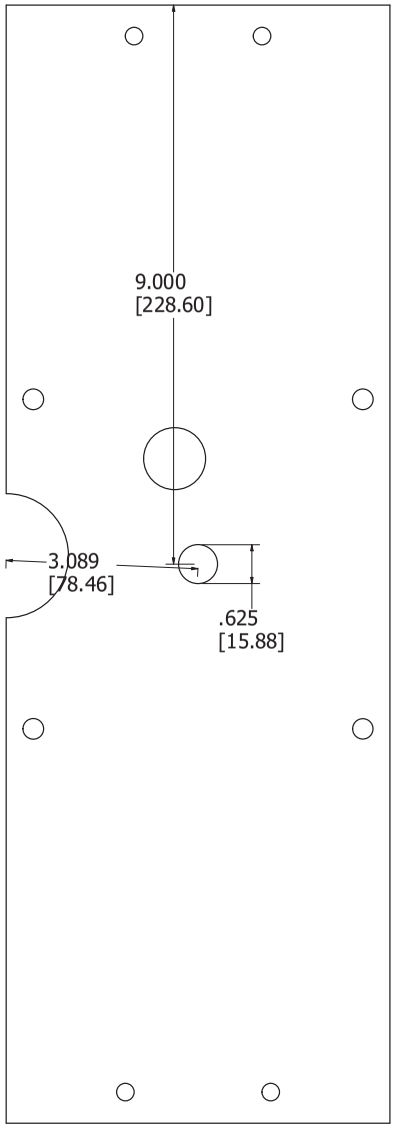

DRAWN rchaffer	1/13/2021		
CHECKED		TITLE	
QA			
MFG			
APPROVED			
		SIZE D	DWG NO Base Plate REV
		SCALE 1 : 1	SHEET 3 OF 4

91

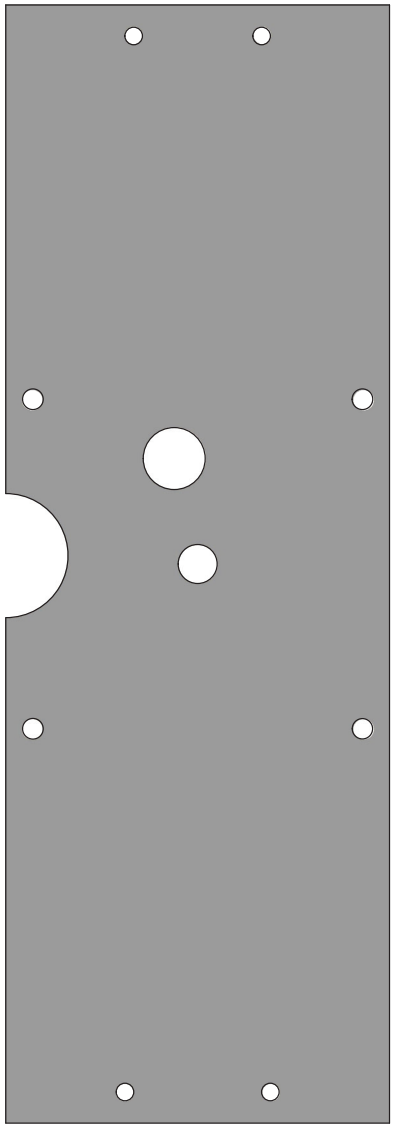

92

DRAWN rchaffer	1/13/2021		
CHECKED		TITLE	
QA			
MFG			
APPROVED			
		SIZE D	DWG NO Base Plate REV
		SCALE 1 : 1	SHEET 4 OF 4

A.4 Combustion Air Distribution System

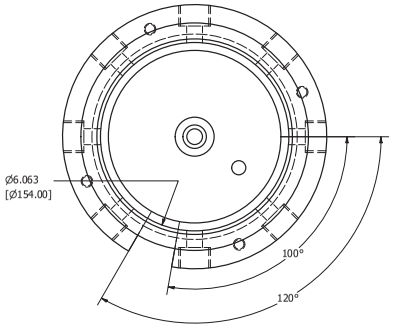

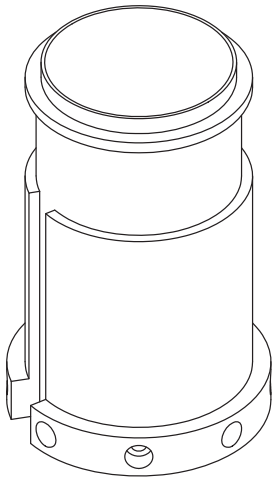

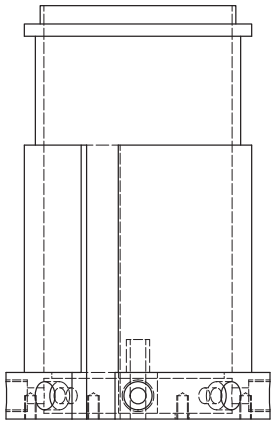

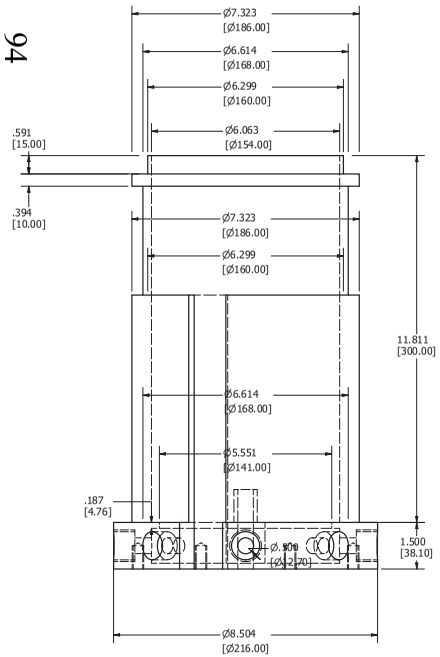

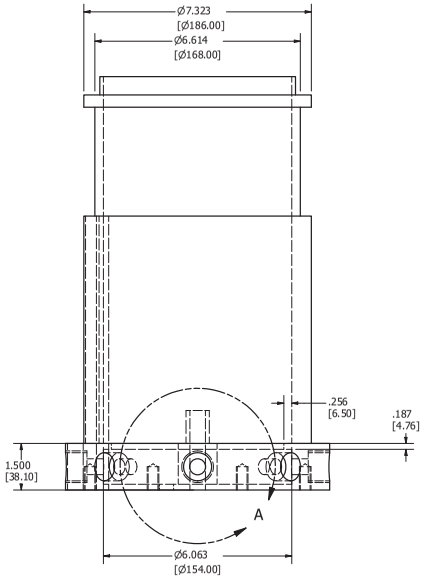

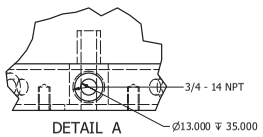

DETAIL A
SCALE 1 / 2

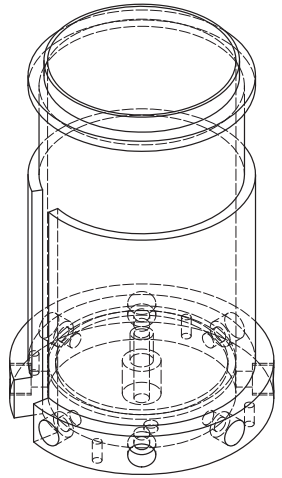

DRAWN rchaffer	8/26/2020	Material: Aluminum
CHECKED		TITLE
QA 1		
MFG		
APPROVED		
Units: inches [mm]		SIZE D / DWG NO Air_DIST_Final / REV
		SCALE 1 / 2 / SHEET 1 OF 13

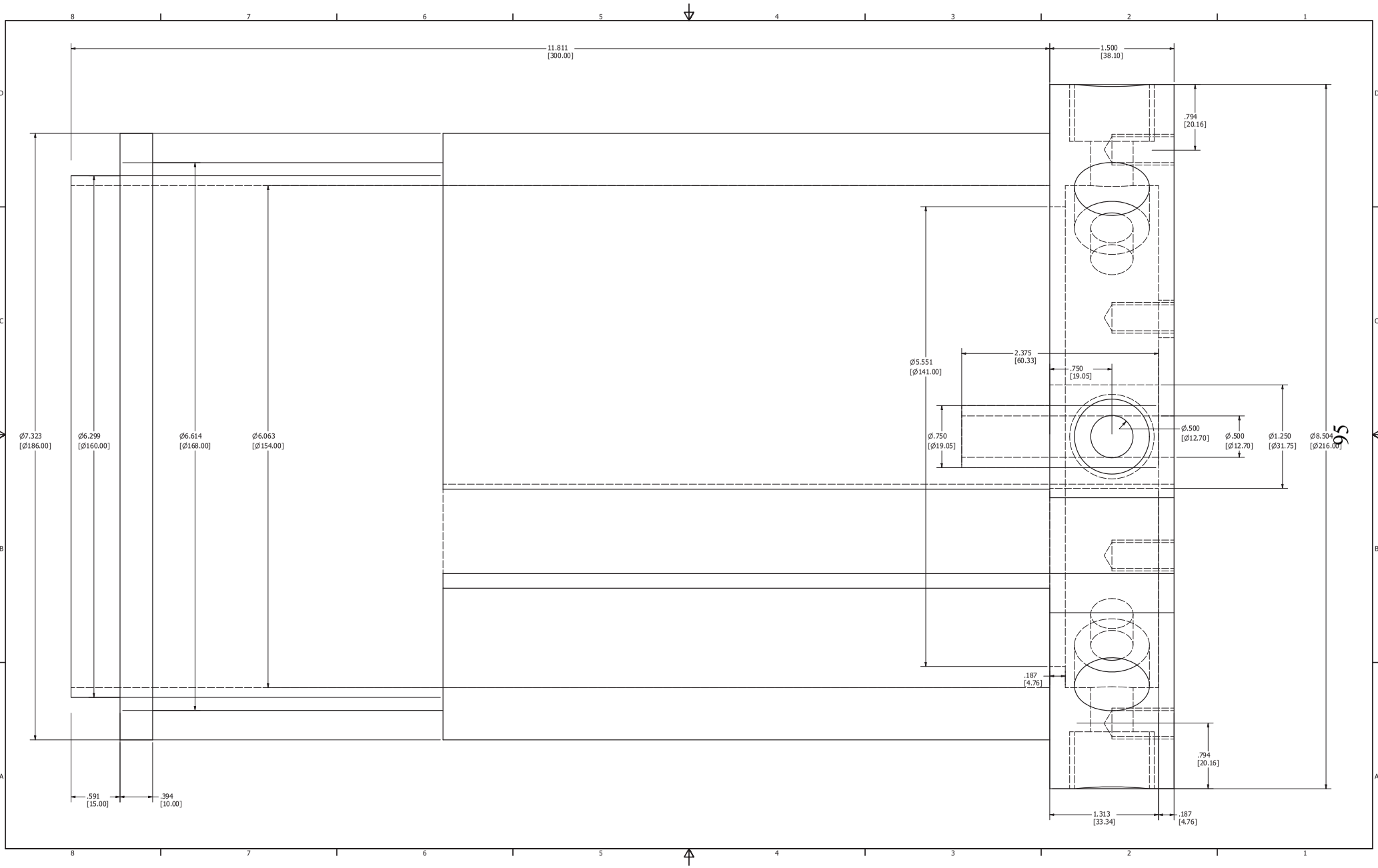
11.811
[300.00]
1.500
[38.10]
.794
[20.16]
Ø5.551
[Ø141.00]
2.375
[60.33]
.750
[19.05]
Ø.750
[Ø19.05]
Ø.500
[Ø12.70]
Ø.500
[Ø12.70]
Ø1.250
[Ø31.75]
Ø8.504
[Ø216.00]
Ø7.323
[Ø186.00]
Ø6.299
[Ø160.00]
Ø6.614
[Ø168.00]
Ø6.063
[Ø154.00]
.187
[4.76]
.794
[20.16]
.591
[15.00]
.394
[10.00]
1.313
[33.34]
.187
[4.76]
95

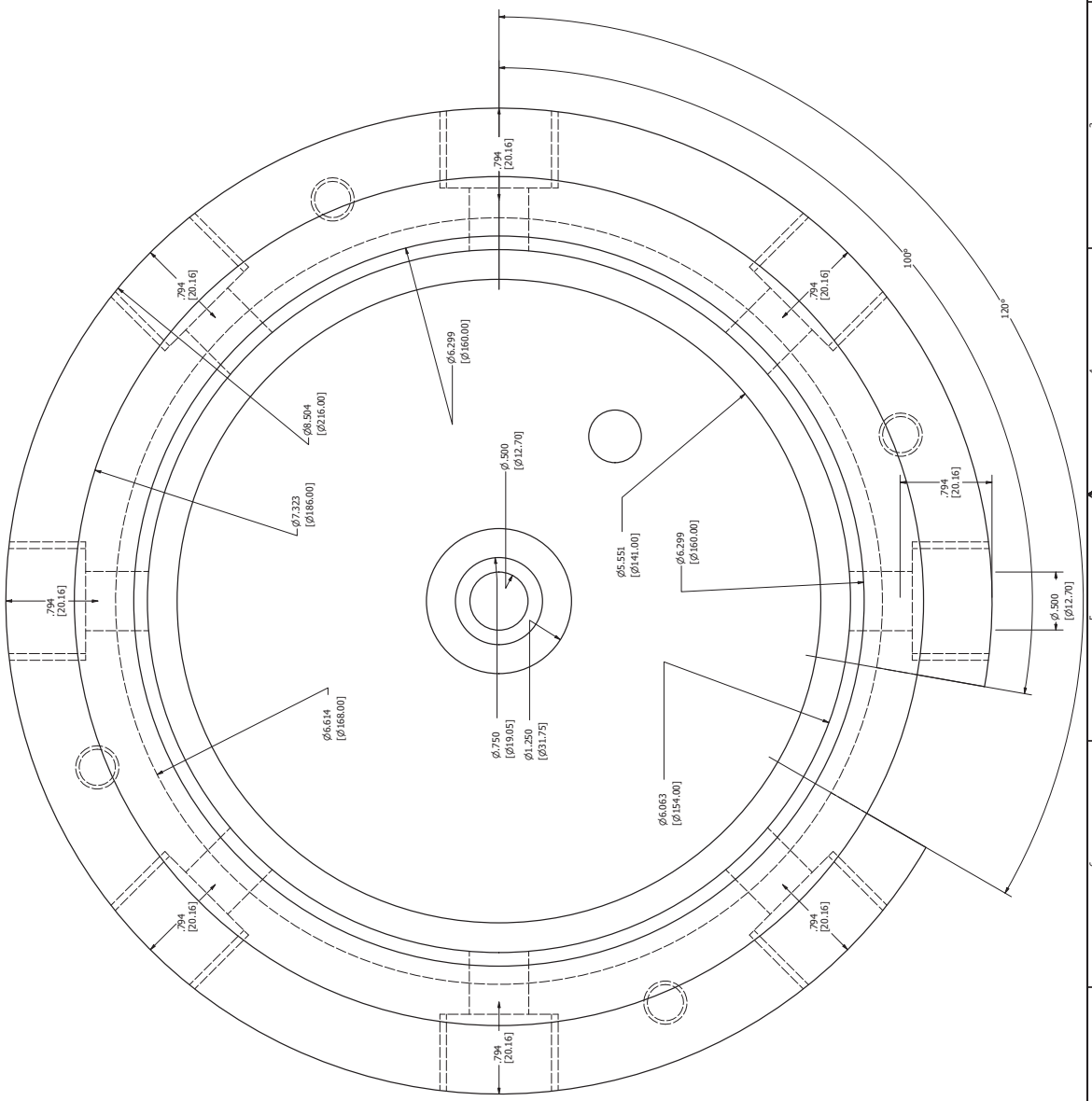
.794 [20.16]
.794 [20.16]
.794 [20.16]
.794 [20.16]
.794 [20.16]
.794 [20.16]
.794 [20.16]
Ø6.299 [Ø160.00]
Ø6.504 [Ø216.00]
Ø7.323 [Ø186.00]
Ø6.614 [Ø168.00]
Ø.500 [Ø12.70]
Ø.750 [Ø19.05]
Ø1.250 [Ø31.75]
Ø5.551 [Ø141.00]
Ø6.299 [Ø160.00]
Ø6.063 [Ø154.00]
Ø.500 [Ø12.70]
100°
120°

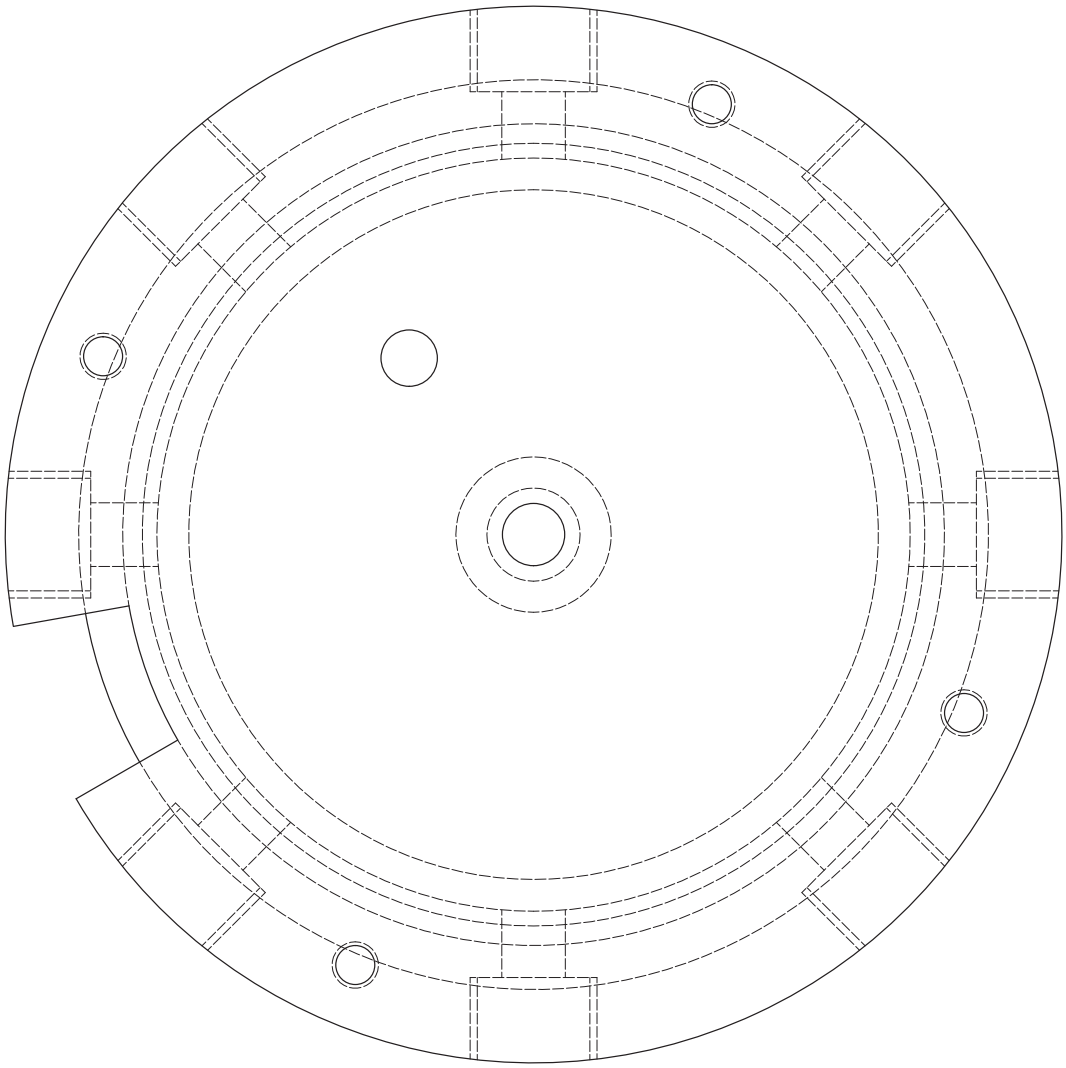

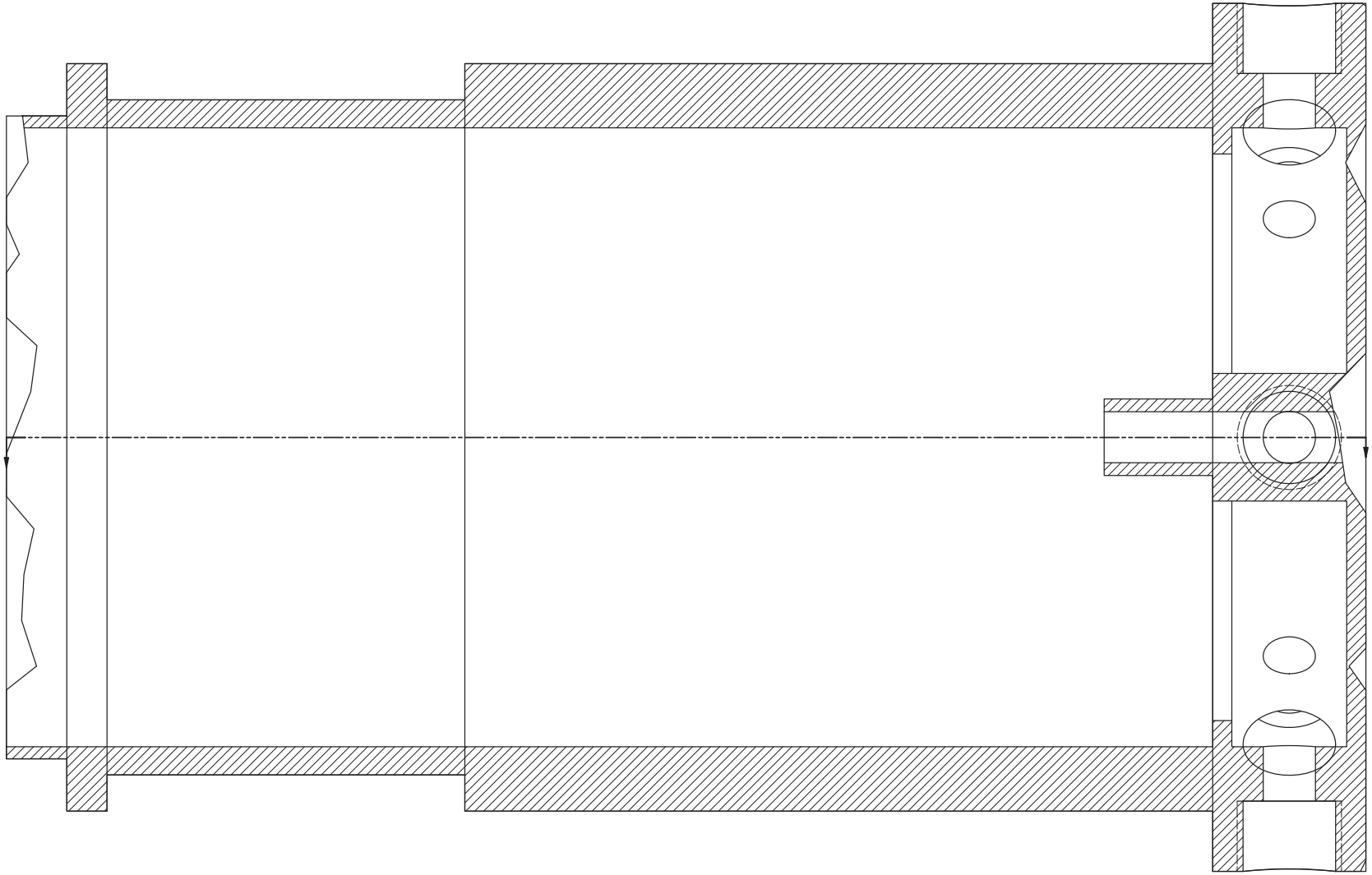

SECTION B-B
SCALE 2 : 1

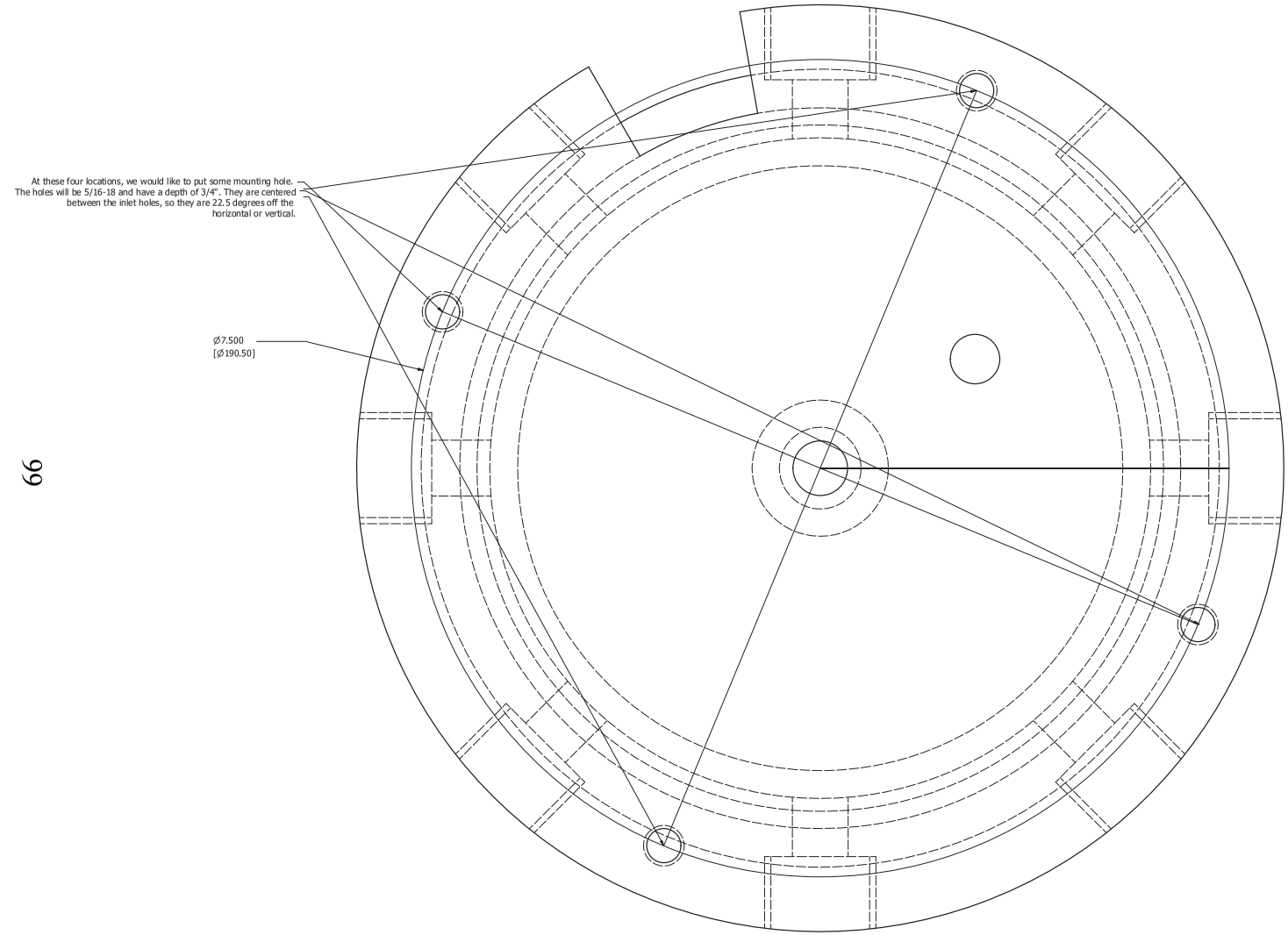
At these four locations, we would like to put some mounting hole. The holes will be 5/16-18 and have a depth of 3/4". They are centered between the inlet holes, so they are 22.5 degrees off the horizontal or vertical.
Ø7.500
[Ø190.50]

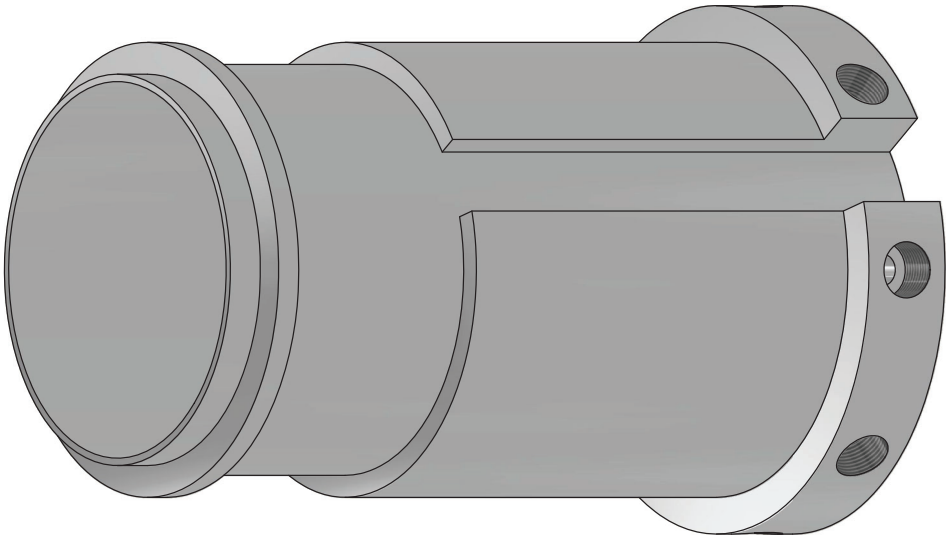

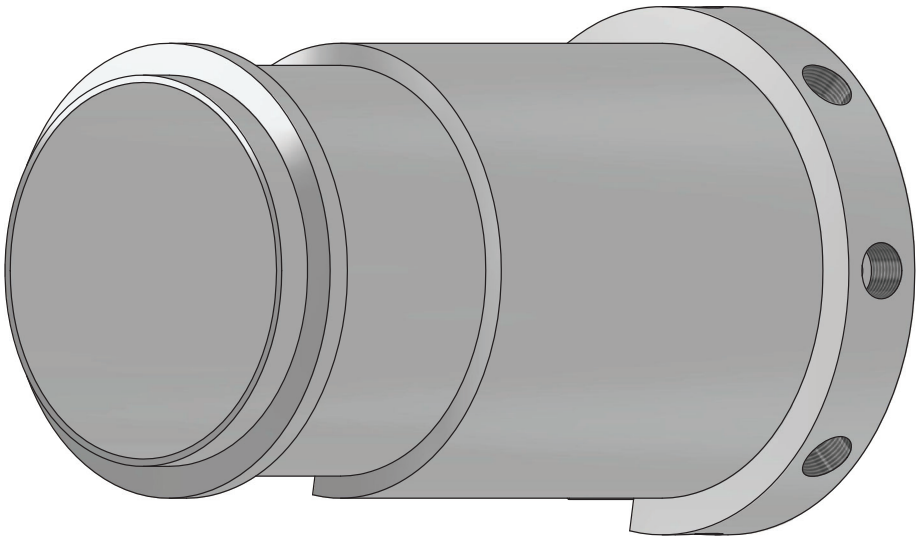

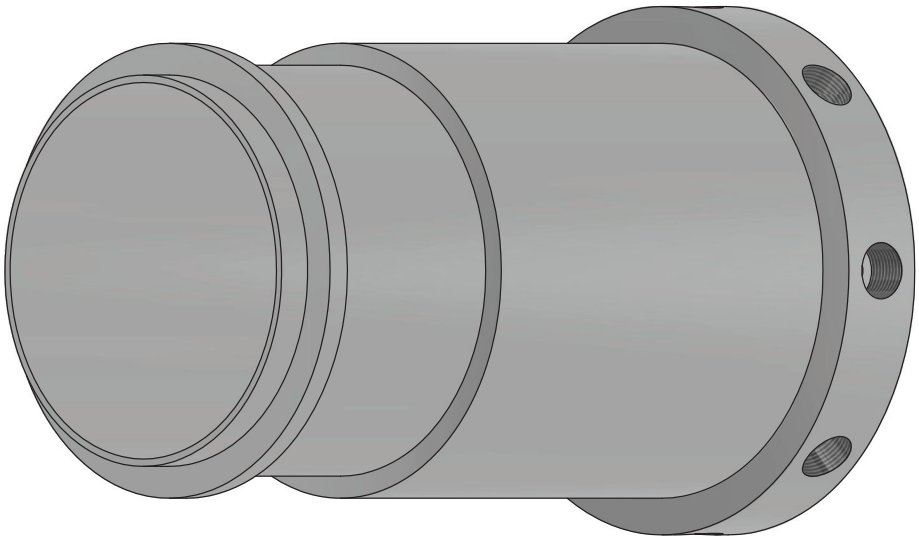

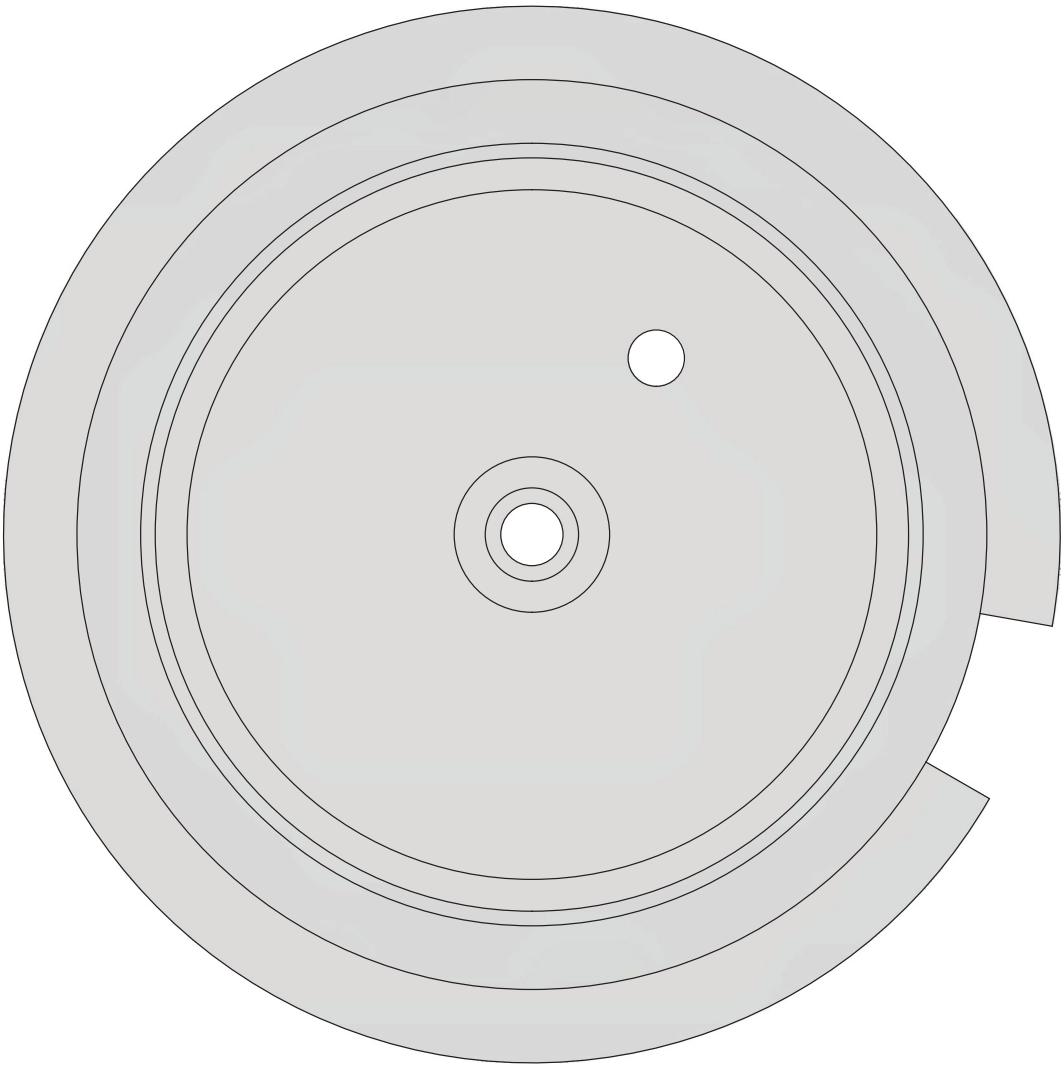

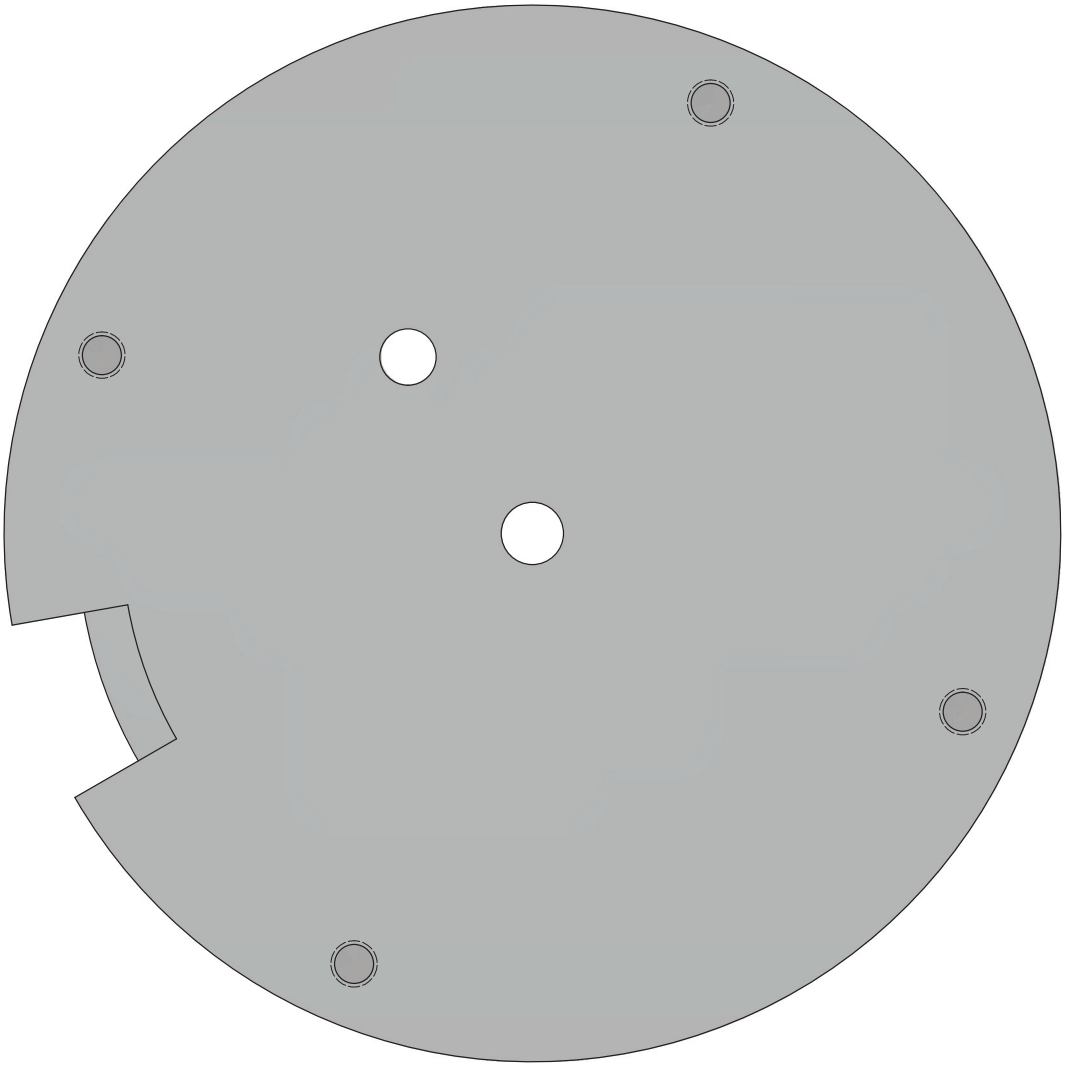

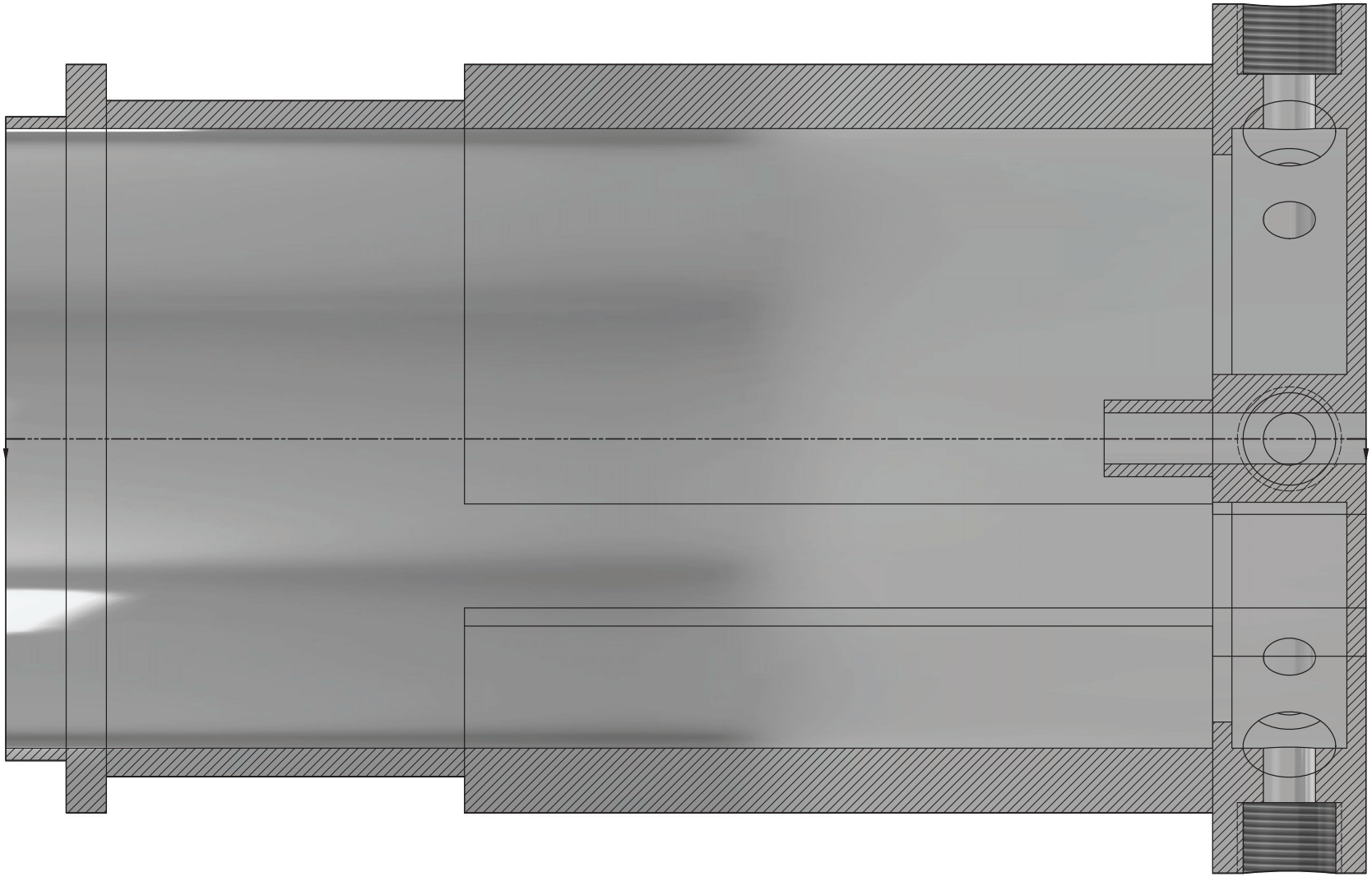

SECTION G-G
SCALE 2 : 1

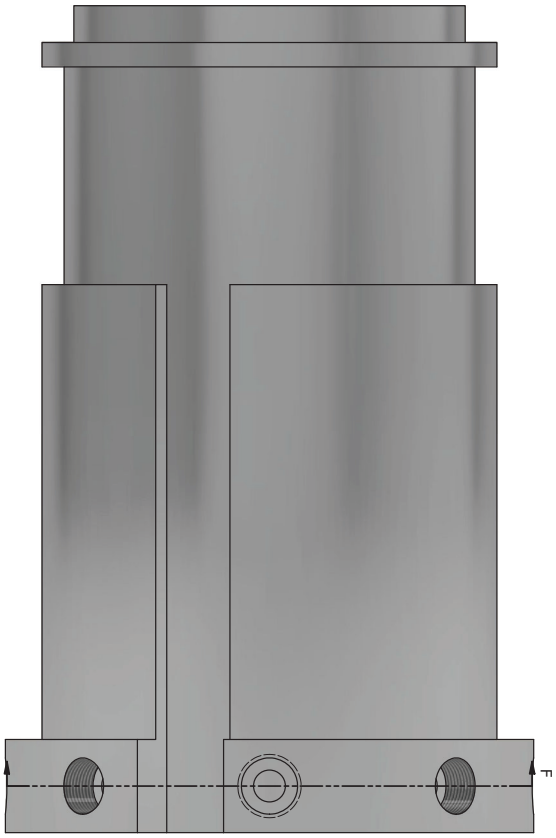

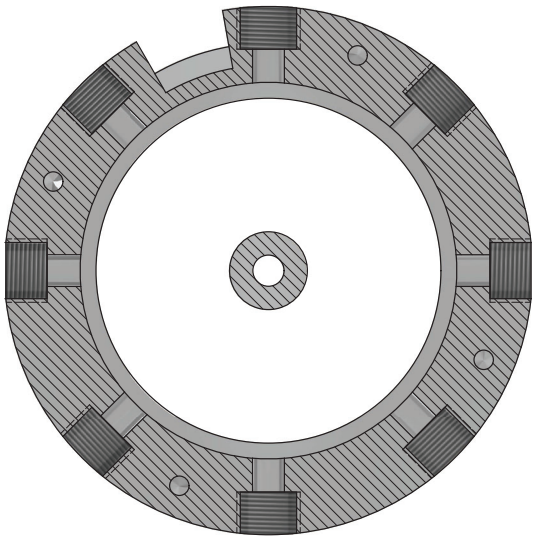

SECTION F-F
SCALE 1 : 1

A.5 Quartz Tube Adapter

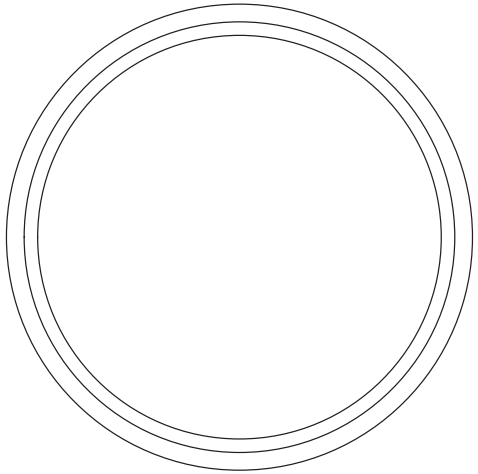

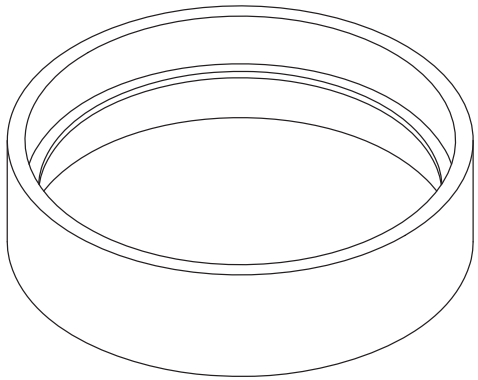

108

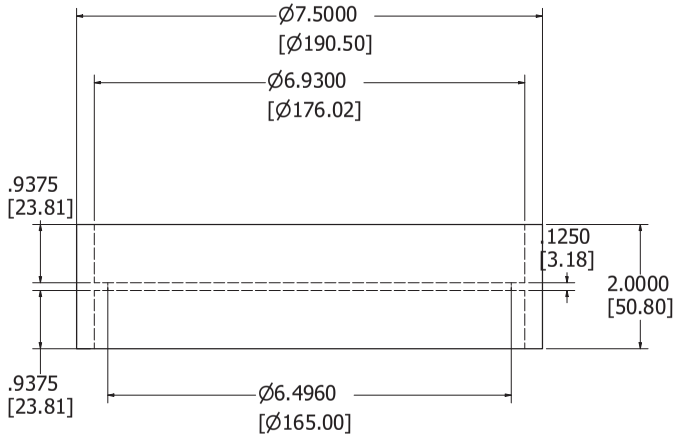

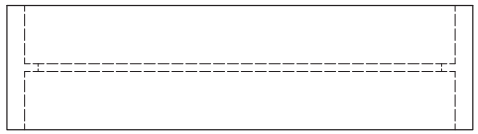

DRAWN rchaffer	6/14/2021		
CHECKED			
QA 1		TITLE Material: Aluminum	
MFG			
APPROVED			
		SIZE D / DWG NO Tube_Adapter / REV	
		SCALE 1 : 1 / SHEET 1 OF 3	

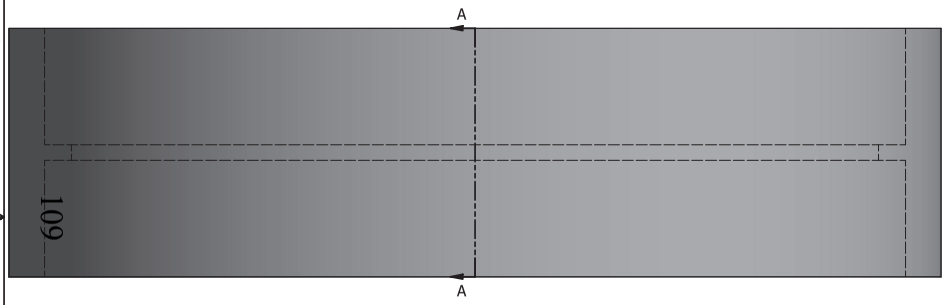

SECTION A-A
SCALE 2 : 1

DRAWN rchaffer	6/14/2021		
CHECKED		TITLE	
QA			
MFG			
APPROVED			
		SIZE D	DWG NO Tube_Adapter REV
		SCALE 2 : 1	SHEET 2 OF 3

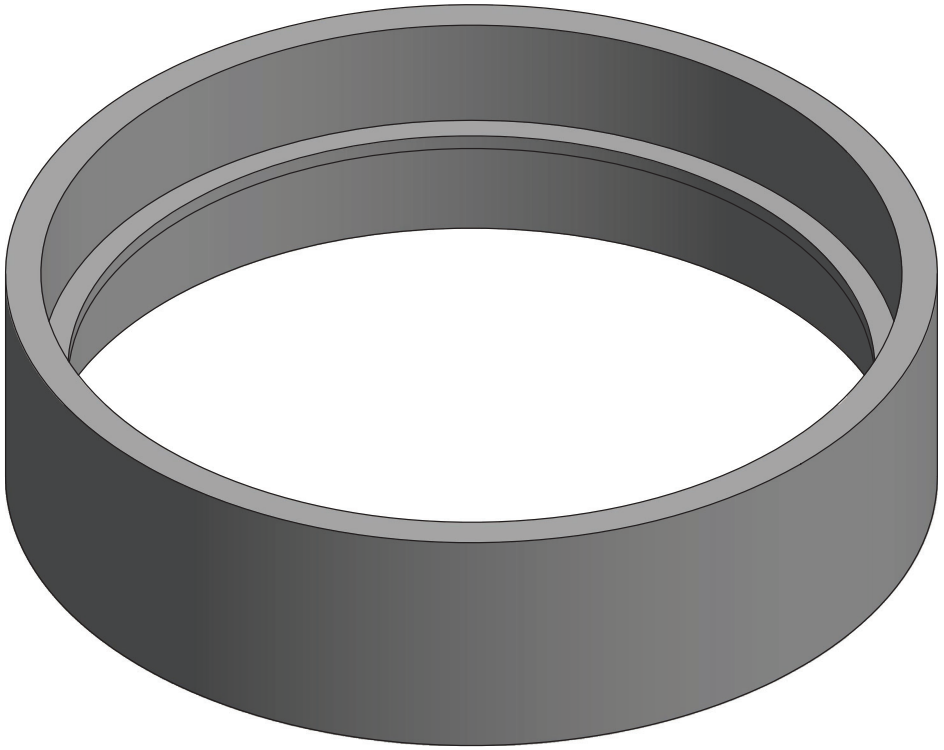

110

DRAWN rchaffer	6/14/2021		
CHECKED		TITLE	
QA			
MFG			
APPROVED			
		SIZE D	DWG NO Tube_Adapter REV
		SCALE 2 : 1	SHEET 3 OF 3

A.6 Water Cooled Outer Shield

112

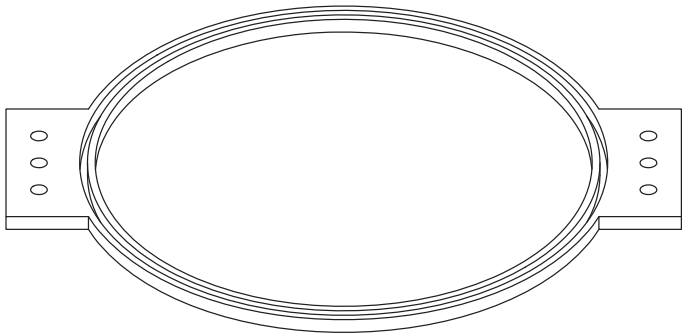

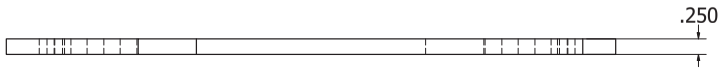

DRAWN rchaffer	2/15/2021		
CHECKED		TITLE	
QA			
MFG			
APPROVED			
		SIZE D	DWG NO Option 4 REV
		SCALE 1 : 1	SHEET 1 OF 3

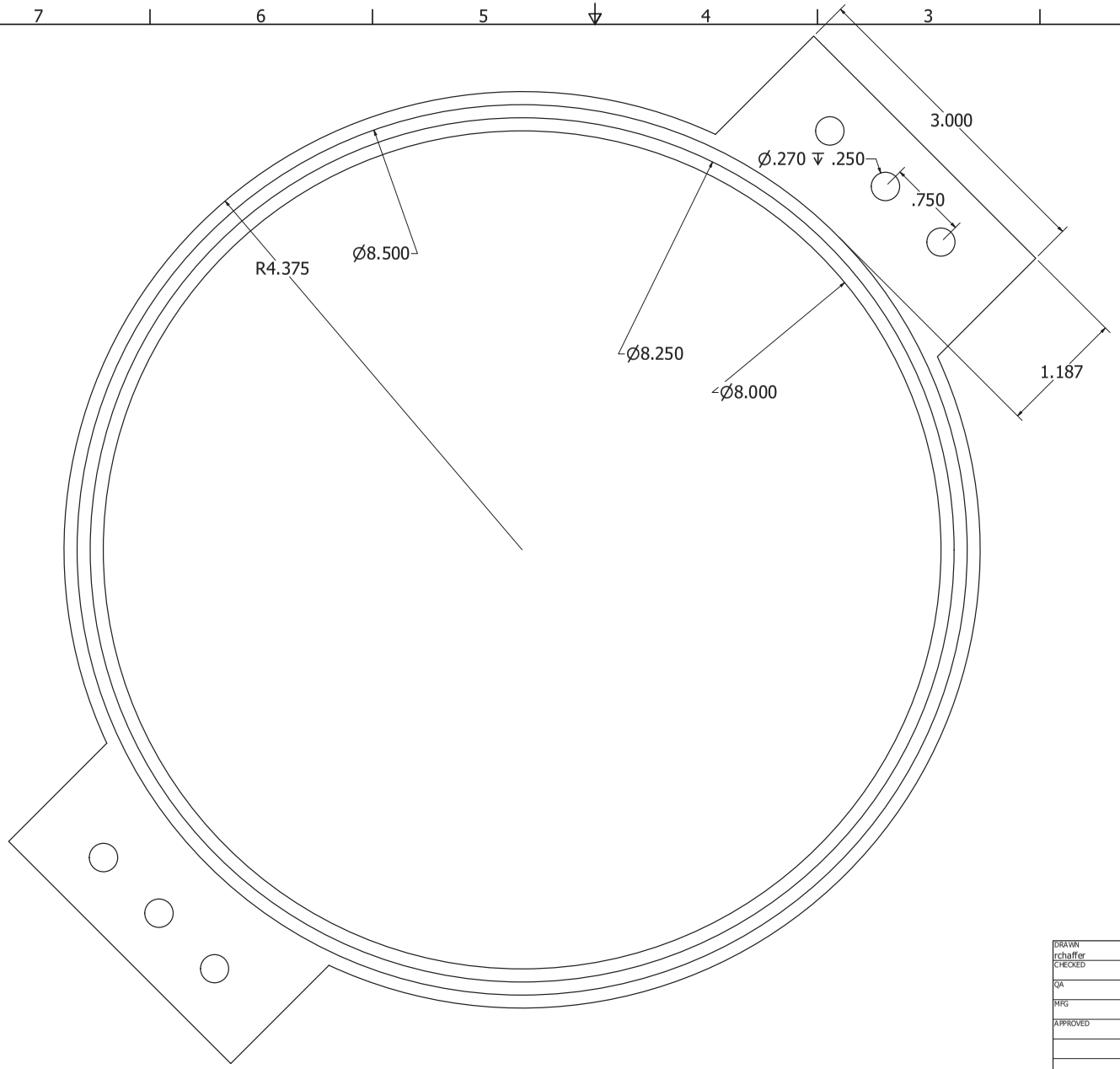

DRAWN rchaffer	2/15/2021		
CHECKED		TITLE	
QA			
MFG			
APPROVED			
		SIZE D	DWG NO Option 4 REV
		SCALE 2 : 1	SHEET 2 OF 3

113

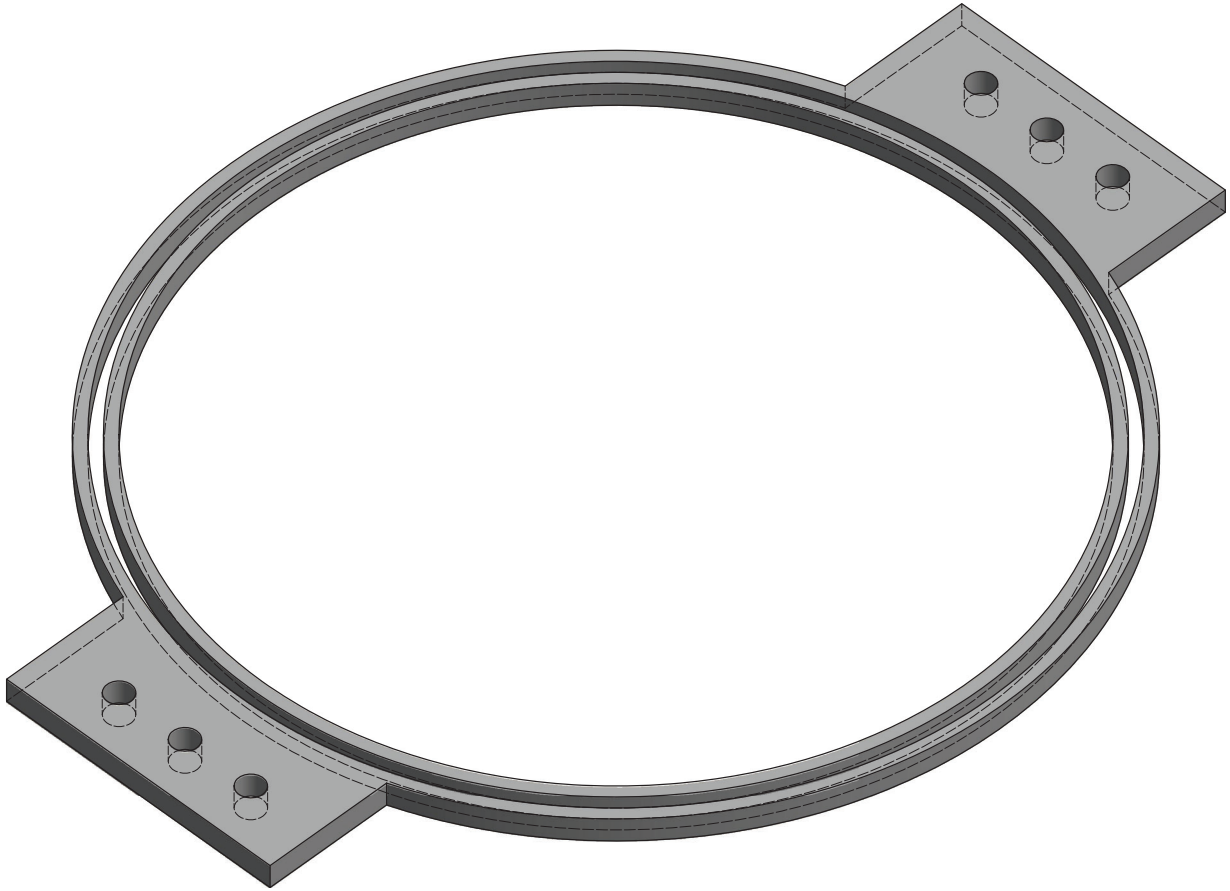

DRAWN	rchaffer	2/15/2021
CHECKED		
QA		
MFG		
APPROVED		

TITLE

SIZE D | DWG NO Option 4 | REV

SCALE 2 : 1 | SHEET 3 OF 3

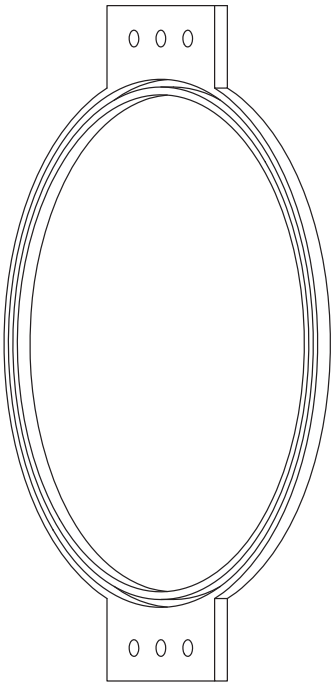

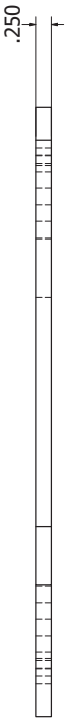

DRAWN	rchaffer	2/15/2021	TITLE		
CHECKED					
QA					
MFG					
APPROVED					

SIZE	DWG NO	REV	
D	Option 4		
SCALE 1 : 1	SHEET 1 OF 3		

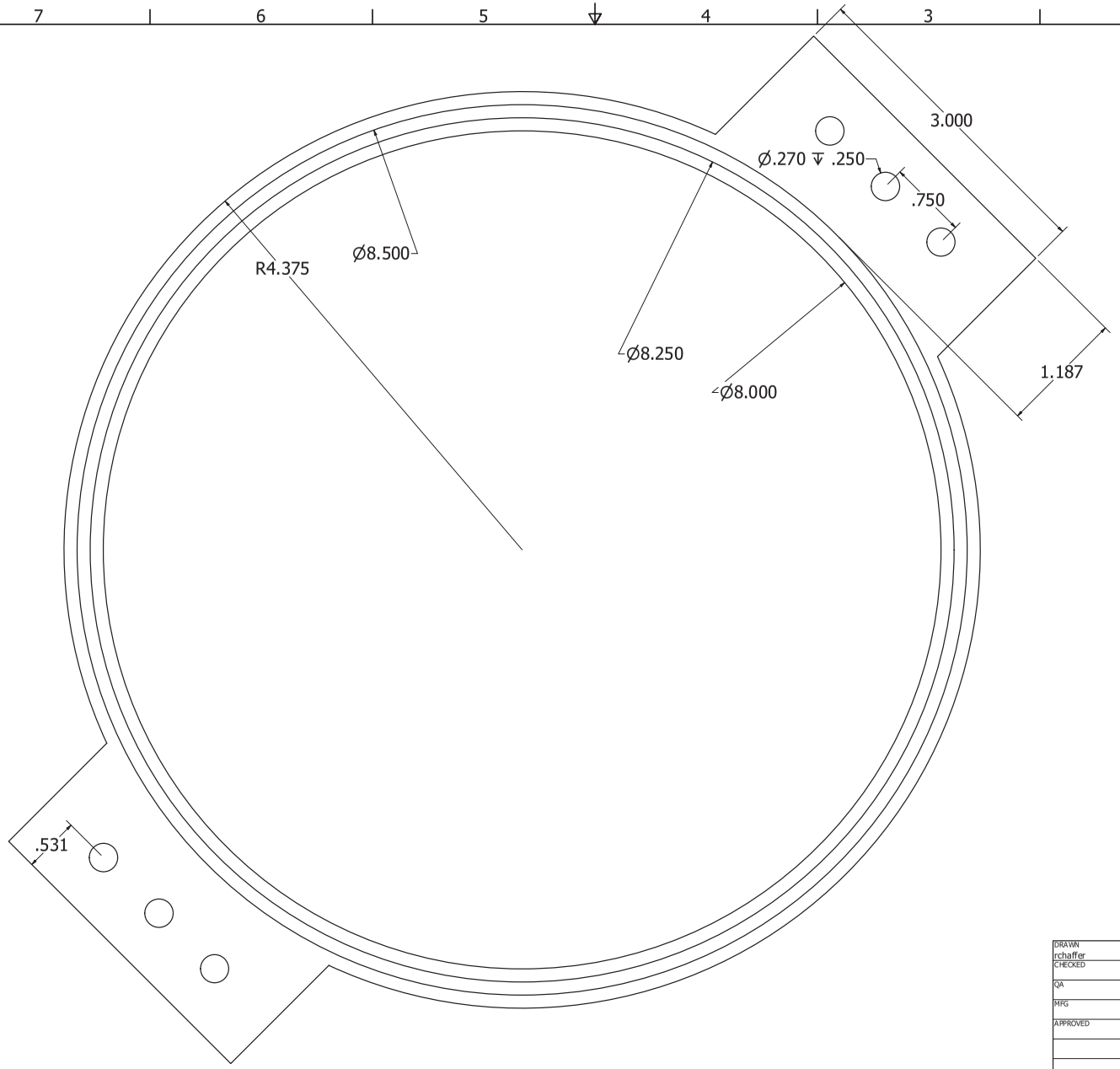

DRAWN rchaffer	2/15/2021		
CHECKED		TITLE	
QA			
MFG			
APPROVED			
		SIZE D	DWG NO Option 4 REV
		SCALE 2 : 1	SHEET 2 OF 3

116

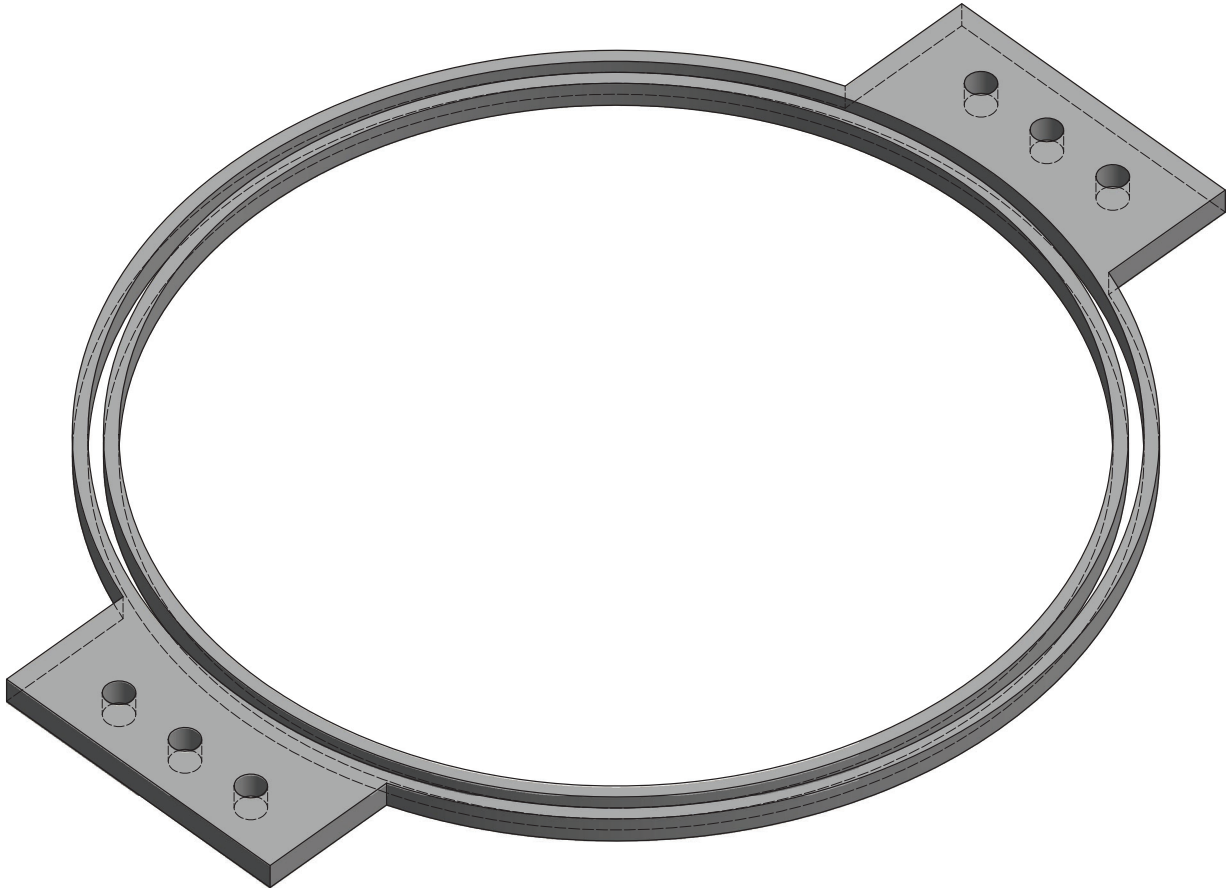

DRAWN rchaffer	2/15/2021		
CHECKED		TITLE	
QA			
MFG			
APPROVED			
		SIZE D	DWG NO Option 4 REV
		SCALE 2 : 1	SHEET 3 OF 3

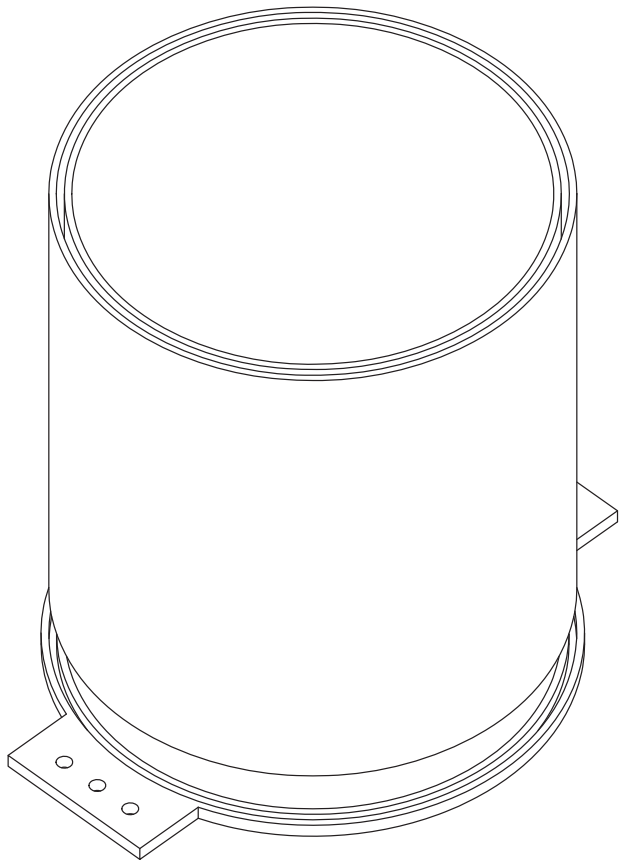

DRAWN rchaffer	3/31/2021	
CHECKED		TITLE
QA		
MFG		
APPROVED		
		SIZE D / DWG NO Option 4_All / REV
		SCALE 1 : 1 / SHEET 1 OF 3

A.7 Pneumatic Air Cylinder Mounts

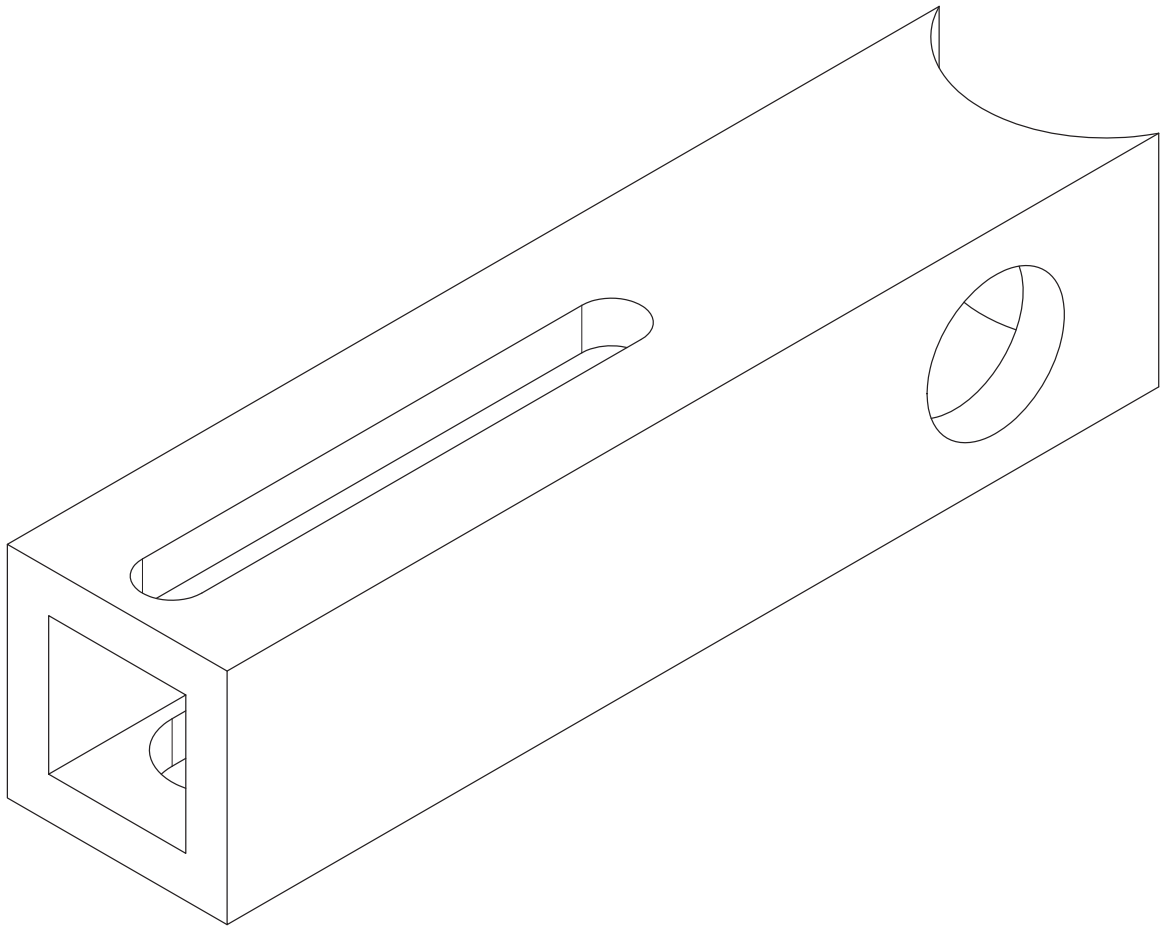

120

DRAWN rchaffer	6/8/2021	
CHECKED		
QA 2		TITLE Material: Aluminum, 3/16" wall, 1" High, 1" Wide
MFG		
APPROVED		
		SIZE D · DWG NO Upper_Air_Cylinder_Mount · REV
		SCALE 5 : 1 · SHEET 1 OF 5

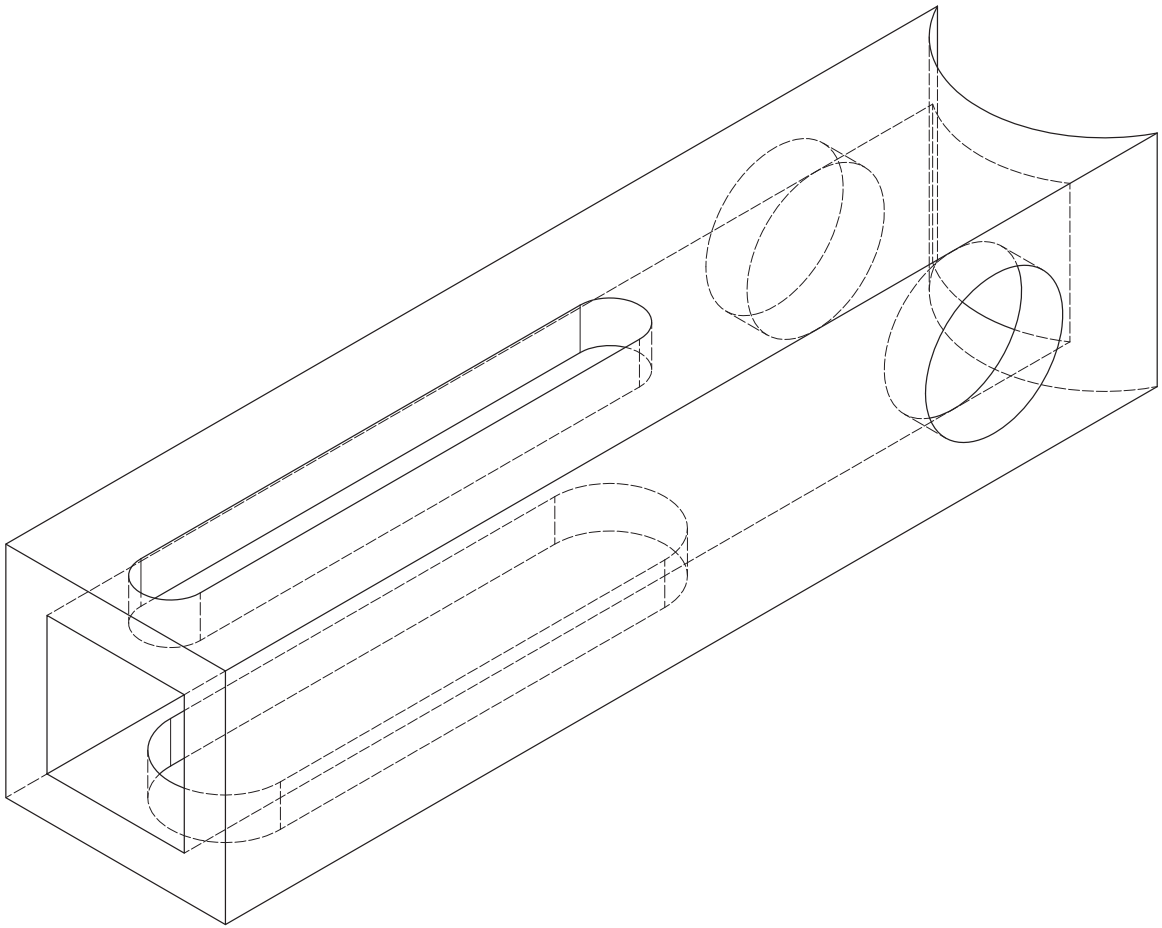

DRAWN rchaffer	6/8/2021	
CHECKED		TITLE
QA		
MFG		
APPROVED		
		SIZE D / DWG NO Upper_Air_Cylinder_Mount / REV
		SCALE 5 : 1 / SHEET 2 OF 5

121

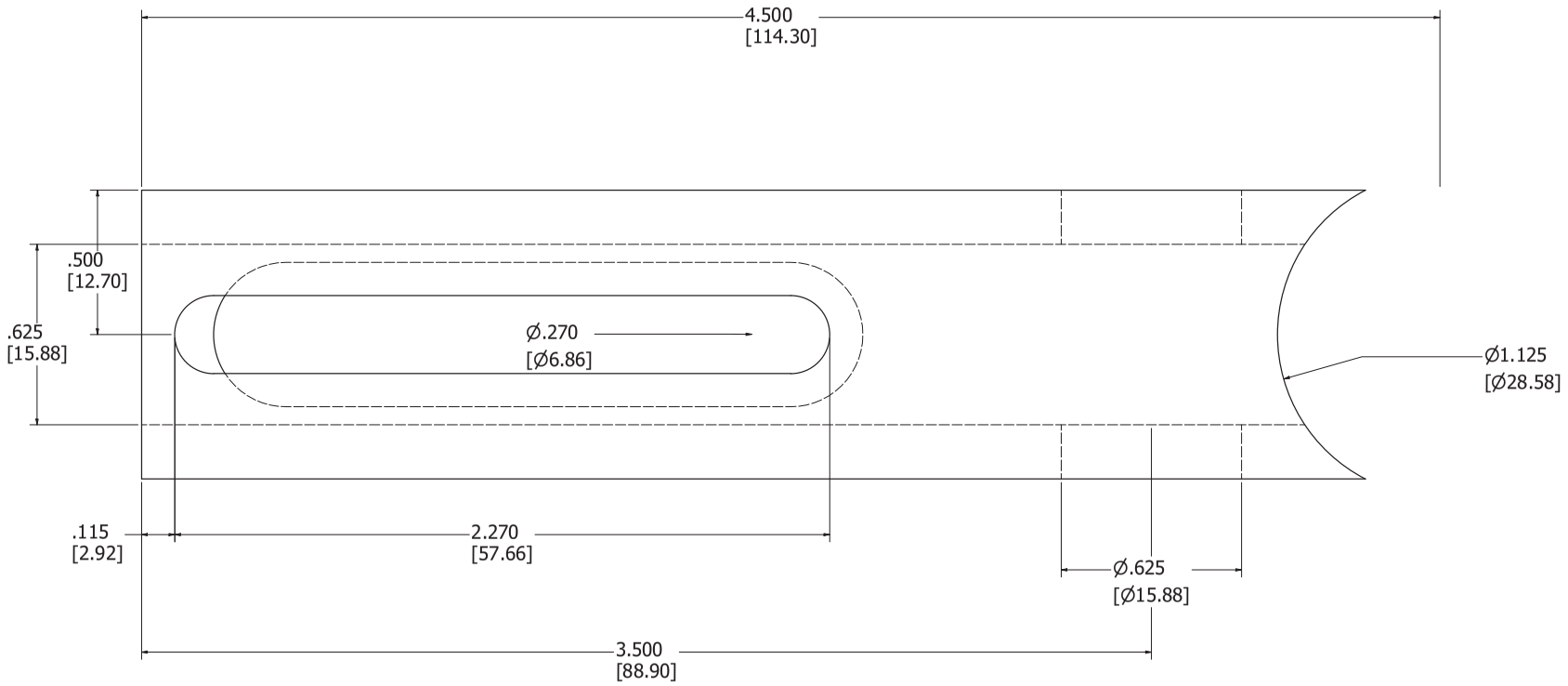

DRAWN rchaffer	6/8/2021	Top View
CHECKED		TITLE
QA		
MFG		
APPROVED		
SIZE D	DWG NO Upper_Air_Cylinder_Mount	REV
SCALE 5 : 1	SHEET 3 OF 5	

122

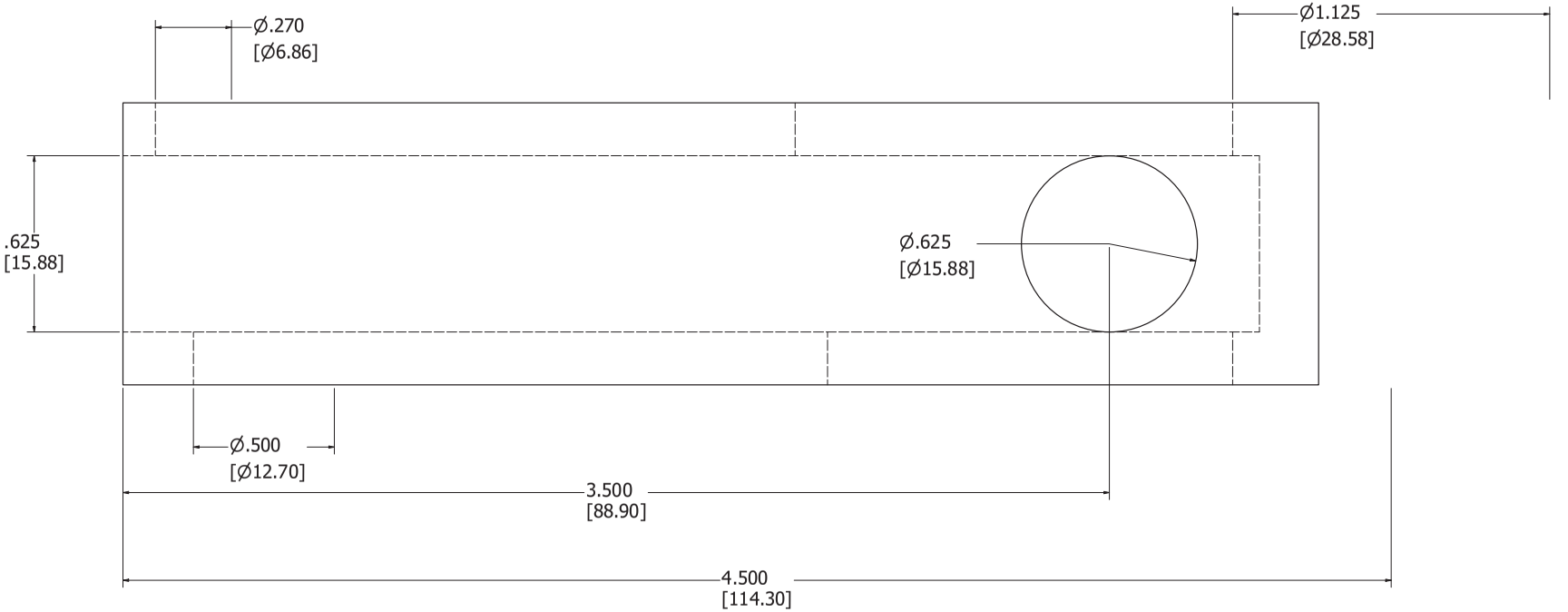

123

DRAWN rchaffer	6/8/2021	Side View
CHECKED		TITLE
QA		
MFG		
APPROVED		
		SIZE D · DWG NO Upper_Air_Cylinder_Mount · REV
		SCALE 5 : 1 · SHEET 4 OF 5

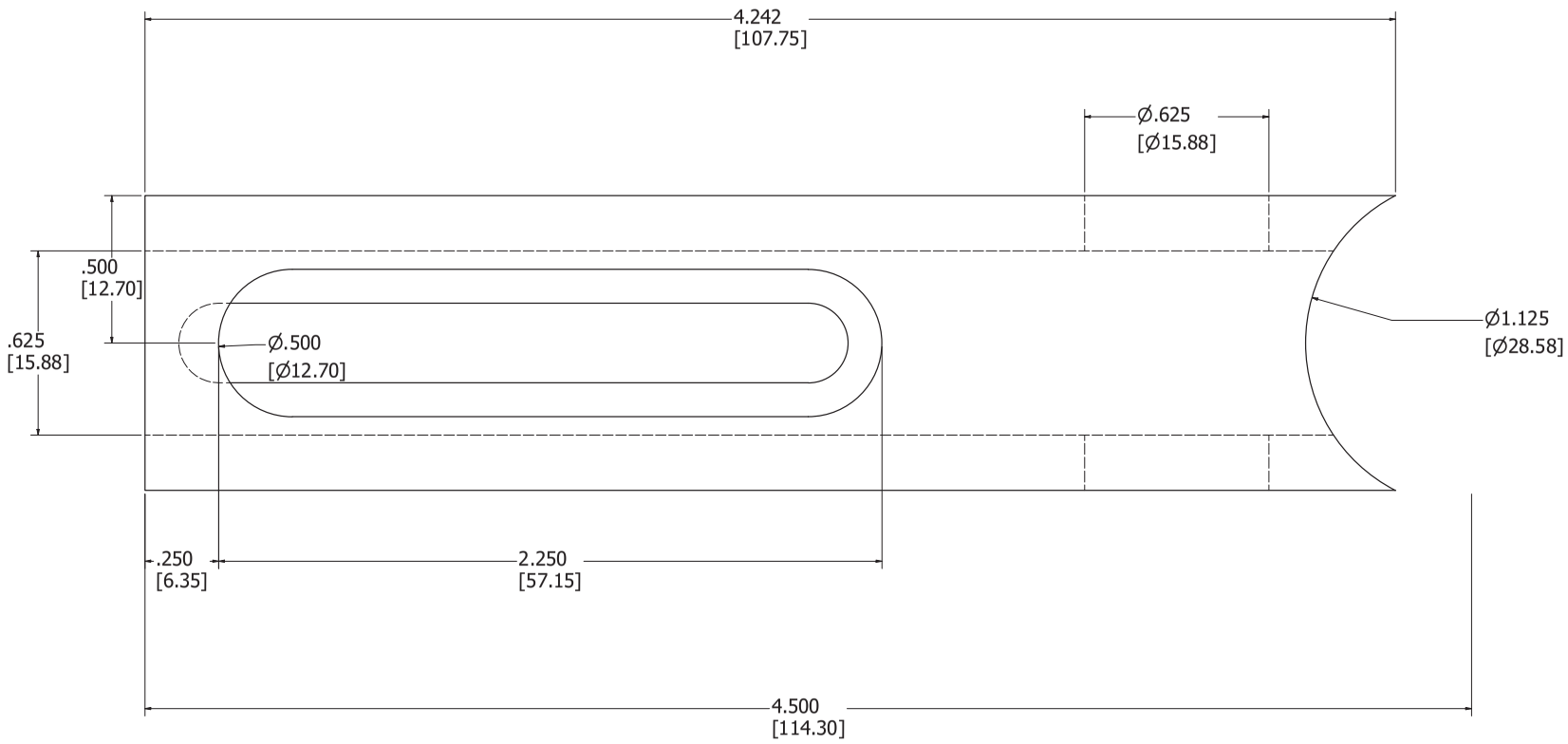

124

DRAWN rchaffer	6/8/2021	Bottom View
CHECKED		TITLE
QA		
MFG		
APPROVED		
		SIZE D · DWG NO Upper_Air_Cylinder_Mount · REV
		SCALE 5 : 1 · SHEET 5 OF 5

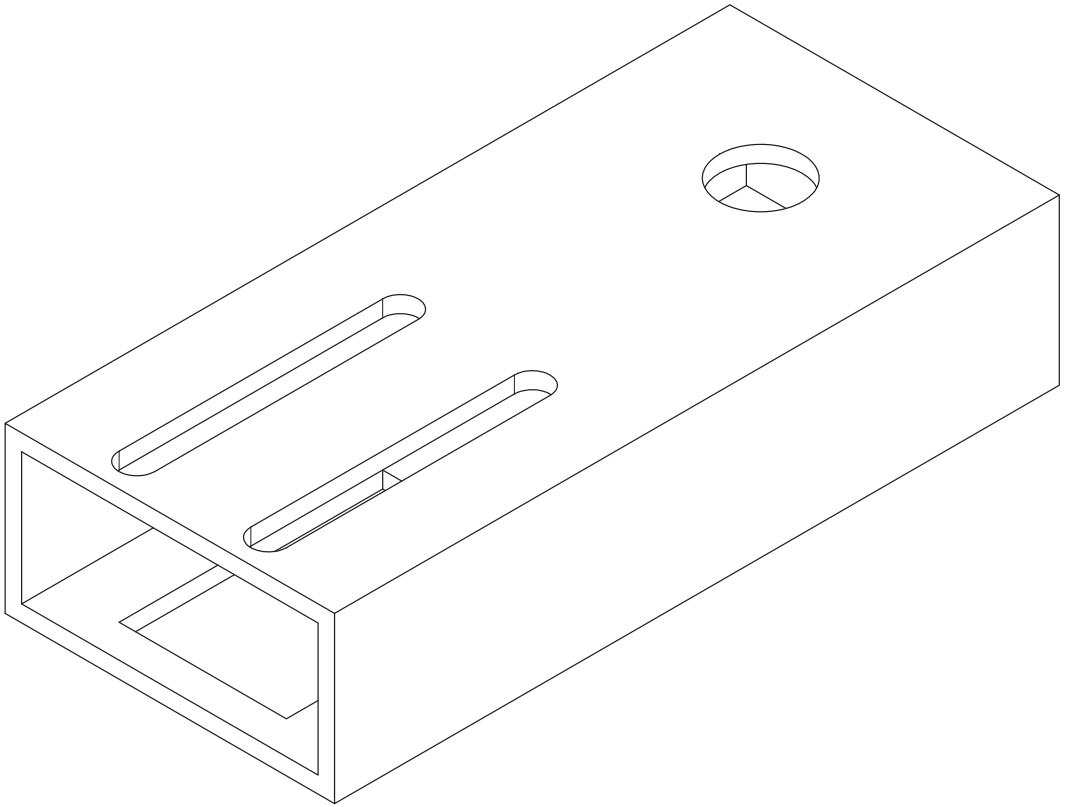

DRAWN rchaffer	6/8/2021	
CHECKED		
QA 2		TITLE: Material: Aluminum, 1/8" Wall, 1-1/4" High, 2-1/2" Wide
MFG		
APPROVED		SIZE D | DWG NO Lower_Bracket | REV
		SCALE 3 : 1 | SHEET 1 OF 5

125

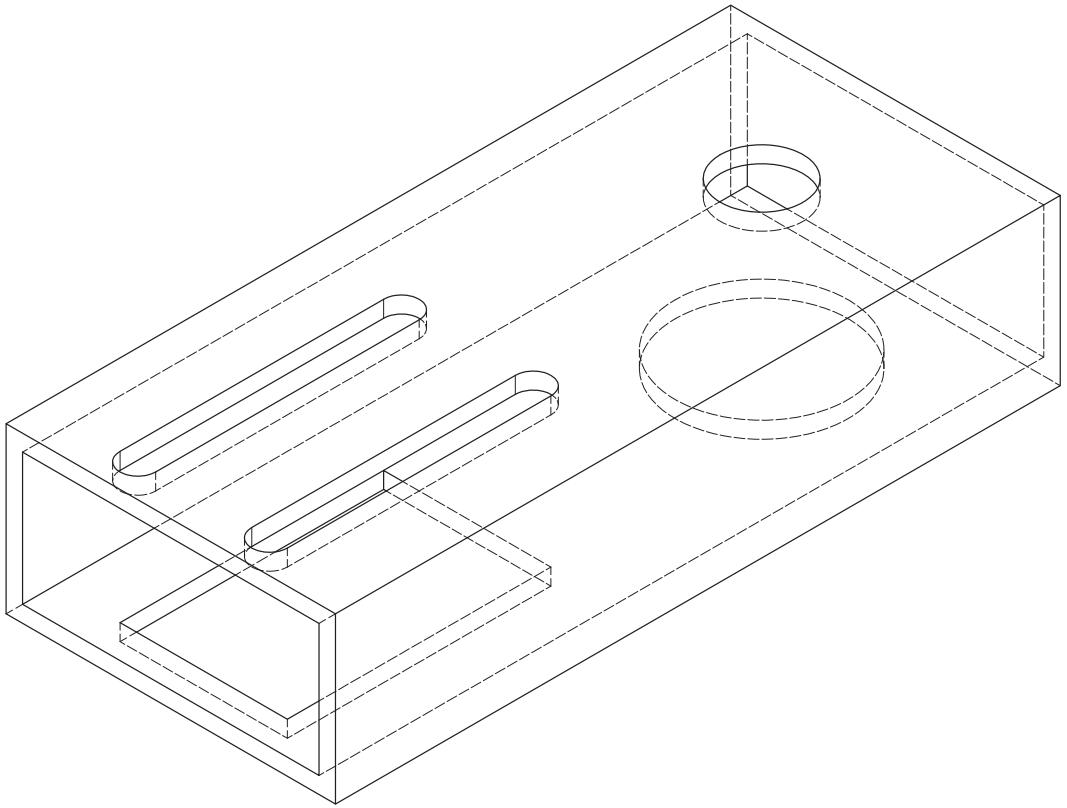

DRAWN rchaffer	6/8/2021		
CHECKED		TITLE	
QA			
MFG			
APPROVED		SIZE D	DWG NO Lower_Bracket REV
		SCALE 3 : 1	SHEET 2 OF 5

126

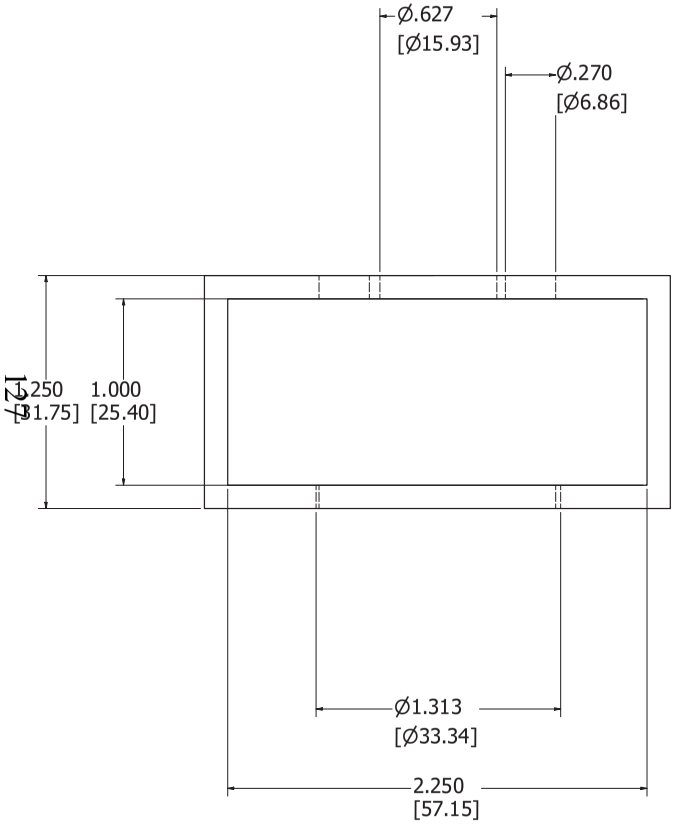

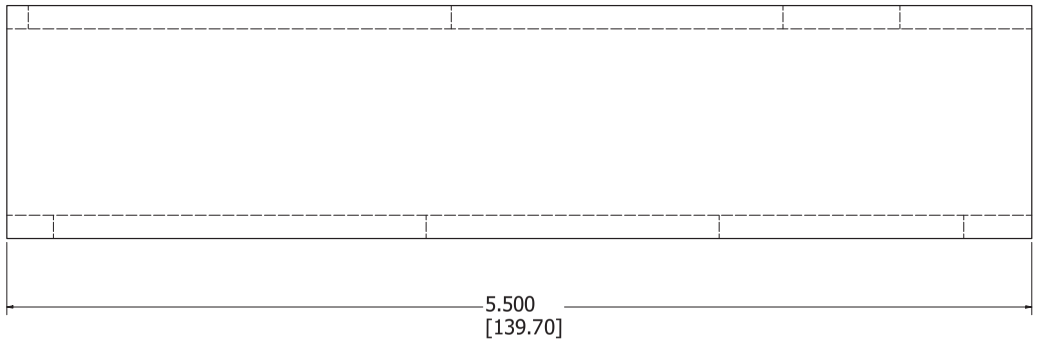

DRAWN rchaffer	6/8/2021	Front and Side View
CHECKED		TITLE
QA		
MFG		
APPROVED		
		SIZE D · DWG NO Lower_Bracket · REV
		SCALE 3 : 1 · SHEET 3 OF 5

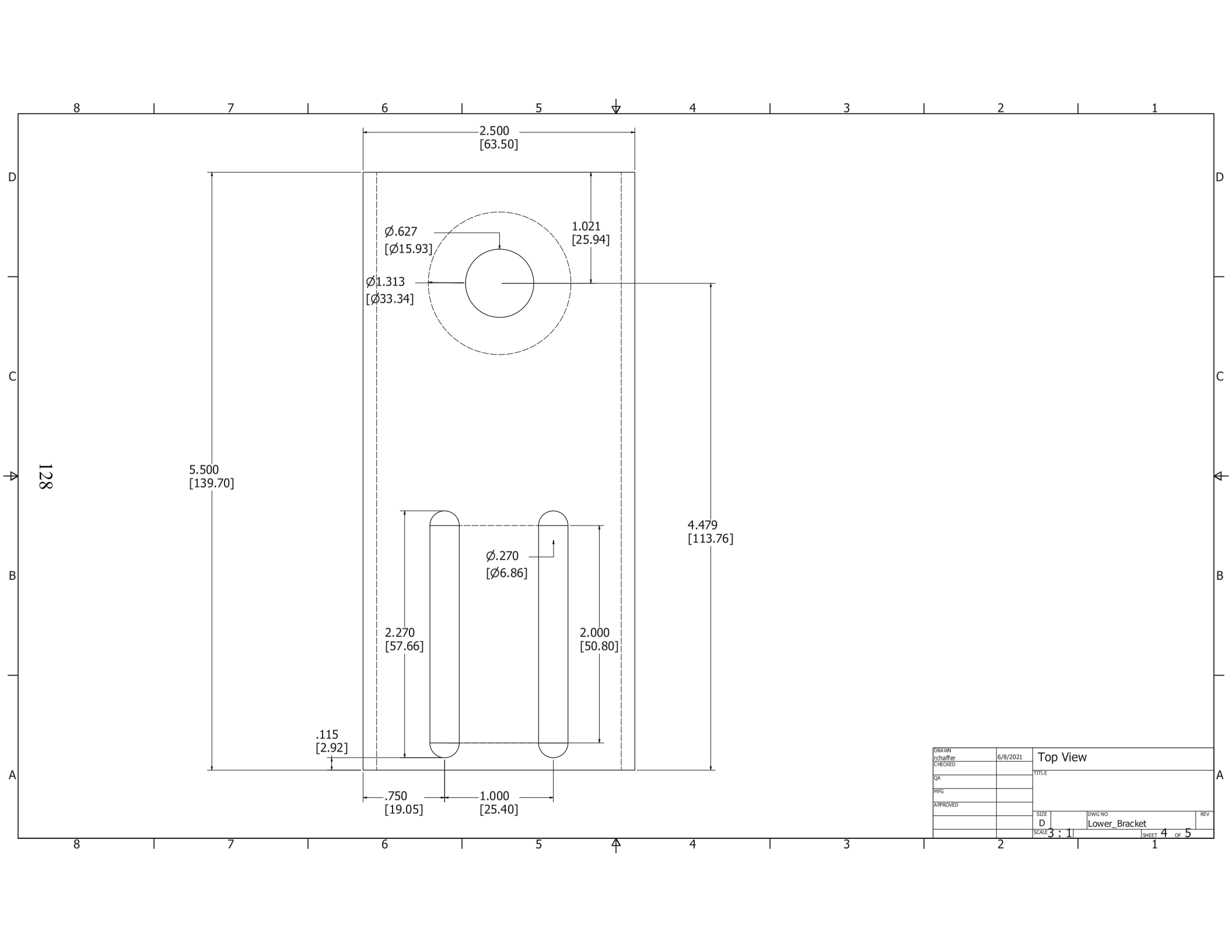
2.500
[63.50]
Ø.627
[Ø15.93]
1.021
[25.94]
Ø1.313
[Ø33.34]
5.500
[139.70]
4.479
[113.76]
Ø.270
[Ø6.86]
2.270
[57.66]
2.000
[50.80]
.115
[2.92]
.750
[19.05]
1.000
[25.40]
DRAWN
rchaffer
6/8/2021
CHECKED
QA
MFG
APPROVED
Top View
TITLE
SIZE
D
DWG NO
Lower_Bracket
REV
SCALE 3 : 1
SHEET 4 OF 5

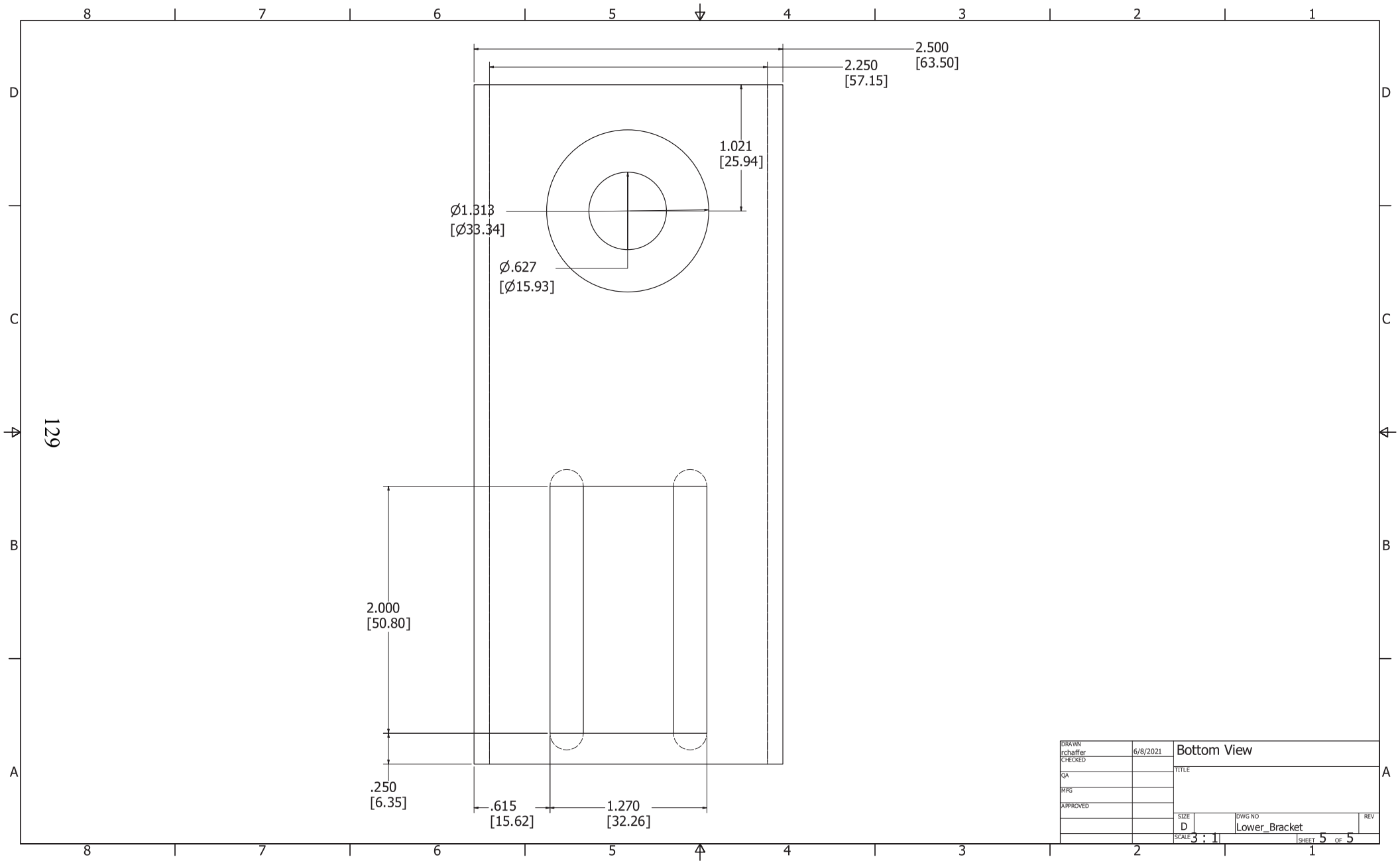
2.500
[63.50]
2.250
[57.15]
1.021
[25.94]
Ø1.313
[Ø33.34]
Ø.627
[Ø15.93]
2.000
[50.80]
.250
[6.35]
.615
[15.62]
1.270
[32.26]
DRAWN
rchaffer
6/8/2021
CHECKED
QA
MFG
APPROVED
Bottom View
TITLE
SIZE
D
DWG NO
Lower_Bracket
REV
SCALE 3 : 1
SHEET 5 OF 5

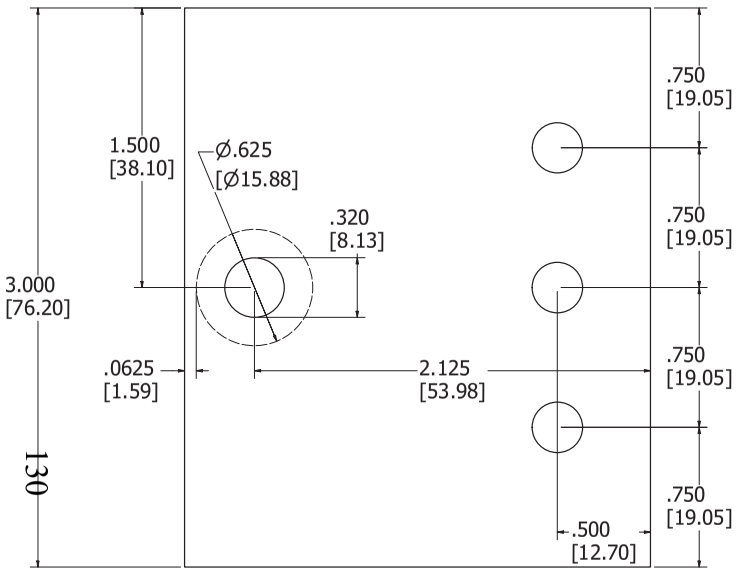

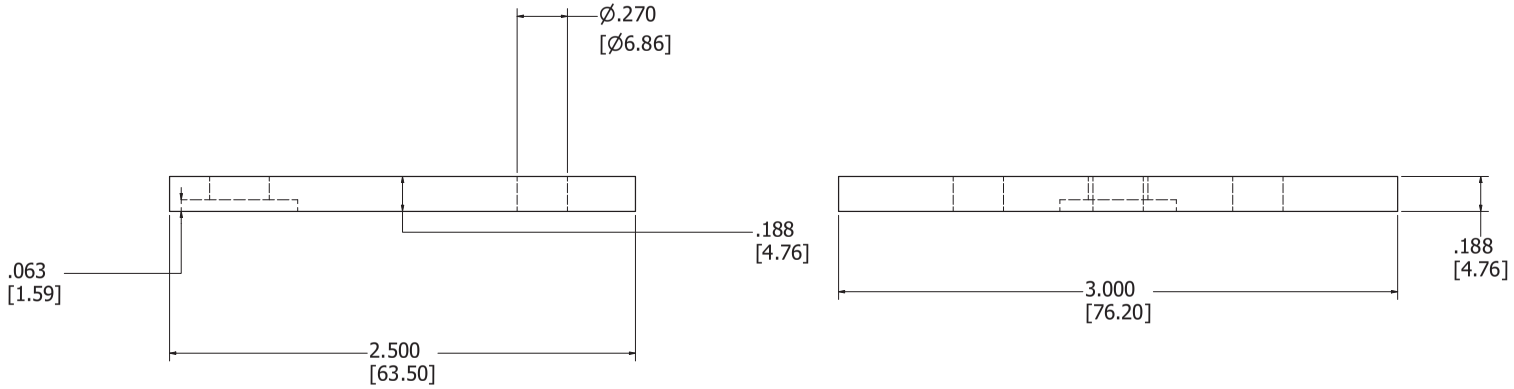

DRAWN rchaffer	6/8/2021	
CHECKED		
QA 2		TITLE Material: Stainless Steel, 3/16" thick, 3" wide
MFG		
APPROVED		SIZE D · DWG NO Mounting_Tab · REV
		SCALE 3 : 1 · SHEET 1 OF 3

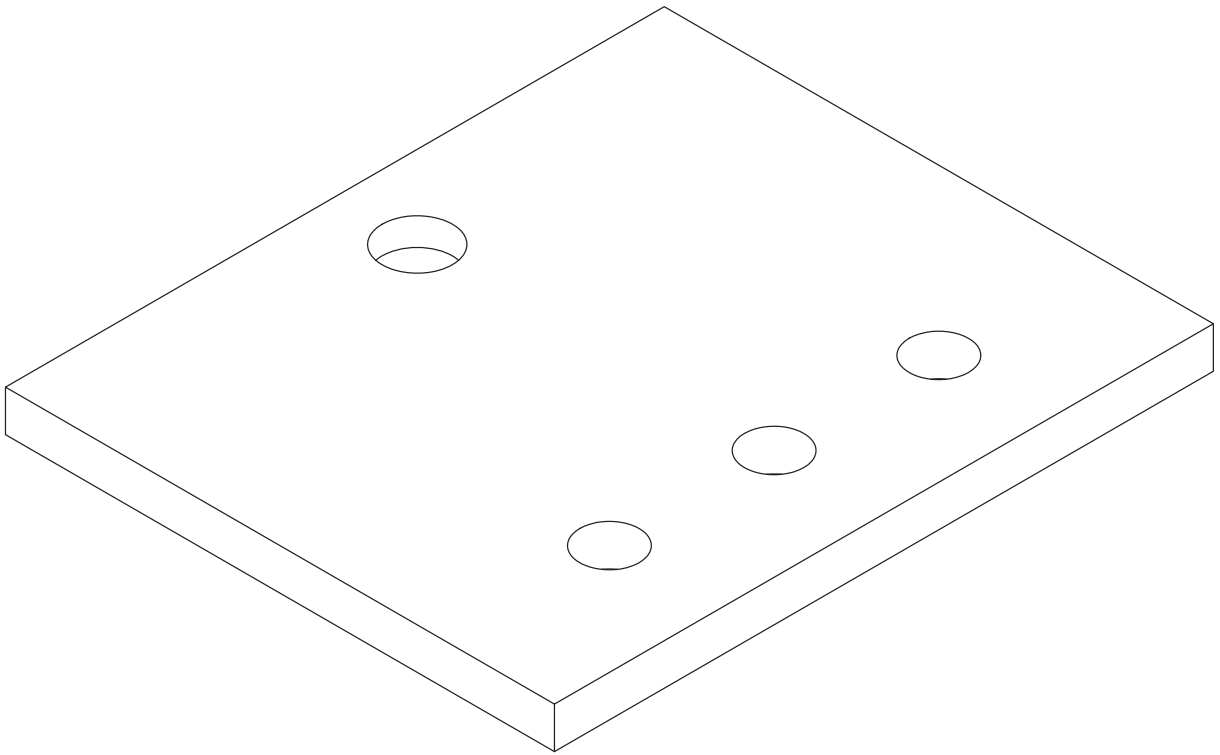

DRAWN rchaffer	6/8/2021	ISO Top
CHECKED		TITLE
QA		
MFG		
APPROVED		
		SIZE D · DWG NO Mounting_Tab · REV
		SCALE 5 : 1 · SHEET 2 OF 3

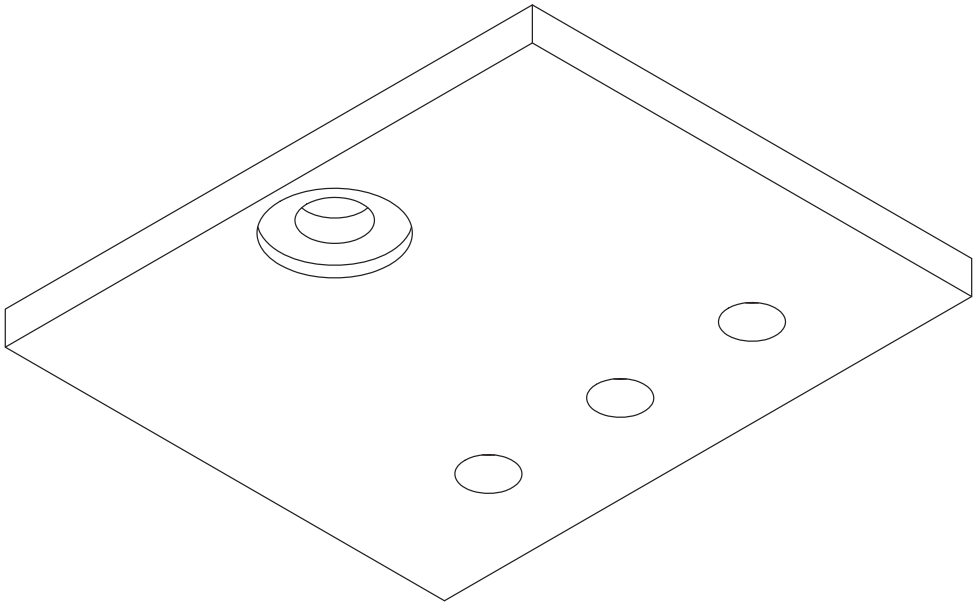

DRAWN rchaffer	6/8/2021	ISO Bottom	
CHECKED		TITLE	
QA			
MFG			
APPROVED			
		SIZE D	DWG NO Mounting_Tab REV
		SCALE 4 : 1	SHEET 3 OF 3

A.8 Load Cell Base Mounting Plate

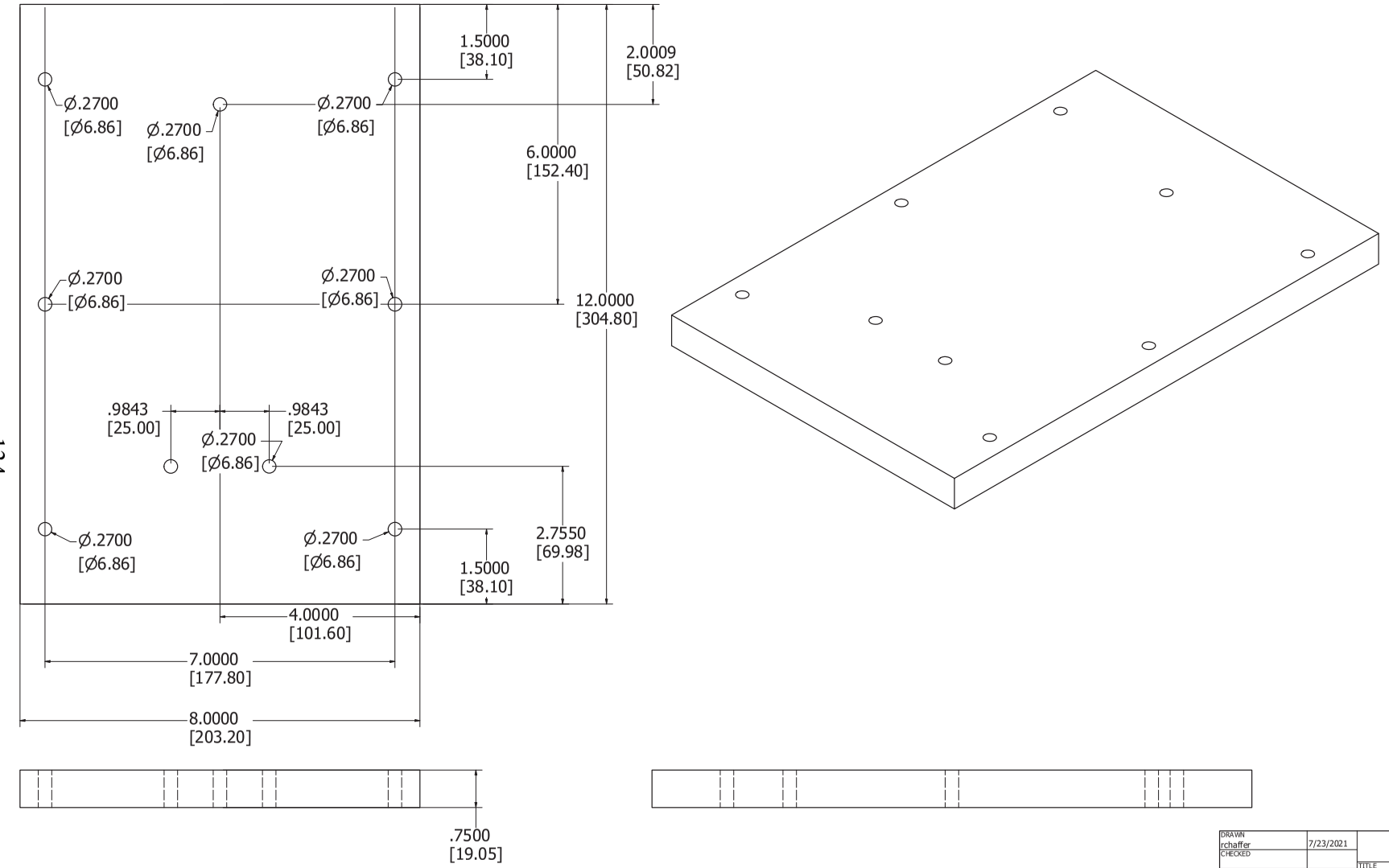

DRAWN rchaffer	7/23/2021	
CHECKED		
QA 1		TITLE Material: Steel
MFG		
APPROVED		
		SIZE D · DWG NO Load_Cell_Base_Plate · REV
		SCALE 1 : 1 · SHEET 1 OF 2

134

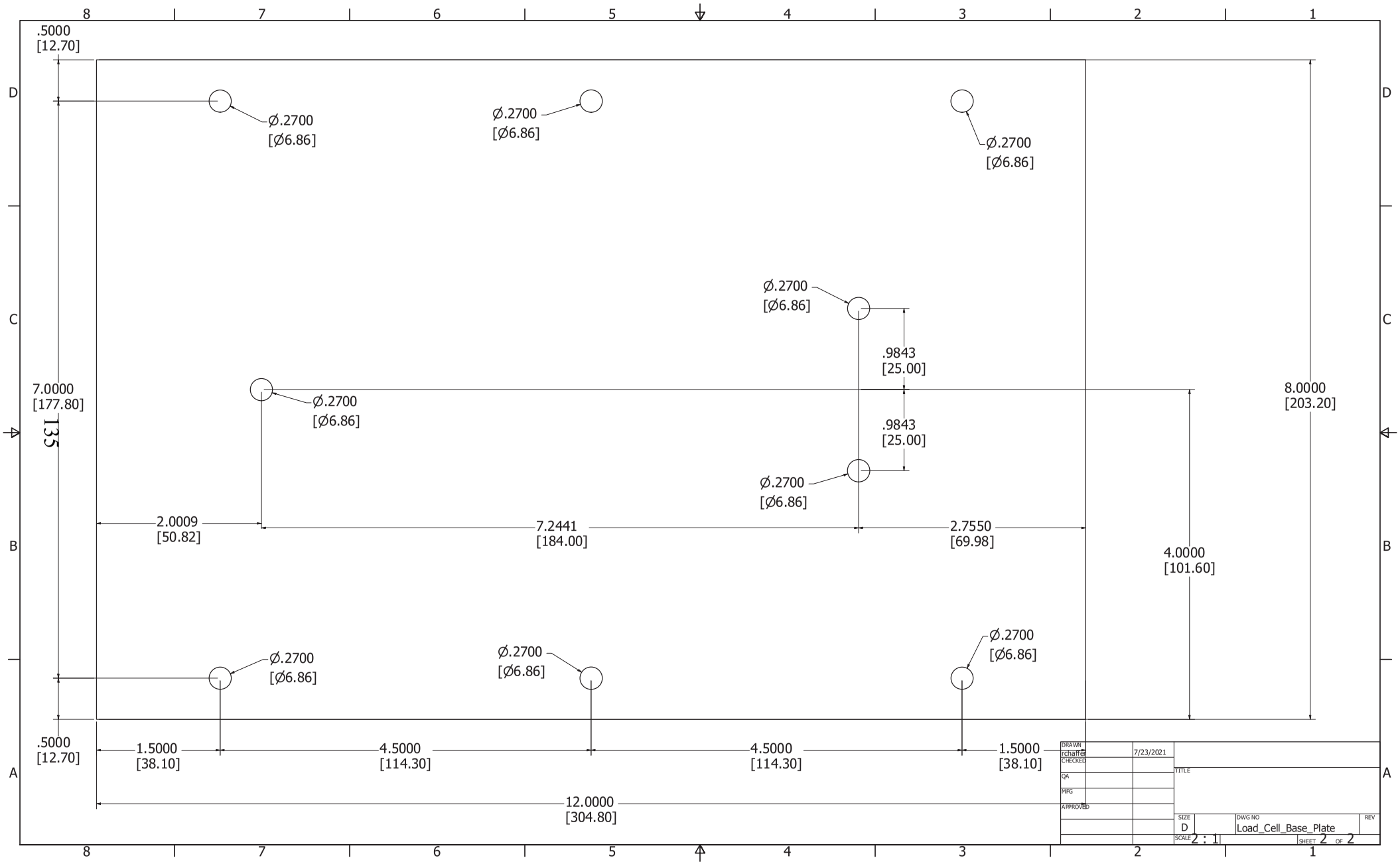
.5000
[12.70]
Ø.2700
[Ø6.86]
Ø.2700
[Ø6.86]
Ø.2700
[Ø6.86]
Ø.2700
[Ø6.86]
.9843
[25.00]
.9843
[25.00]
Ø.2700
[Ø6.86]
Ø.2700
[Ø6.86]
7.0000
[177.80]
135
8.0000
[203.20]
4.0000
[101.60]
2.0009
[50.82]
7.2441
[184.00]
2.7550
[69.98]
Ø.2700
[Ø6.86]
Ø.2700
[Ø6.86]
Ø.2700
[Ø6.86]
.5000
[12.70]
1.5000
[38.10]
4.5000
[114.30]
4.5000
[114.30]
1.5000
[38.10]
12.0000
[304.80]
DRAWN
rchaffee
7/23/2021
CHECKED
QA
MFG
APPROVED
TITLE
SIZE
D
DWG NO
Load_Cell_Base_Plate
REV
SCALE
2 : 1
SHEET
2
OF
2

A.9 Sample Support Assembly and Horizontal Sample Dish

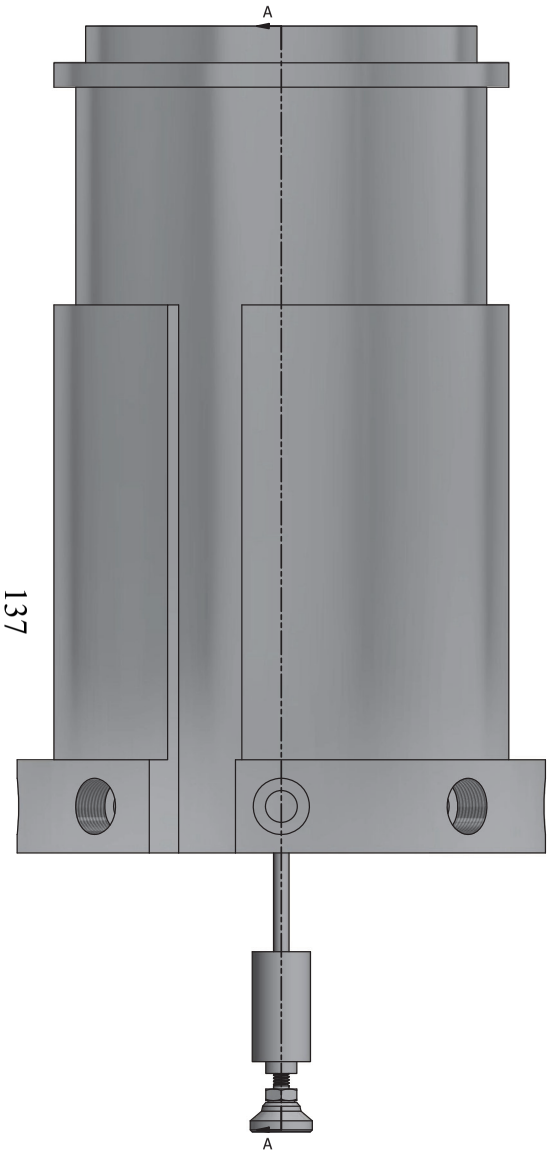

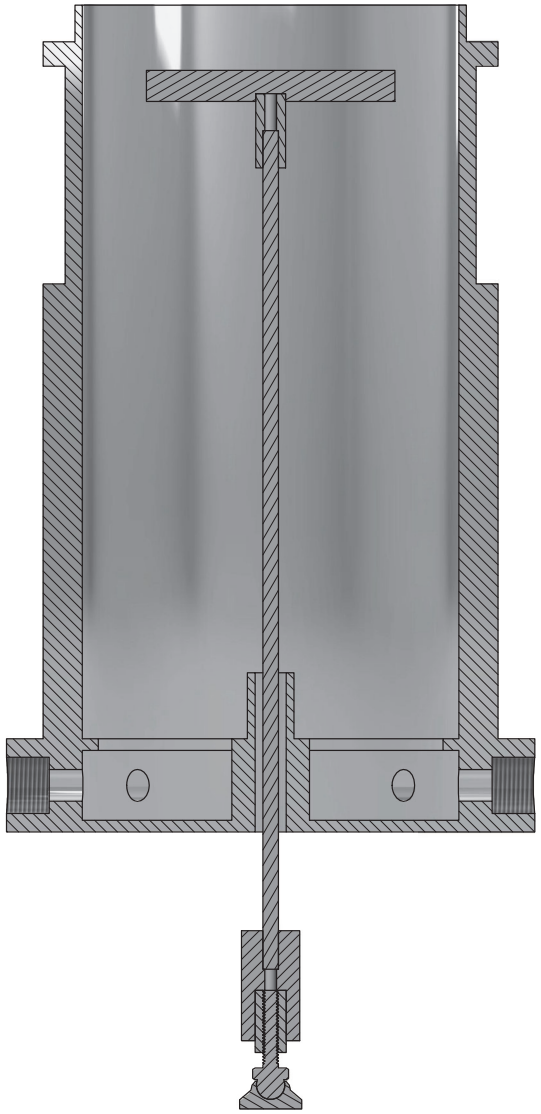

SECTION A-A
SCALE 1 : 1

DRAWN rchaffer	5/27/2021		
CHECKED			
QA		TITLE	
MFG			
APPROVED			
		SIZE D	DWG NO ADC_and_Sample_Holder REV
		SCALE 1 : 1	SHEET 1 OF 1

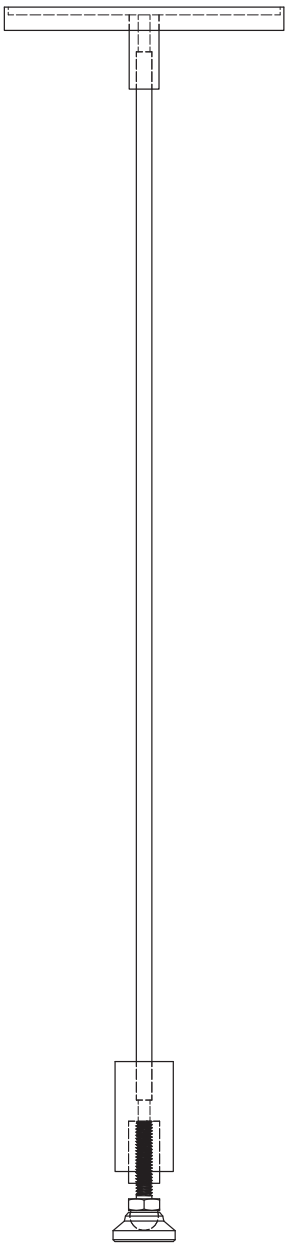

DRAWN	rchaffee		
CHECKED			
QA			
MFG			
APPROVED			
		9/29/2021	
SIZE	D	TITLE	
SCALE	1 : 1		
DWG NO	Sample_Holder		
REV			
SHEET 1 OF 2			

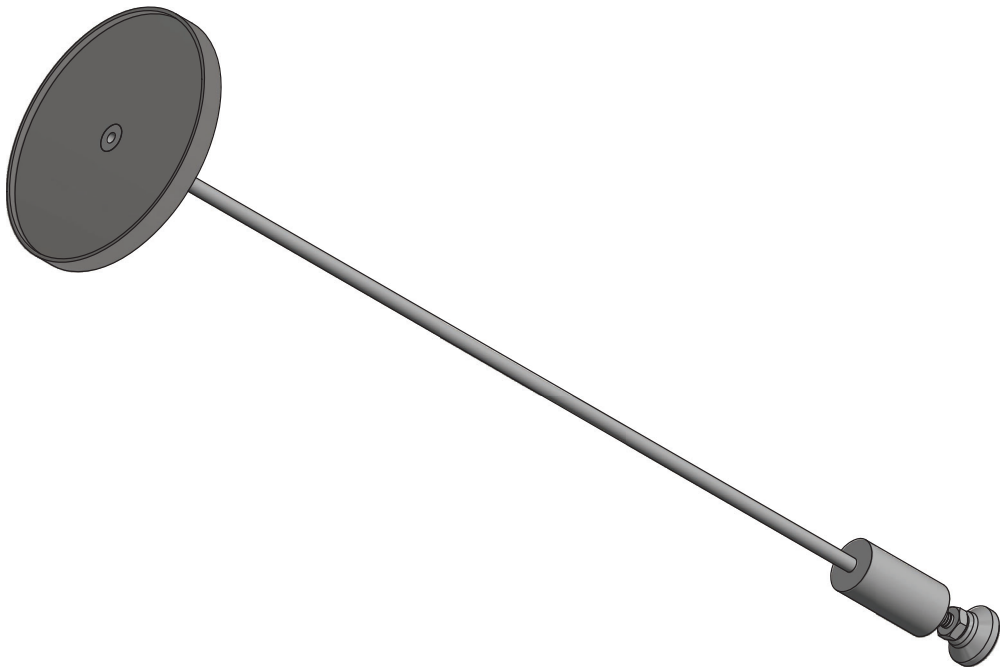

DRAWN rchaffer	9/29/2021		
CHECKED		TITLE	
QA			
MFG			
APPROVED		SIZE D	DWG NO Sample_Holder REV
		SCALE 1 : 1	SHEET 2 OF 2

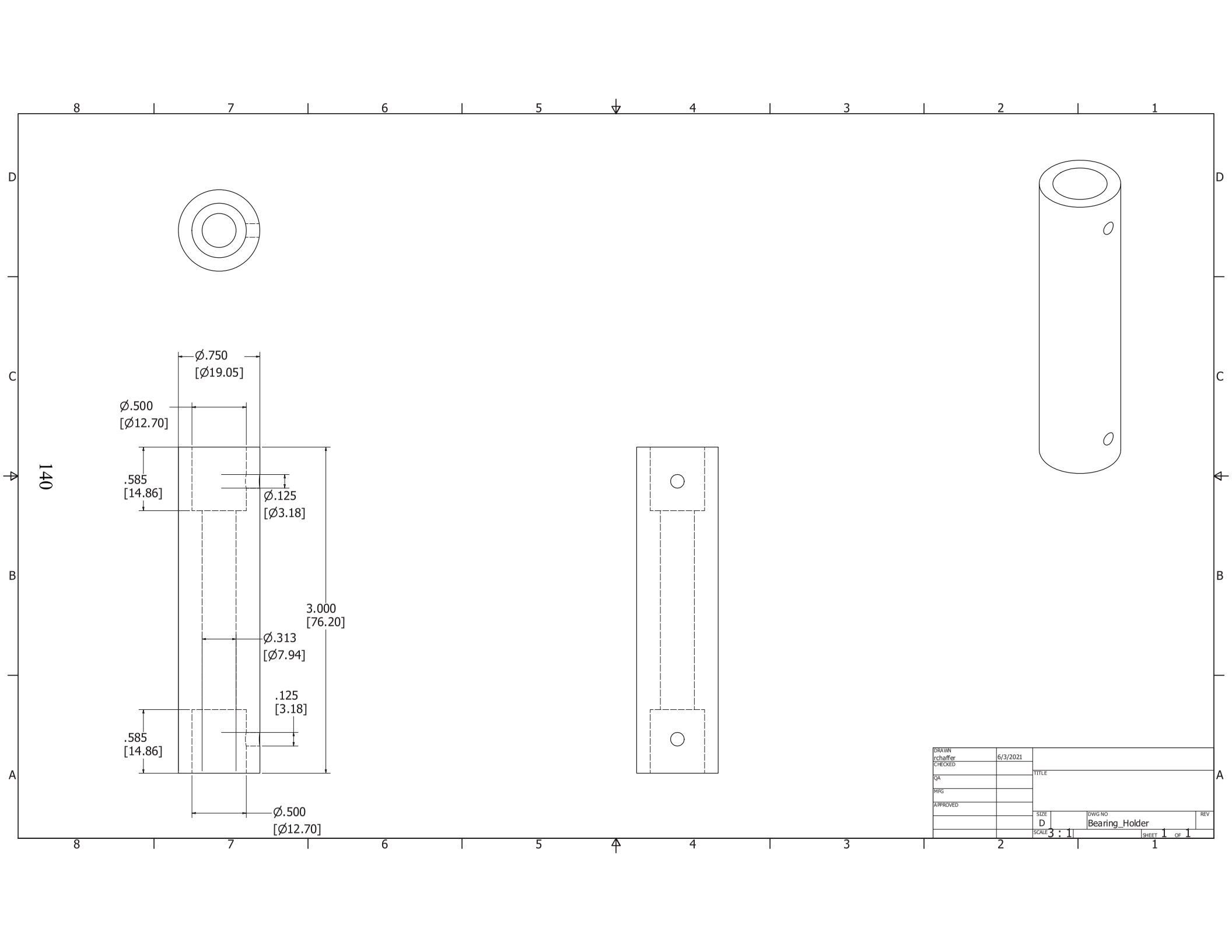
Ø.750
[Ø19.05]
Ø.500
[Ø12.70]
.585
[14.86]
Ø.125
[Ø3.18]
3.000
[76.20]
Ø.313
[Ø7.94]
.125
[3.18]
.585
[14.86]
Ø.500
[Ø12.70]
140
DRAWN
rchaffer
6/3/2021
CHECKED
QA
MFG
APPROVED
TITLE
SIZE
D
DWG NO
Bearing_Holder
REV
SCALE
3 : 1
SHEET 1 OF 1

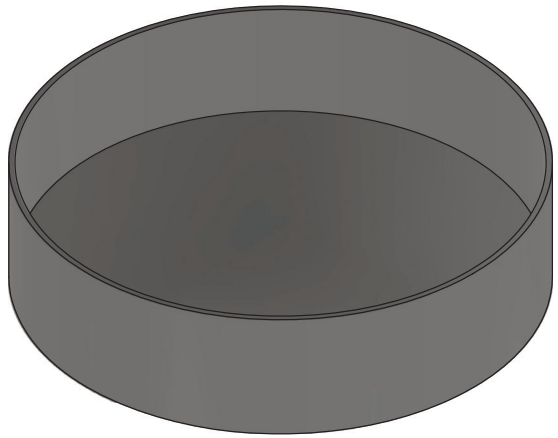

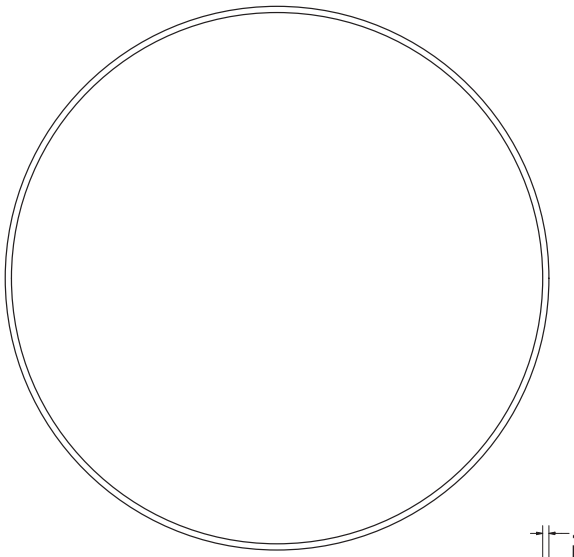

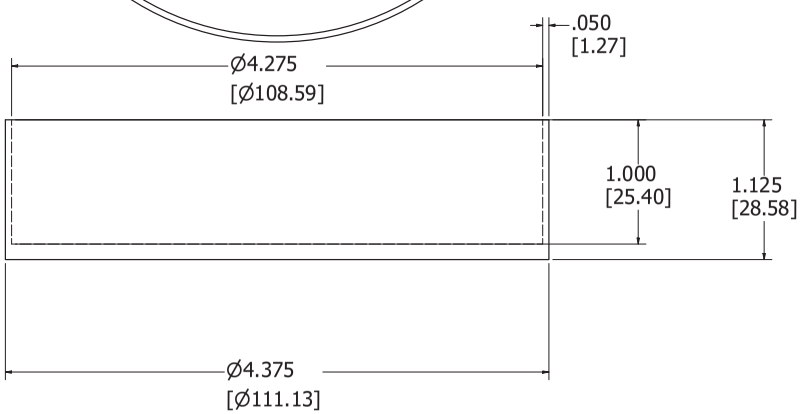

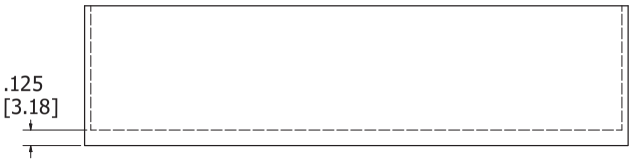

DRAWN rchaffer	6/3/2021		
CHECKED			
QA		TITLE	
MFG			
APPROVED			
		SIZE D	DWG NO Sample_Dish REV
		SCALE 2 : 1	SHEET 1 OF 1

141

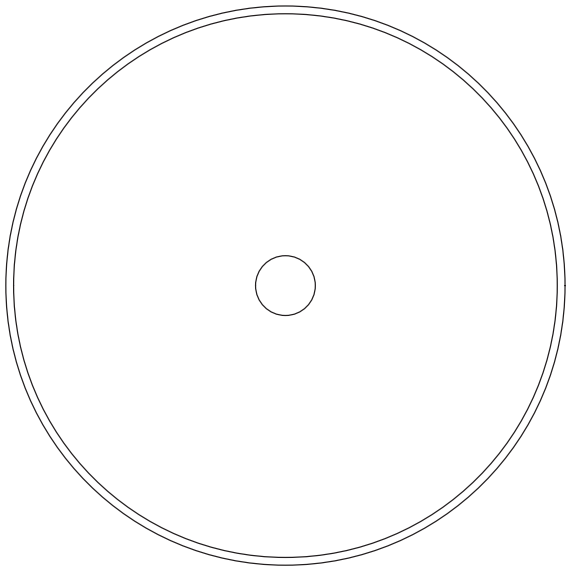

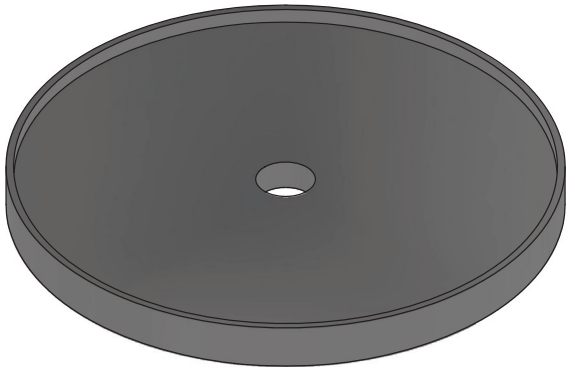

142

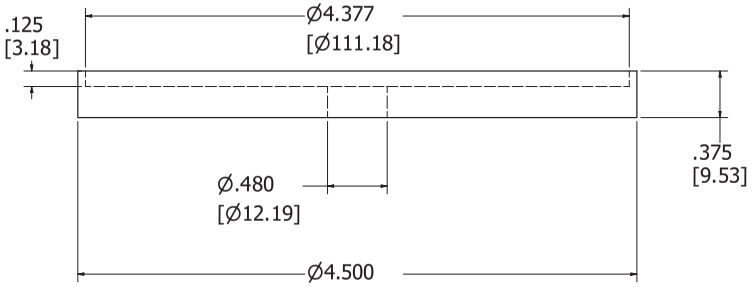

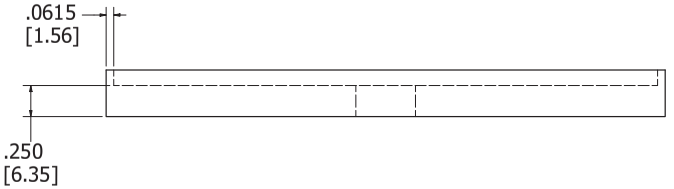

DRAWN rchaffer	6/3/2021	
CHECKED		TITLE
QA		
MFG		
APPROVED		
		SIZE D / DWG NO Top_Sample_Mount_Plate / REV
		SCALE 2 : 1 / SHEET 1 OF 1

A.10 Heat Flux Gauge Mount

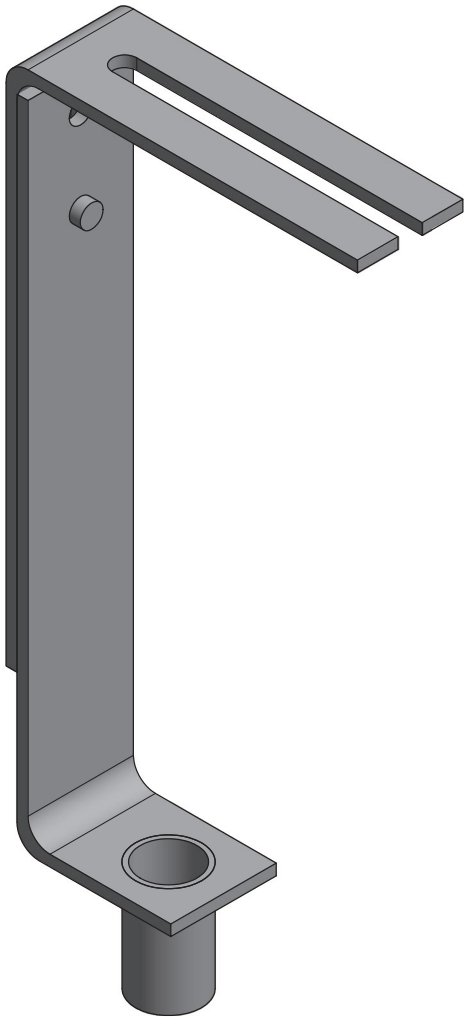

DRAWN rchaffer	5/17/2021	
CHECKED		TITLE
QA		
MFG		
APPROVED		
		SIZE D / DWG NO HFG_Mount / REV
		SCALE 2 : 1 / SHEET 1 OF 4

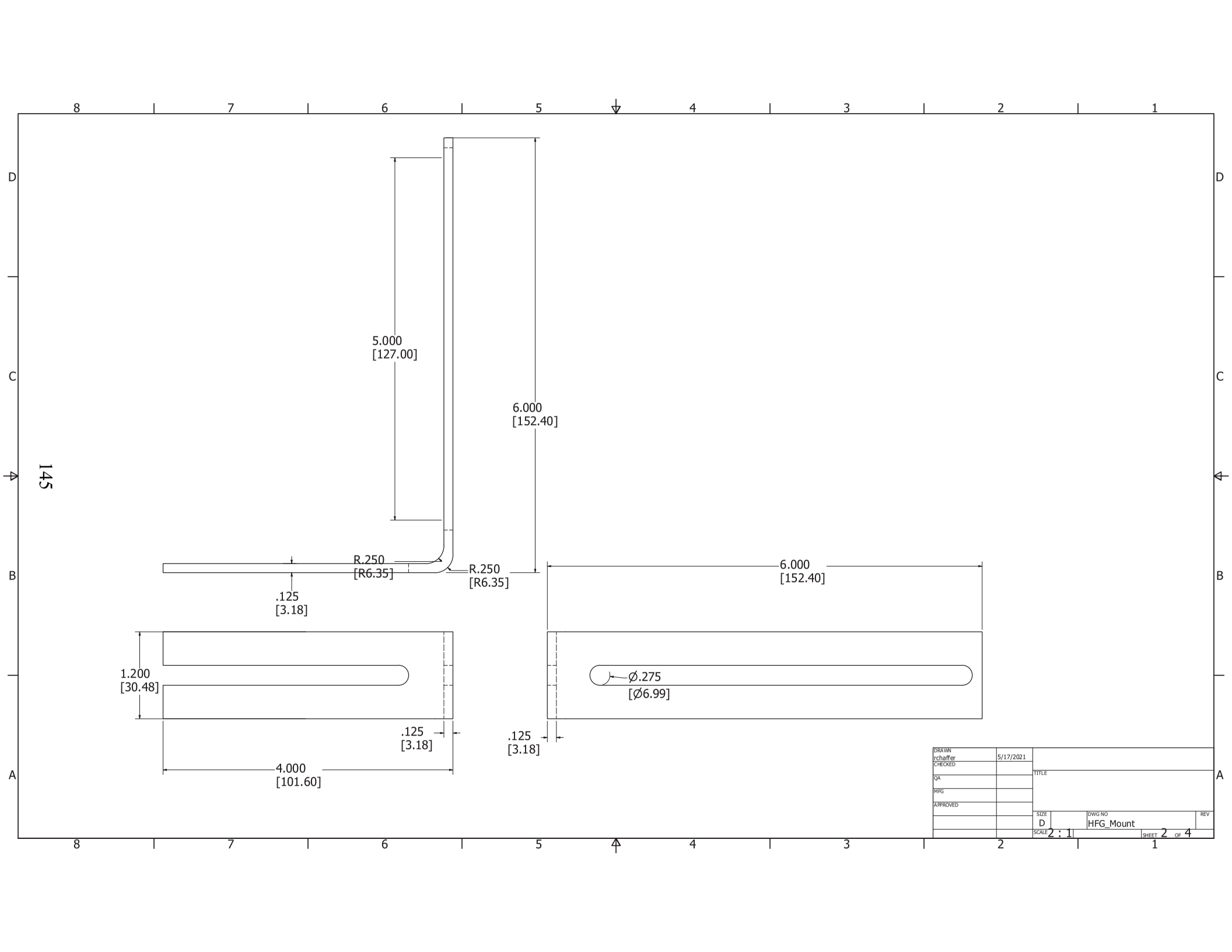
5.000
[127.00]
6.000
[152.40]
R.250
[R6.35]
R.250
[R6.35]
.125
[3.18]
6.000
[152.40]
1.200
[30.48]
Ø.275
[Ø6.99]
.125
[3.18]
.125
[3.18]
4.000
[101.60]
145
DRAWN
rchaffer
5/17/2021
CHECKED
QA
MFG
APPROVED
TITLE
SIZE
D
DWG NO
HFG_Mount
REV
SCALE
2 : 1
SHEET
2
OF
4

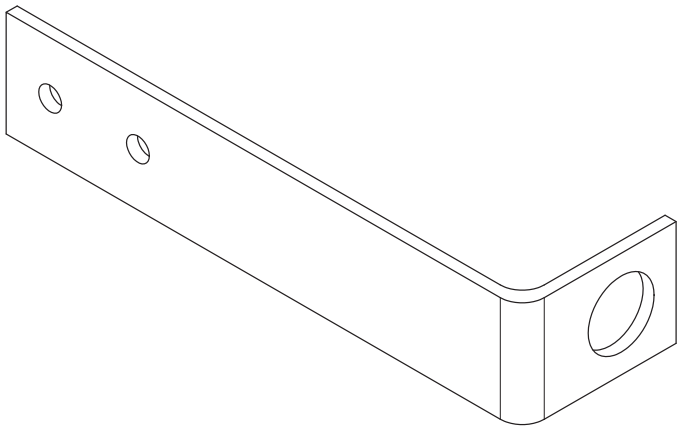

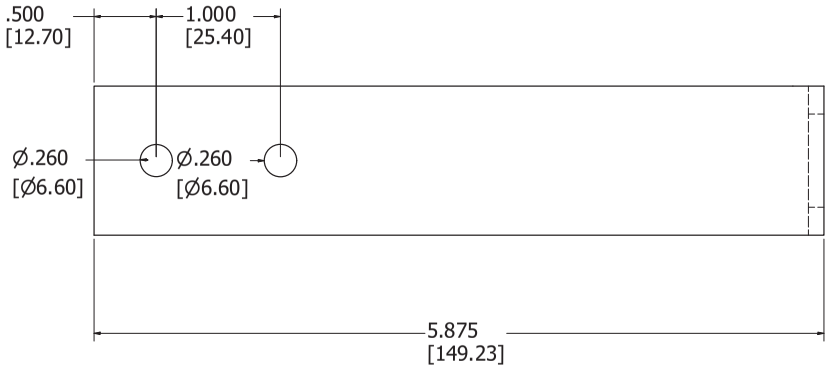

146

DRAWN rchaffer	5/17/2021	
CHECKED		
QA		TITLE
MFG		
APPROVED		
		SIZE D / DWG NO HFG_Mount / REV
		SCALE 2 : 1 / SHEET 3 OF 4

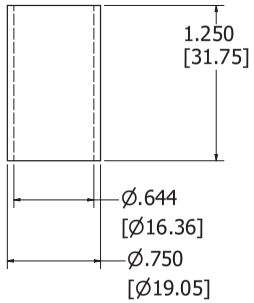

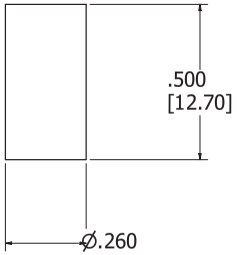

147

DRAWN rchaffer	5/17/2021	
CHECKED		TITLE
QA		
MFG		
APPROVED		
SIZE D	DWG NO HFG_Mount	REV
SCALE 2 : 1	SHEET 4 OF 4	

B: FPA Standard Operating Procedures

B.1 FPA Start Up Procedure

Step 1: Visually inspect the Apparatus and its supporting amenities for damage or wear. If damage is present, resolve the issue before proceeding to step 2. Additionally, take preventative measures to ensure the safety of yourself and others. This includes the use of protective eye equipment, covering the window on the door and turning in both safety lights to notify others the FPA is running and to not enter.

Figure B.1: *All doors are shut with safety lights on.*

Step 2: Clean Lamp quartz lenses before use. Before each use, wipe the lamp lenses with a Kimwipe to ensues they are free of fingerprints and dirt.

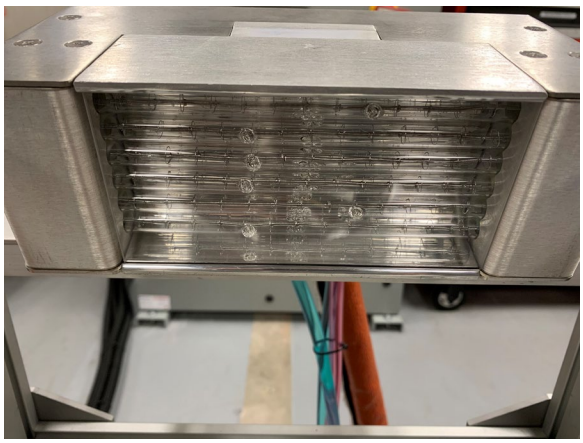

Figure B.2: *Example of clean quartz lamp lens.*

Step 3: Turn on the main water feed line for the FPA located above the sink. Rotate the green handle counterclockwise 90 degrees to start water flow.

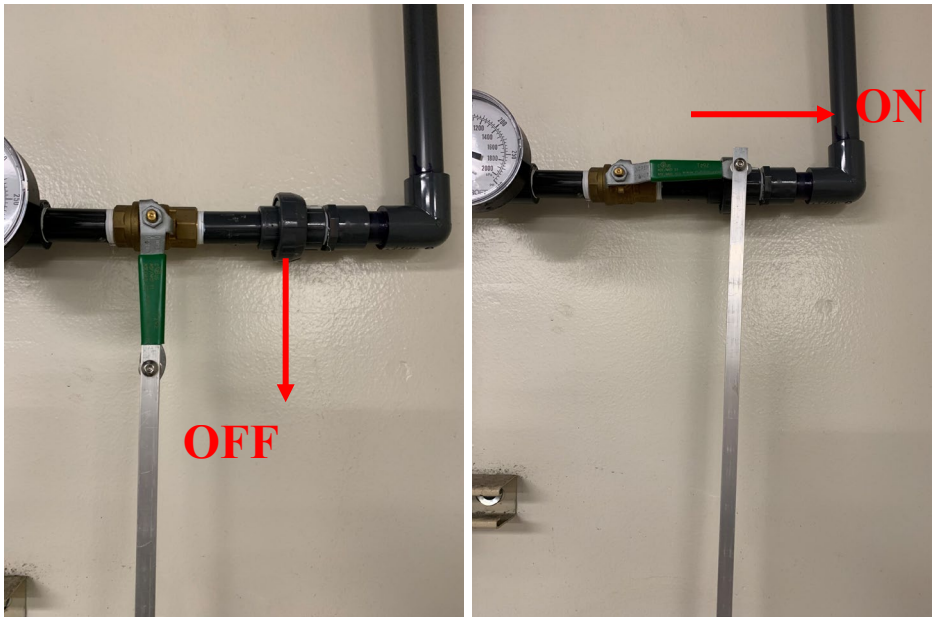

Figure B.3: *Main water feed valve (green handle) rotated 90 degrees to the on position.*

Step 4: Walk over to the FPA Control Area. On the wall there is a red handle valve. Rotate this handle 90 degrees counterclockwise. This is the water valve for the entire FPA cooling system. At this step, the only active cooling circuit is the Air Distribution Camber Coil. Additional steps are needed for the Lamp and Outer shield cooling circuits, as discussed in steps 6 and 7.
Step 5: Turn on the compressed air, used for FPA cooling and air distribution chamber experiment air. Next to the red handle valve in step 4, there is a yellow handle valve. Slowly rotate the yellow handle counterclockwise 90 degrees. The air system will be under 60psi of pressure. Be ready to turn the valve off in a leak occurs.

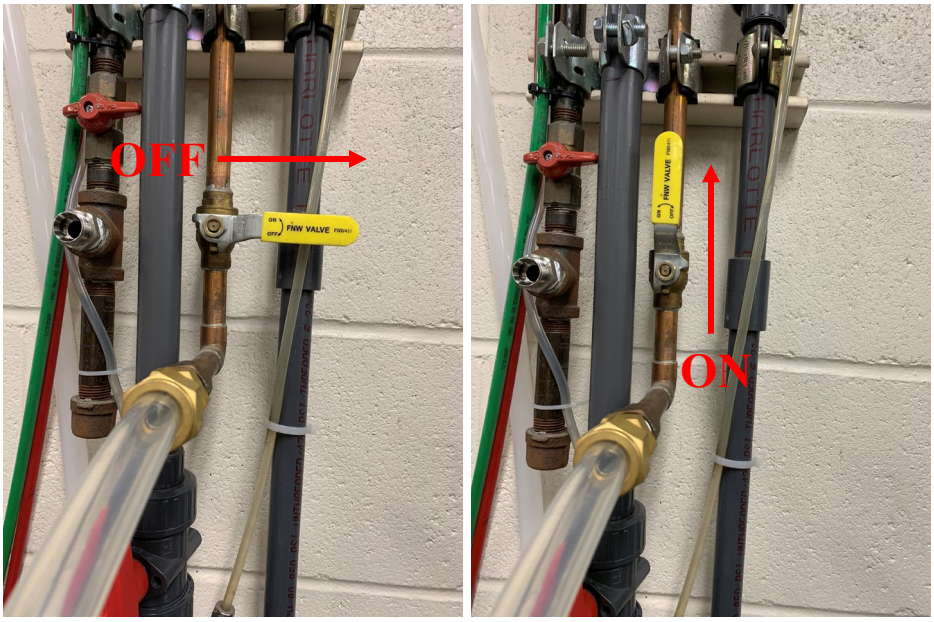

Figure B.5: *Compressed air valve turned 90 degrees counterclockwise to the on position.*

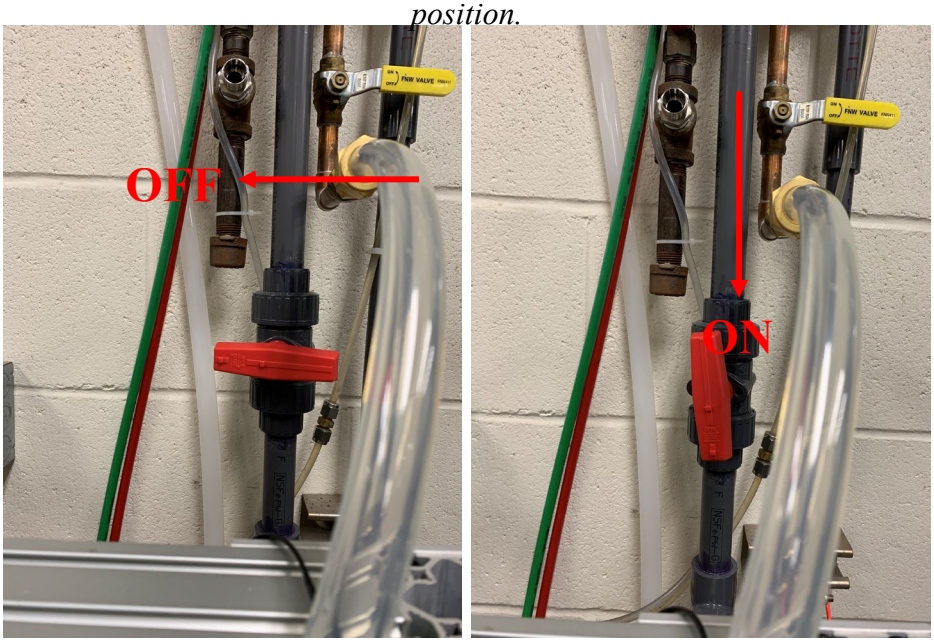

Figure B.4 *FPA cooling system water valve rotated 90 degrees to the on position.*

Step 6: Turn Power on for FPA.

A: Turn the main power disconnect switch on. This is located on the wall next to the FPA Control Panel Area. Push the handle upwards to the "ON" position.

Figure B.6(a): *Main power disconnect turn to the on position.*

B: Turn the power switch on for FPA Lamp Controller. This is located on the front face of the Lamp control Panel. Rotate the red handle clockwise 90 degrees to the "ON" position. At this point the lamp controller will begin booting up. The process may take a few seconds, but when it has finished, the control screen will light, and you will be able to interface with and control the lamps.

Figure B.6(b): *FPA lamp controller power switch turned to the on position.*

Step 7: Activate the lamp cooling circuit. This is done by pushing the "COOLING START" button on the lamp controller screen, located on the bottom left-hand side. When pressed, you should have audible and visual confirmation of flow going to the lamps. The lamp cooling floe meters, located on the front of the FPA Control Panel, should be reading and set to 4 GPM for Water and 13 SCFM for air. These flow rates allow for ample lamp cooling while also allowing flow for additional FPA operations. If no flow is detected by the Lamp Controller, the cooling will automatically stop, an alarm will be present on the lamp controller screen. The Lamp cooling will turn on and off through the cycle of heater use. This is the only cooling that should be turned on and off when the FPA is in operation.

Figure B.7(a): *FPA Lamp controller dashboard.*

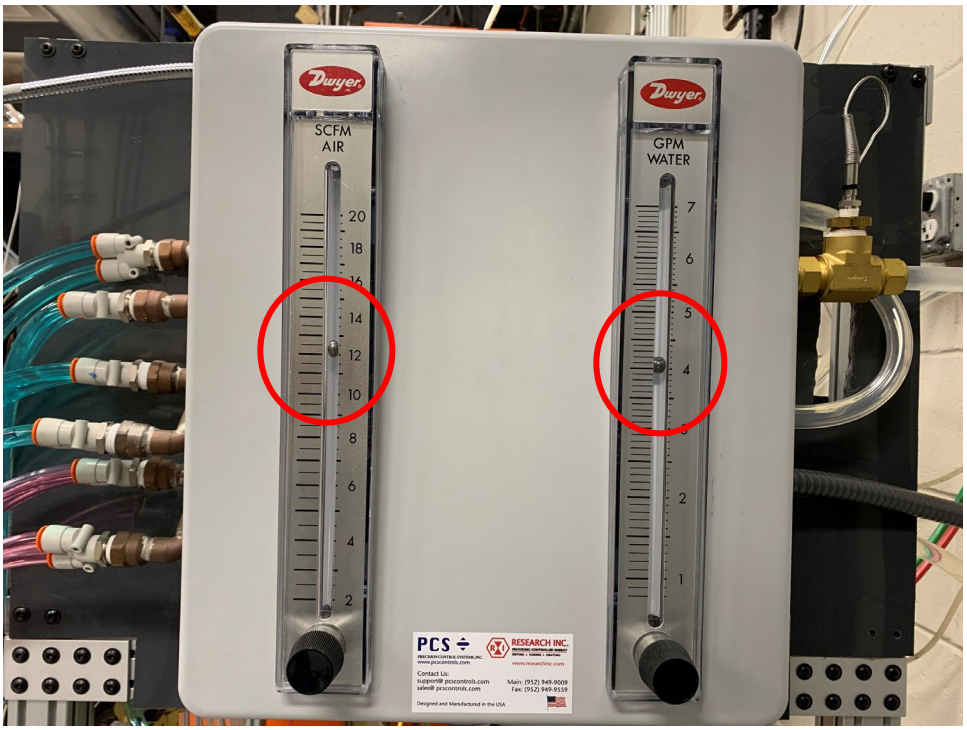

Figure B.7(b): *FPA Cooling flow meters at desired set point.*

Step 8. After the Lamp cooling has run for 5 minutes, it is time to turn the Outer Shield cooling circuit on. The valve is located on the back side of the FPA Control Panel Front Face. Rotate this valve counterclockwise 90 degrees. Allow 5 minutes for the water to circulate through the system.

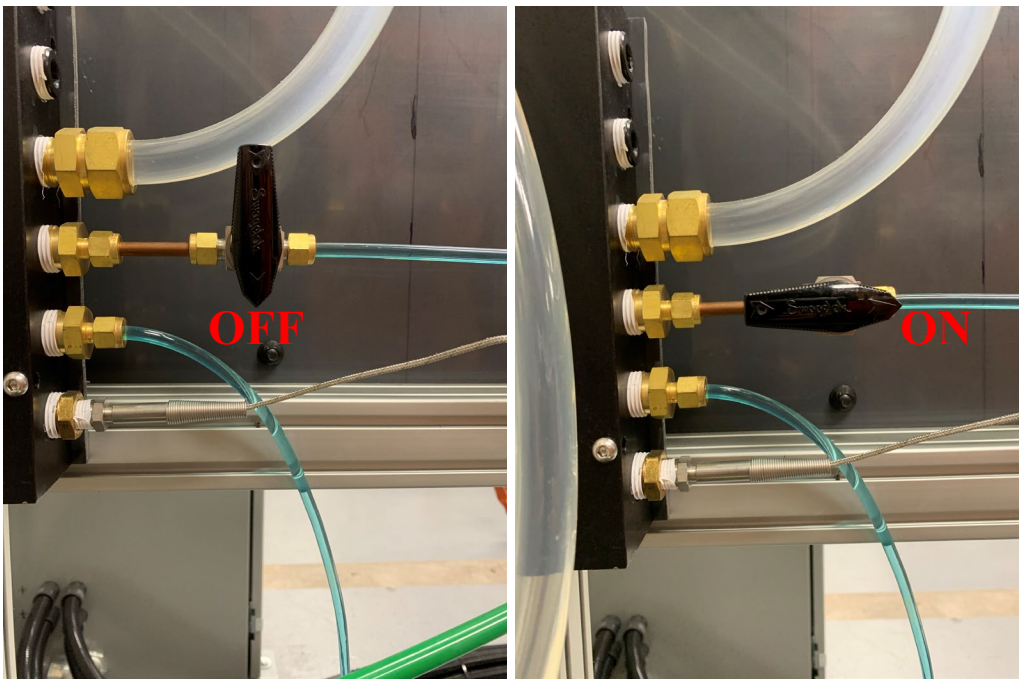

Figure B.8: *Outer shield cooling circuit valve, turned fron the off to on position.*

Step 9: Go to the FPA Laptop and open the LABVIEW Code "FPA_Temp_Data_Logging - Copy.vi". This code will monitor the water temperature of all cooling circuits and the heat flux produced by the lamps, only when a heat flux gauge is present. When viewing the temperature at the start of the day, they should all read ± 2°C from each other. If the viewed measurements do not meet this threshold, inspect the thermocouples for damage and proper connection.

Step 10: Select the power level of the lamps. This is done by "Output %" button on the lamp controller screen. The power is measured in percentage and ranges from 0% to 100%. You can use the Power to Heat Flux Curve to gain a first order estimate of what power level will yield the desired heat flux.

Figure B.9(a): *Location of where to press to change power level.*

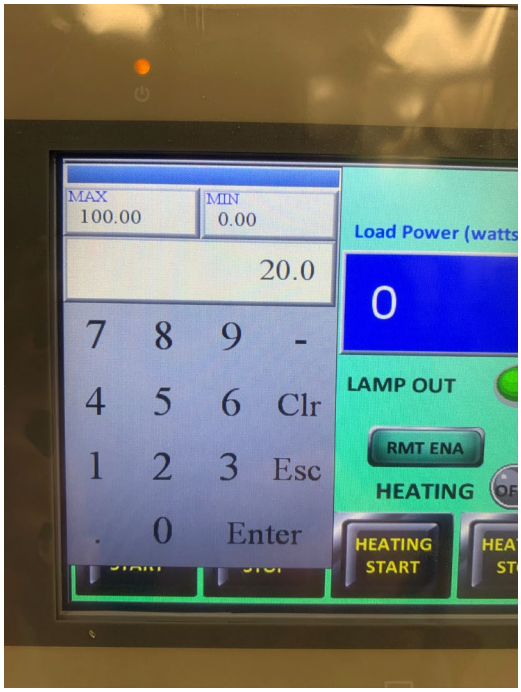

Figure B.9(b): *Input screen for change of power level.*

Step 11: Turn the Lamps on. The last step is to turn the lamps on. This is done by pushing the "HEATER START" button on screen. When you are done, you press the "HEATER STOP" to turn the lamps off.

Figure B.10: *Heater start and stop location on screen.*

B.2 FPA Heat Flux Gauge Procedure

Step 1: Obtain heat Flux Gauge and Heat flux gauge mount.

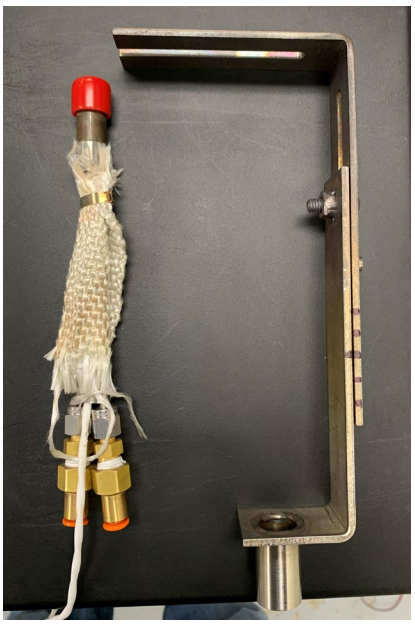

Figure B.11: *Heat flux gauge and mount used in the FPA.*

Step 2: Slide heat flux gauge into the upper slot on the mount. It should slide in nicely, with no space between the mount surface and the gauge surface.

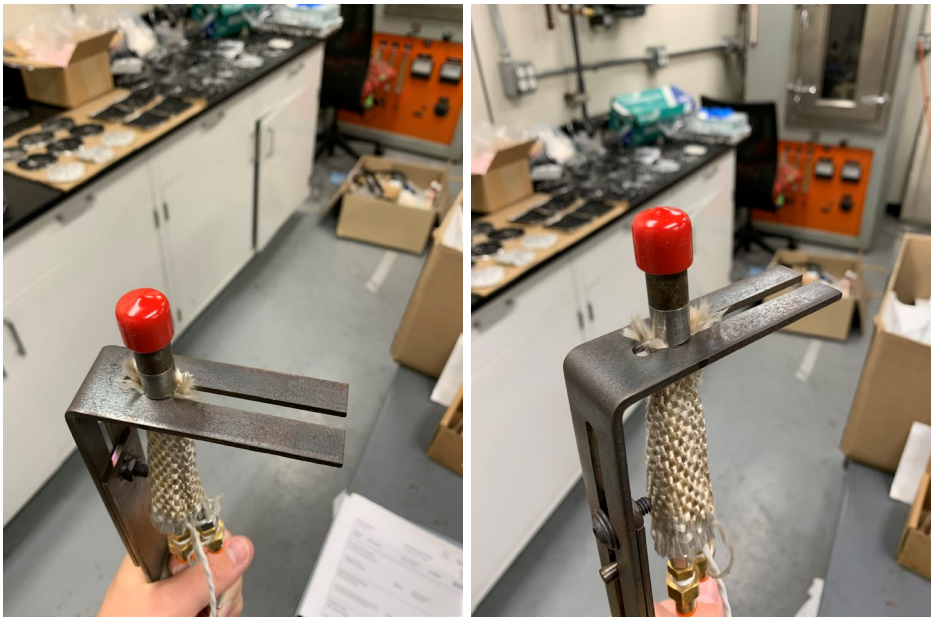

Figure B.12: *Heat flux gauge slid into mount.*

Step 3: Slide Heat flux gauge connection wires through the passthrough at the bottom of the mount.

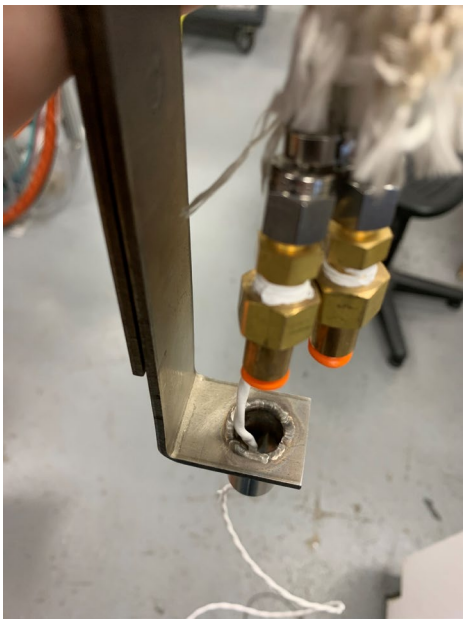

Figure B.13: *Heat flux gauge sensor wires run through mount center passthrough.*

Step 4: Run Water lines for the heat flux gauge. Take the Blue water lines and attach to a water inlet and outlet. There are various location in the lab, anyone will work.

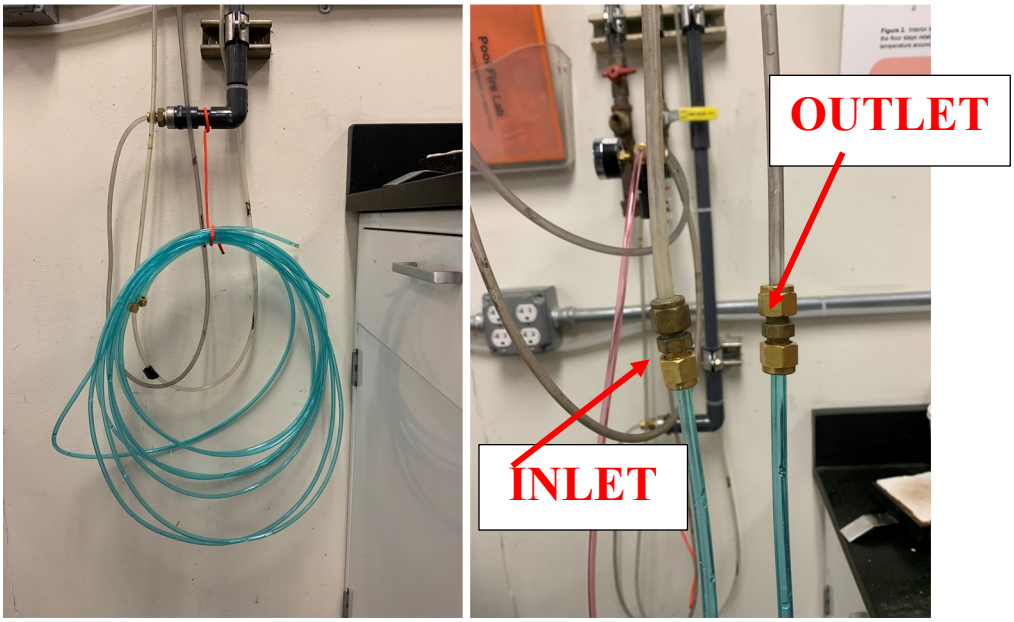

Figure B.14: *Water Lines used for the heat flux gauge (left), inlet and outlet connections made (right).*

Step 5: Take the open end of the water lines over to the FPA. Set them aside for use in a later step.

Figure B.15: *Open ends of water lines set aside at FPA.*

Step 6: Take the heat flux gauge and mount over to the FPA. From the top, feed the connection wires down through the center of the FPA until the portion covered in black heat shrink tubing is completely visible on the underside of the air distribution chamber.

Figure B.16: *Heat flux gauge wires feed through the top with the heat shrink portion visible on the underside.*

Step 7: Connect the Water lines to the Heat flux gauge. From the bottom of the air distribution chamber, feed the water lines up through the same passage at the heat flux gauge connection wires. Following the same path as the connection wires, take the water lines and insert one into each push-to-connect fittings on the gauge. You may need to slide the gauge out of the mounting slot to perform this operation. Once the water lines are connected, wrap all exposed plastic water lines with aluminum foil. There will be 80.0 mm of exposed line that needs to be covered.

Figure B.17: *The four stages of running the water lines into the heat flux gauge.*

Step 8: Insert heat flux gauge mount into the fitting at the bottom of the air distribution chamber. By pulling slightly on the water lines and connection wires from the underside of the chamber, you can help guide the mount into position. DO NOT pull forcefully the water lines or wires, you should only use this as a guide to help get the mount in position by keeping the lines and wires straight, allowing them to slide easily through the hole. If force is required for install, inspect everything for damage or if it is caught on something.

Figure B.18: *Heat flux gauge mounted in air distribution chamber fitting.*

Step 9: Now that all water connections are made, it is time to turn the water on for the heat flux gauge. Rotate the water valve 90 degrees to the on position, this could be clockwise or counterclockwise depending on its location. When the water is turned on, it will purge the air out of the system. As a check, watch the transparent blue water lines, when water flow is seen, that is a good indication the heat flux gauge is ready to use.

Step 10: Walk back to the air distribution chamber and visually inspect the heat flux gauge for water leaks. If water is leaking, turn the water off and address the issue.

Step 11: Make electrical connection to data acquisition system. This is done via a white thermocouple connection. Screw the heat flux gauge wire leads into the male side and plug it into the female side. To ensure proper connection and response, start the LABVIEW Code "FPA_Temp_Data_Logging - Copy.vi" and run a lighter close to the surface of the gauge. There should be an increase in heat flux. if no increase is detected, troubleshoot for the problem. In addition to temperature monitoring, this code will read the heat flux when a gauge is properly connected.

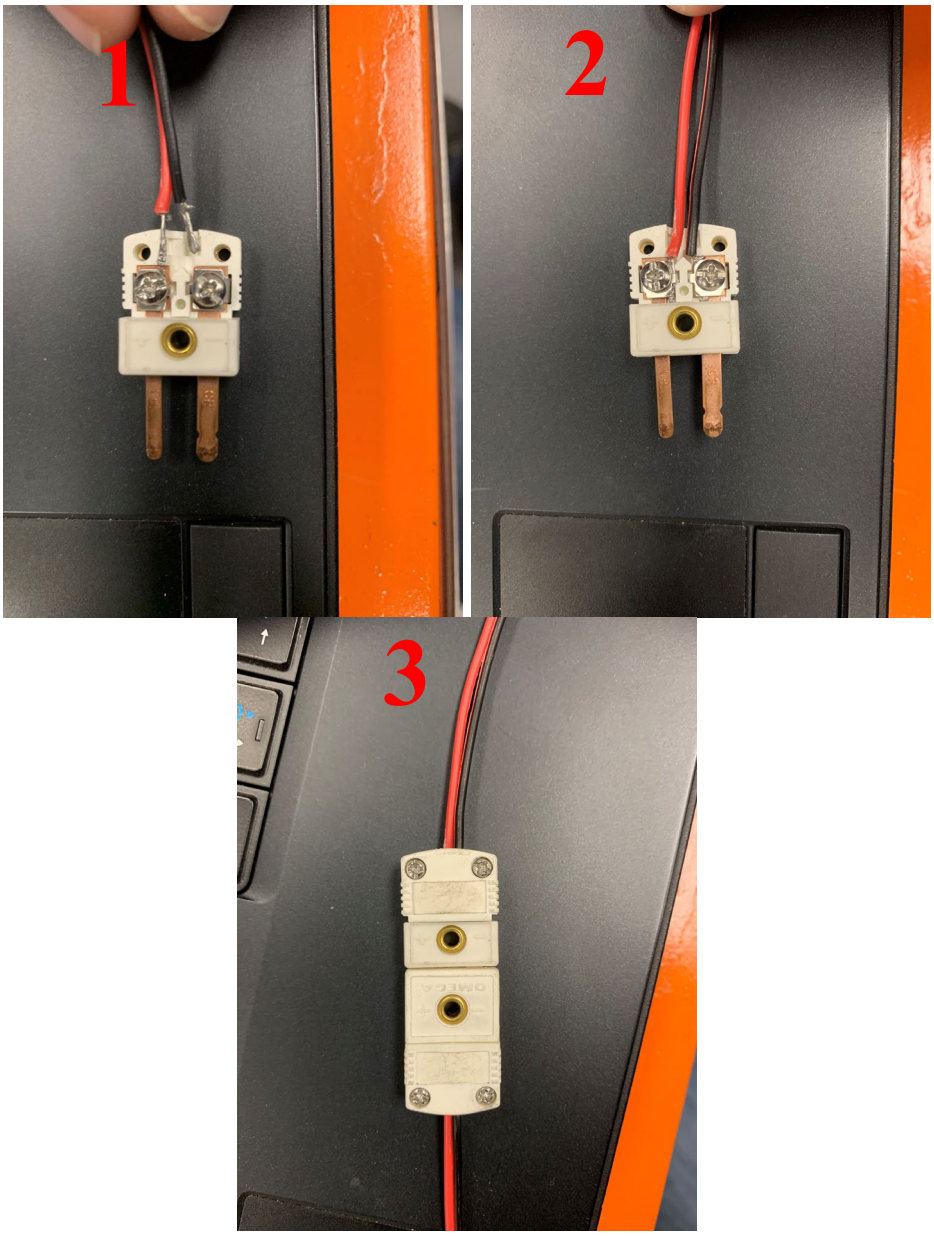

Figure B.19: *Three stages of connection the heat flux gauge to the computer.*

Step 12: Place Quartz tubes on top of air distribution chamber. The taller one goes in the bottom, then the aluminum adapter followed by the shorter one. Each quartz tube connection point should have an insulation gasket to promote an airtight seal. If gaskets are damaged, replace with a new one.

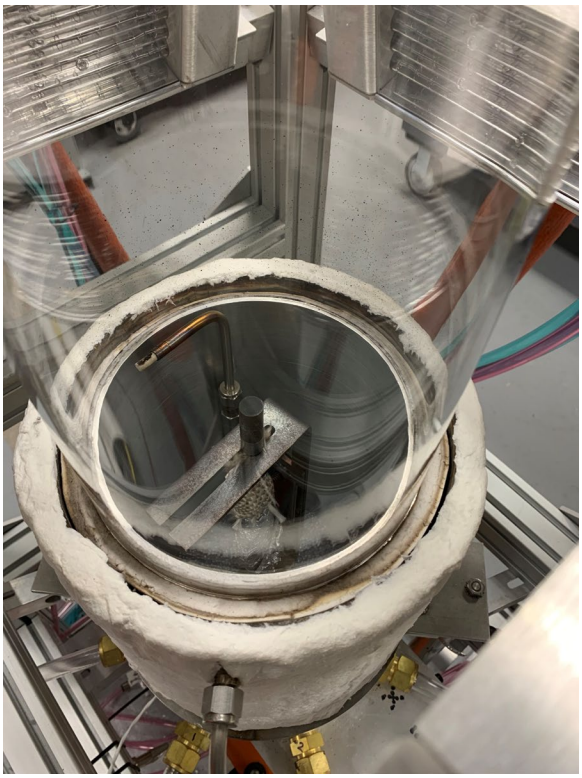

Figure B.20: *Heat flux gauge mounted with quartz tube installed.*

Step 13: Turn on experiment air for the air distribution chamber. When the heat flux is taken, it is done with air flowing through the air distribution chamber. Turn on the flow controller and change the set point to 200 SLPM of air. If the setpoint is made and the digital display does not depict a flow being present, ensure the Main air is on and there are no leaks in the system.

Figure B.21: *Experiment air flow controler with set point of 200 SLPM.*

Step 14: The heat flux of the apparatus is now ready to be taken. Raise the outer cooling shield and follow steps 1 through 11 of FPA Start Up Procedure. The Lamps should have a 2-minute warm up time before dropping the shield and exposing the gauge. It may take a few iterations to get the desired heat flux.

> **Note**: due to the nature of the apparatus, the heat flux drifts through the duration of exposure. Due to this, the heat flux is taken to be the average values from 45 seconds to 75 seconds after the gauge is exposed to the lamps.

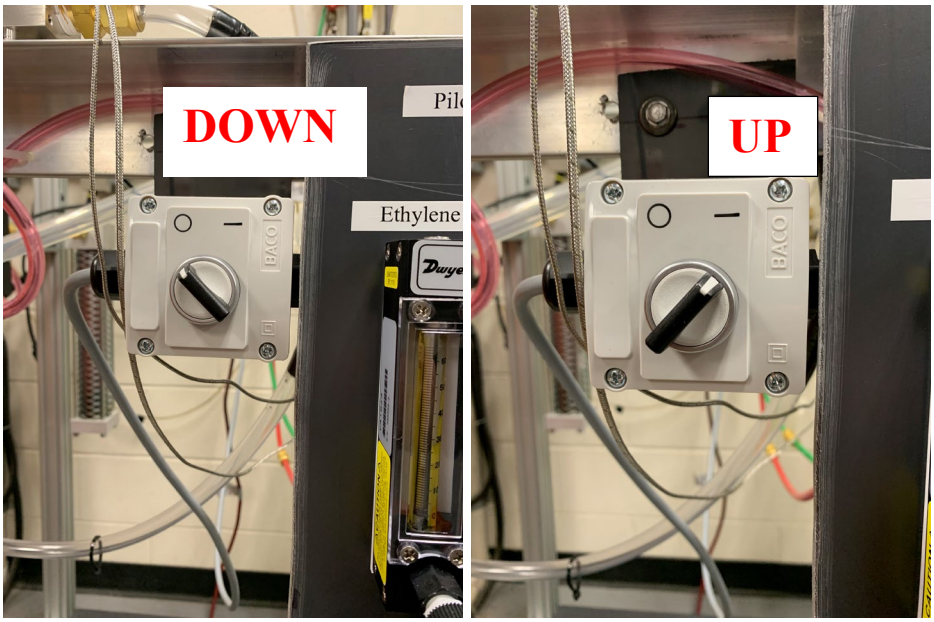

Figure B.21(a): *Outer shield switch for location control.*

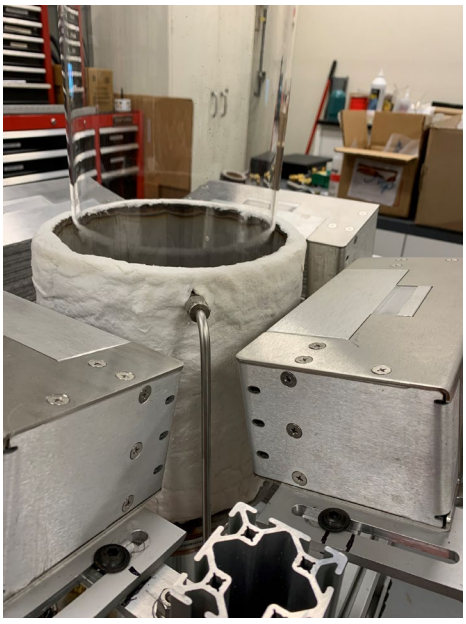

Figure B.21(b): *Outer shield in the up position.*

Step 15: When the desired heat flux is found, and its corresponding power level, reverse the above steps to remove the heat flux gauge from the apparatus.

> **Note**: The apparatus will be hot after this. Allow some time for the apparatus to cool, about 15 minutes before trying to remove the gauge.

B.3 Experiment Running Procedure

Note: This procedure is written under the pretense that the FPA Heat Flux Gauge Procedure was run. If that is not the case, it is imperative that the experiment air is on, as outline in step 13 of " the FPA Heat Flux Gauge Procedure", for the duration of this procedure.

Step 1: Take the prepared sample and place it in the sample dish.

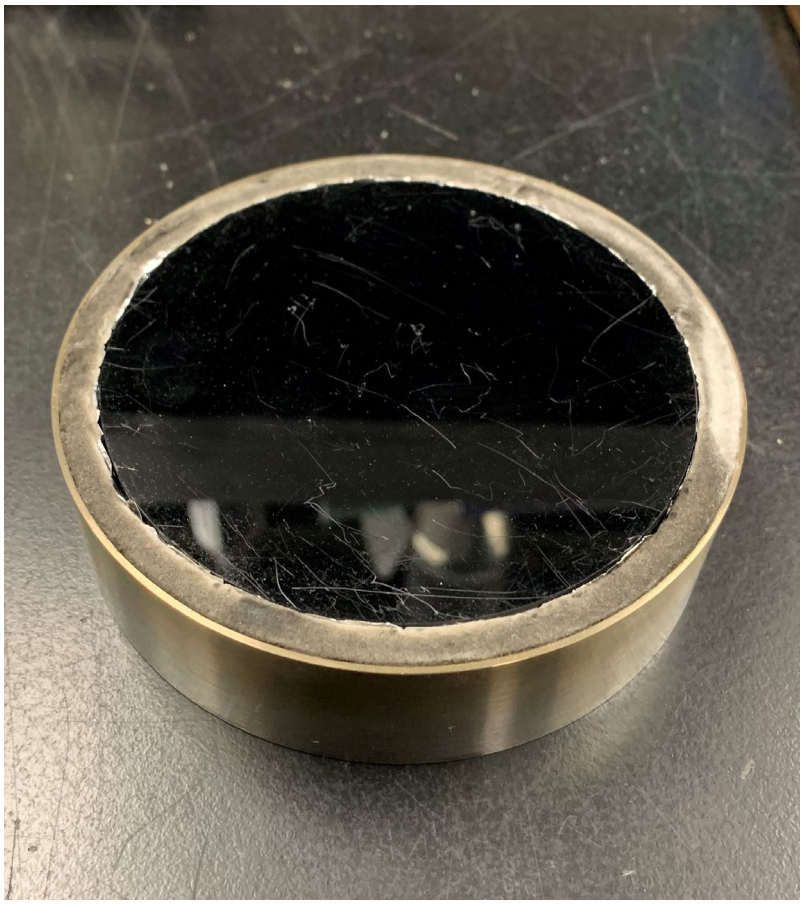

Figure B.22: *Representative example of what a sample in the sample dish looks like.*

Step 2: Install Sample bearing holder into air distribution chamber. Install the bearing holder in the fitting, tighten into place by hand. If the bearing is over tightened, and the fitting begins to spin loose, it will need to be re tightened on the lower connection.

Figure B.23(a): *Bearing holder.*

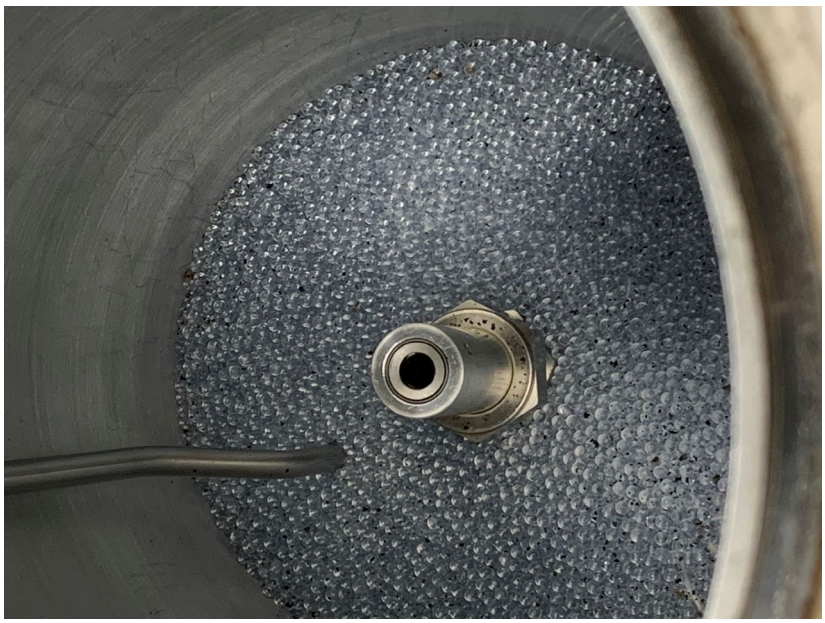

Figure B.23(b): *Bearing holder mounted in air distribution chamber.*

Step 3: Install Sample holder into air distribution chamber. The sample holder will drop in from the top through the bearing holder. When it passes through the bottom of the air distribution chamber, install the adjustable base foot, and place it onto the load cell.

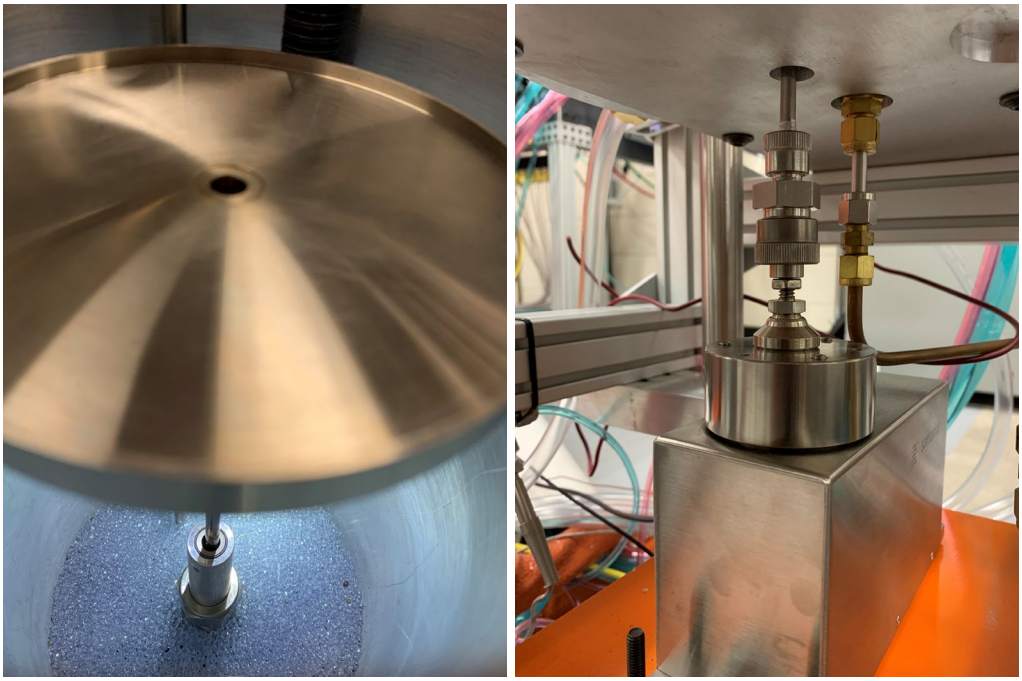

Figure B.24: *Sample holder through the bearing with the adjustable base foot installed.*

Step 4: Center and level the sample holder to allow the load cell to be zeroed. This process may take some time, if necessary, place a piece of metal between the load cell and the sample holder. This will help reduce the fluctuation in mass signal. When the mass signal variation is no more than ±0.03 grams it is time to proceed.

Step 5: Ensure proper connectivity with computer. Run the mass recording software "SmartLux Simple Data Logger". Change the output file name before running the program. Press start and ensure data is being transferred and no errors are present. If errors occur, troubleshoot the issue.

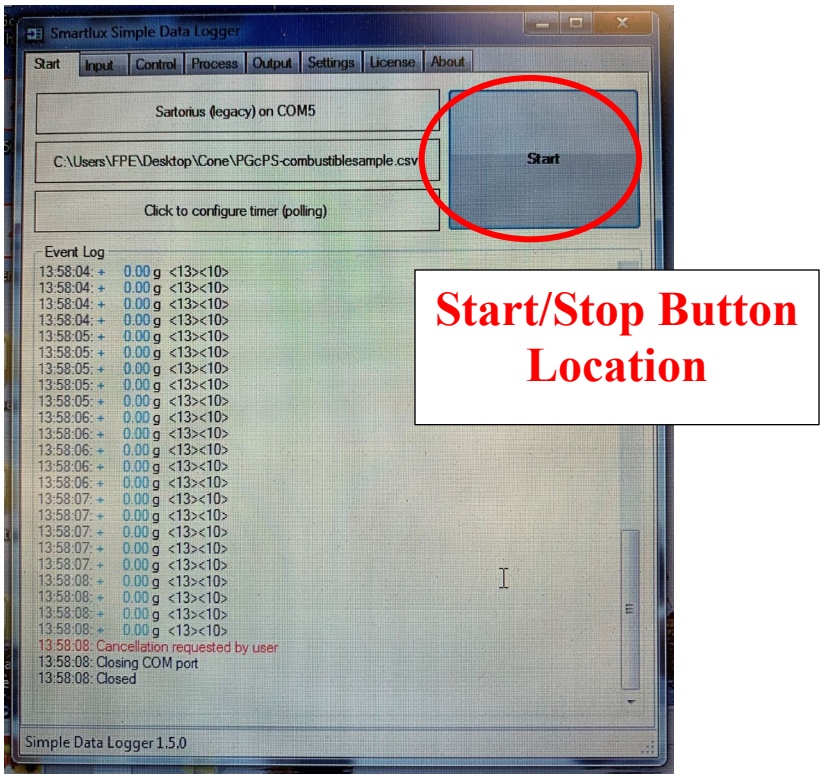

Figure B.25(a): *Mass recording software start screen.*

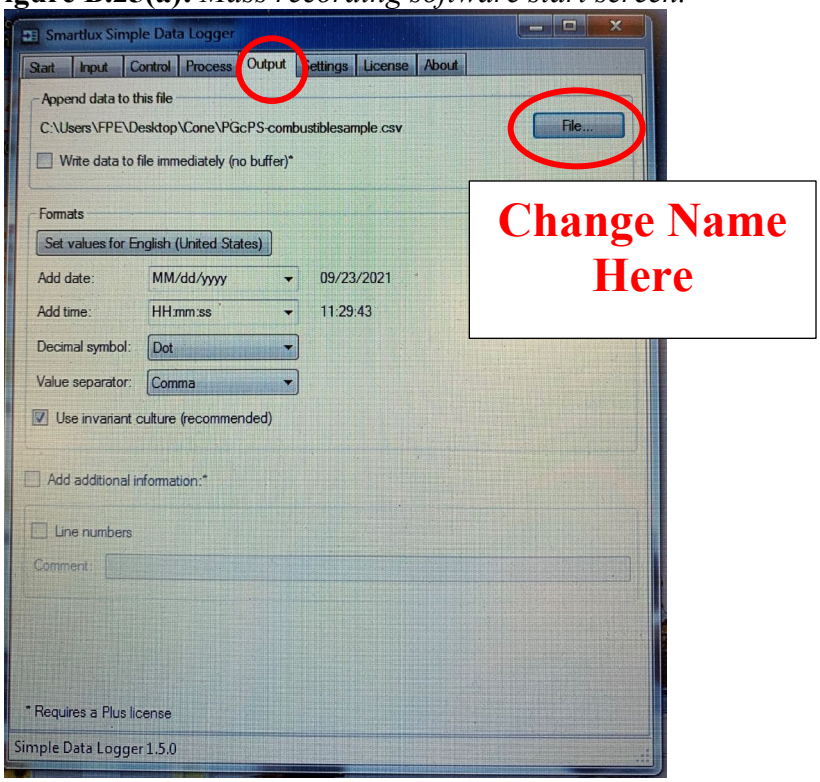

Figure B.25(b): *Mass recording software output screen.*

Step 6: Follow the Pilot flame starting procedure outline lined in " FPA Pilot Flame Procedure".

Step 7: place the sample dish and prepared sample onto the sample holder assembly. The sample dish and sample holder are a matching set, meaning the sample holder is machined to accept the dish. The dish will sit inside the sample holder recessed area. The mass readout should match that of an external bench top mass balance with a range of ±0.50 grams.

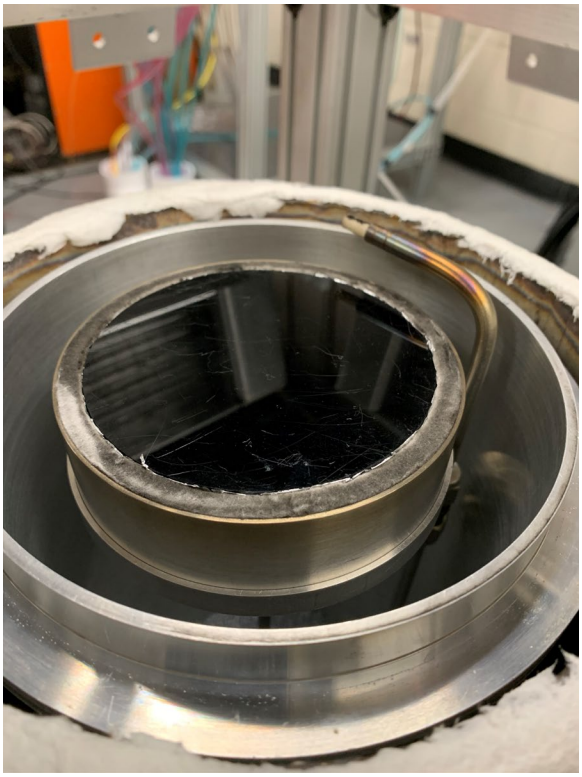

Figure B.26: *Sample dish mounted on top of sample holder.*

Step 8: Similar to step 4, ensure the mass fluctuation is within ±0.03 grams with the sample dish and prepped sample installed. This is done by rotating the sample dish.

Step 9: Reignite the pilot flame. Leave the pilot flame to the side, it will be rotated into place in a later step.

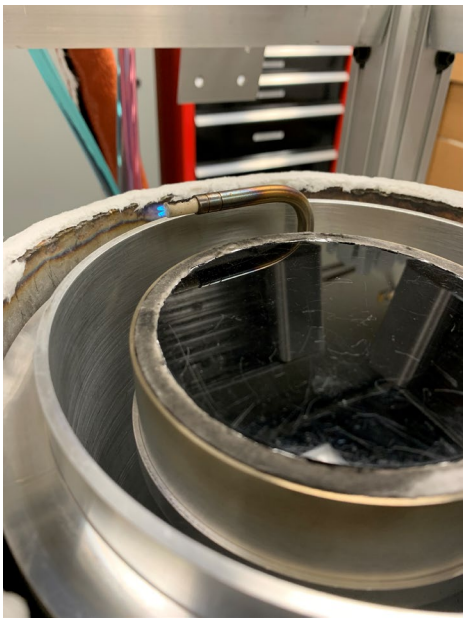

Figure B.27: *Pilot flame running off to the side with sample in place.*

Step 10: Place Quartz tubes on top of air distribution chamber. The taller one goes on the bottom, then the aluminum adapter followed by the shorter one. Each quartz tube connection point should have an insulation gasket to promote an airtight seal. If gaskets are damaged, replace with a new one.

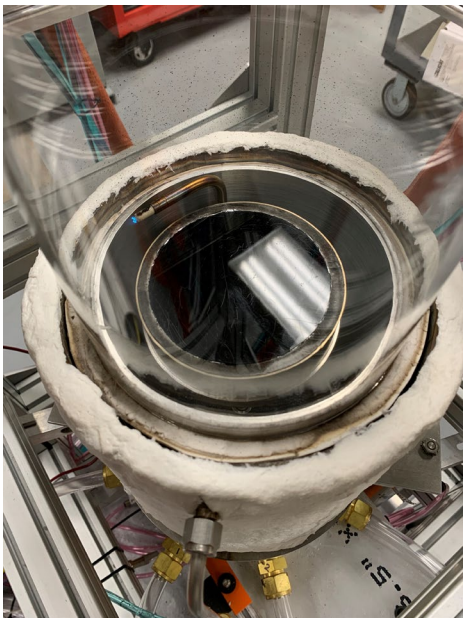

Figure B.28: *Quartz tubes in place.*

Step 11: Raise the outer shield.

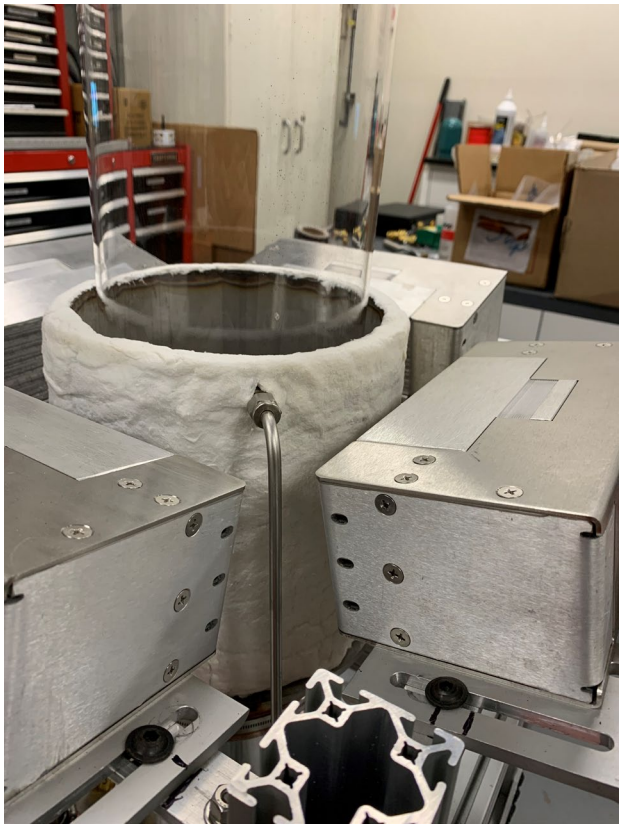

Figure B.29: *Outer Shield raised into position.*

Step 12: Start mass recording program. Through the use of an external stopwatch, record the following times via a lap function.

1. Start of experiment (Time zero), Start mass recording and stopwatch at the same time
2. Lamp Power on. This is when the lamps are powered on, historically this has been done 30 seconds after the start of mass recording.
3. Dropping of the outer shield, exposing the sample. This is done 120 seconds after the lamps are power on.
4. Time to ignition initial. This is when a flame from the sample is first visible.
5. Tine to ignition final. This is when the sample has flaming across the entire surface.
6. Time to extinction. This is when the sample has extinguished.
7. End. This is when the mass recording was stopped.

Notes:
The pilot flame should be spun into place 1 minute into the lamp warmup period.
If desired, the user can also run the LABVIEW Code "FPA_Temp_Data_Logging - Copy.vi" to monitor the apparatus temperatures throughout the experiment.
When the sample reaches extinction, the lamps should be shut off.
Allow the apparatus to cool for at least 5 minutes before removal of quartz tubes and sample dish.
During the experiment, visually inspect the apparatus for damage or overheating. If something is present, shut lamps down immediately and address the issue.

Step 13: Repeat the procedure as needed for various material and heat fluxes.
Note: The quartz tubes should be wiped clean after/before each use. This is done in four stages. Take proper safety measures to prevent contact with soot.

1. Using a dry shop towel/paper towel, wipe the bulk of the soot out.
2. Using a shop towel/paper towel with acetone, wipe the tube out until it is visually clean.
3. Using a large Kimwipe, wipe the inside of the tube. This should be repeated until the quartz tubes are clean.
4. Ensure no fingerprints are present on the quartz tube before installing.

B.4 FPA Pilot Flame Procedure

Step 1: Ensure the downstream pilot flame valve is in the off position. This for safety purposes to endure the premixed ethylene and air are not exiting the system when a flame is not present.

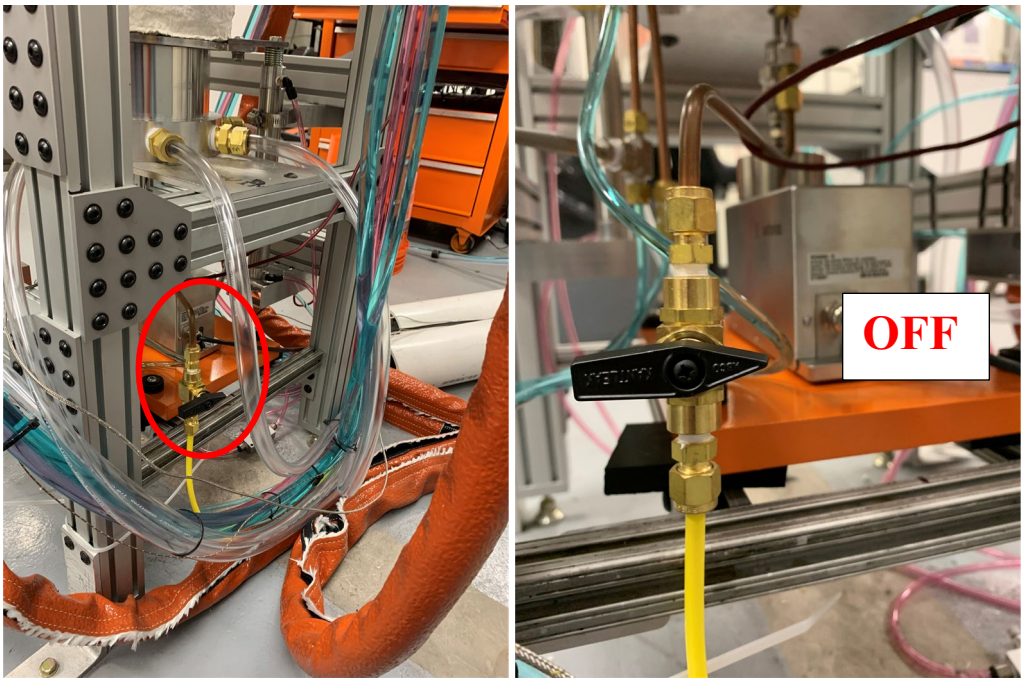

Figure B.30: *Pilot flame downstream valve location, in the off position.*

Step 2: Turn on Ethylene and Compressed air gas cylinders. Turn the main valve on top of the tank counterclockwise and the safety valve, lower left side of the regulator clockwise. The regulator pressure should be preset. The Ethylene should be set at 38 PSI and the Compressed Air at 40 PSI.

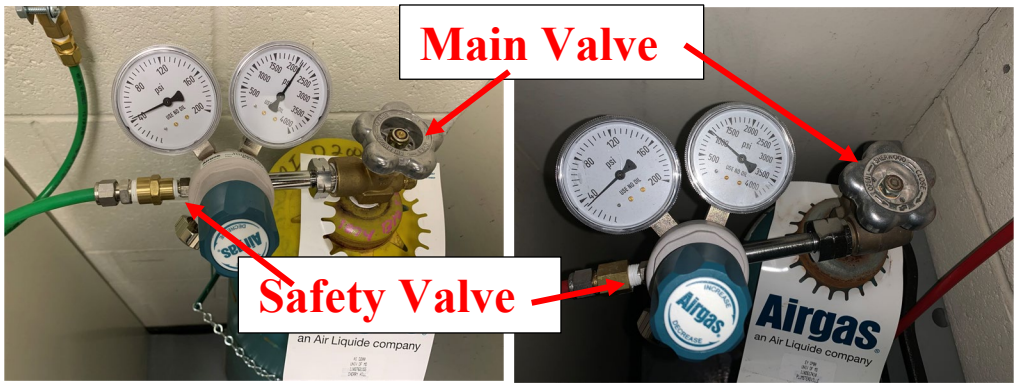

Figure B.31: *Air regulator (left) and ethylene regulator (right) at their pressure set point.*

Step 3: On the pilot flame control panel, turn the needle valve counterclockwise 9.5 rotations to the open position.

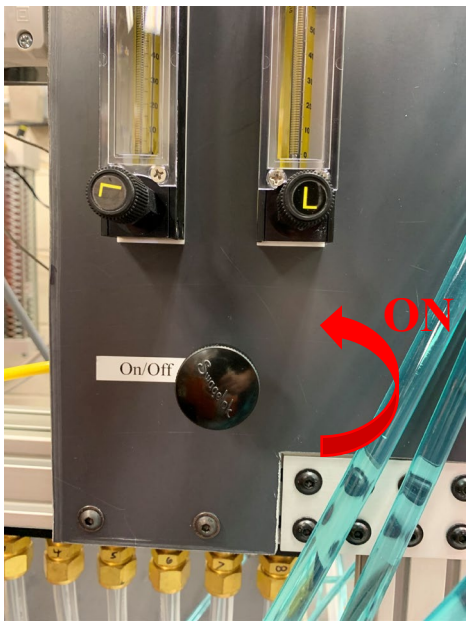

Figure B.32: *Pilot flame control panel on/off valve.*

Step 4: Take a lighter and hold it at the pilot flame location. Slowly turn the downstream valve counterclockwise 90 degrees to allow the prefixed fuel to exit and produce the flame.

> **Note**: It may take a few seconds for a flame to be visible due to the low flow rate of the mixture.

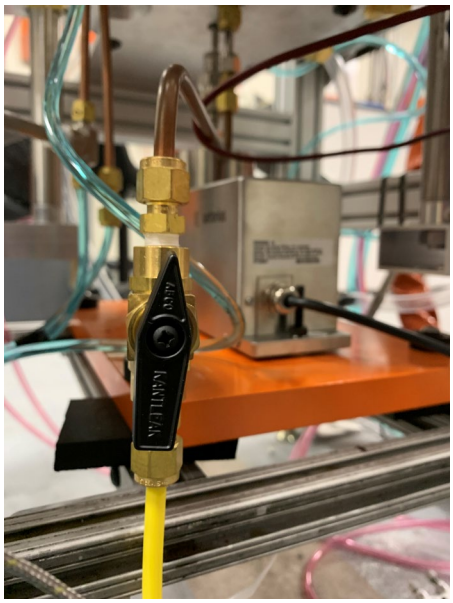

Figure B.33: *Pilot flame downstream value in the on position.*

Figure B.34: *Pilot flame before and after lighting.*

Step 5: Check the flow rates of the ethylene and air on their flow meters. In order ensure the flame is stoichiometry, the Ethylene flow rate should be set to 37 and the compressed air 38.

> **Note**: the flow meters have a scaled reading, meaning the number seen is not the true flow rate. The desired flow rate of Ethylene and Compressed Air is 20.75 ml/min and 297.5 ml/min respectively. At the prescribed flow rates, the flame is stoichiometric and has a length of 10 mm.

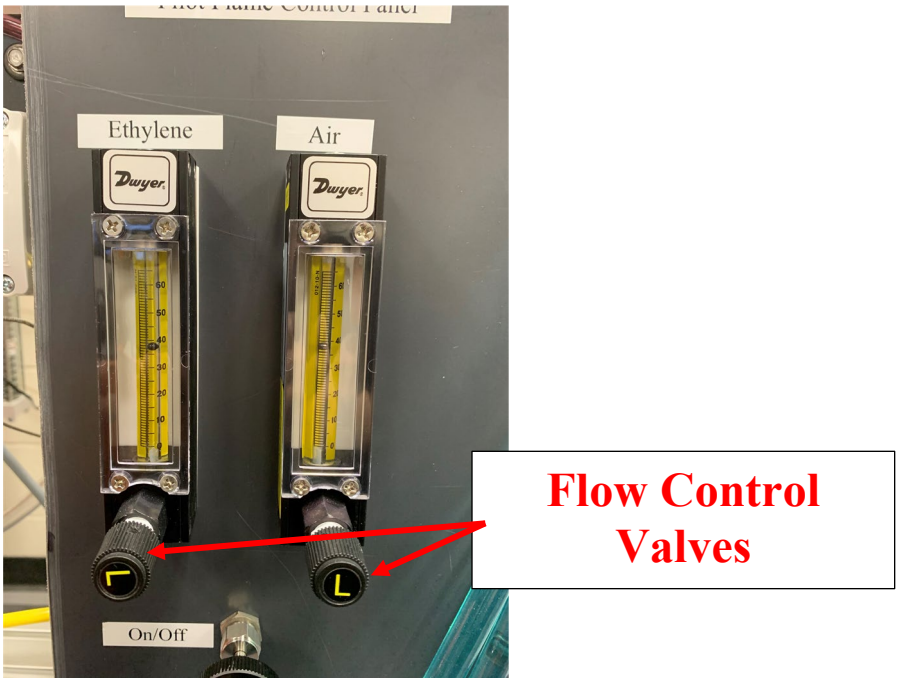

Figure B.35: *Pilot flame flow meters for ethylene and air.*

Step 6: Allow the pilot flame to run uninterrupted for 5 minutes to ensure constant flow. After this run time, turn the downstream valve off.

Step 7: Follow the procedure outlined in "Experiment Running Procedure".

> **Note**: When the pilot flame needs to be put into place over the sample, simply line the marks on the pully wire up and put into place. The black mark on the wire should be the starting point to wrap the wire around the stud.

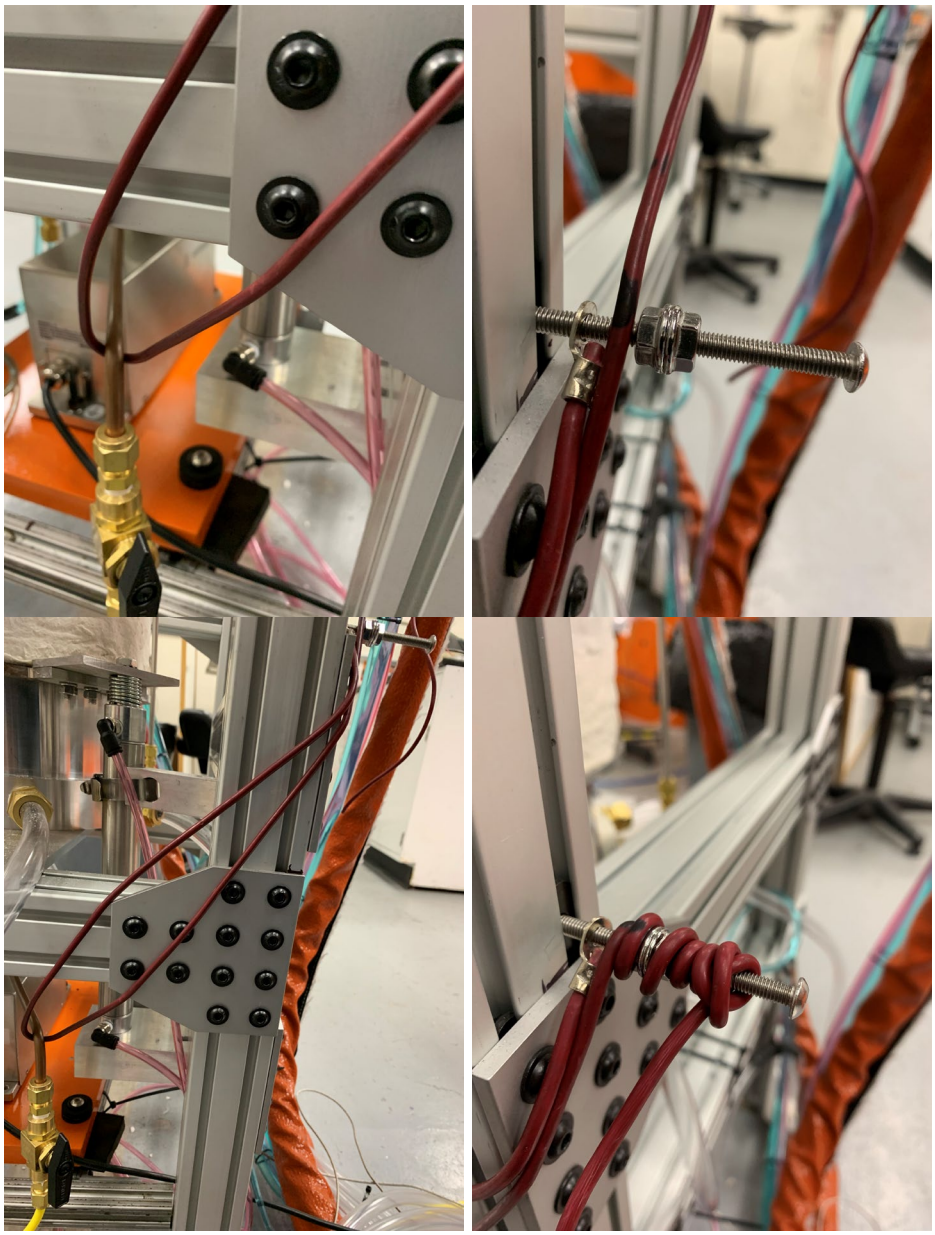

Figure B.36: *Visual representation of what the pilot flame location asjutment should look like.*

Figure B.37: *Location of Pilot flame over sample surface.*

Step 8: Reverse the procedure followed in steps 2 through 4 to disable the pilot flame safely and properly. Remember, the upstream valve is always the first to be shut off and the last to be turned on.

C: Load Cell Menu Settings

Menu Structure (Overview)

Level 1 [•]	Level 2 [••]	Level 3 [•••]	Codes
SETUP	BAL.SCAL. (Weigh cell functions)	AMBIENT Ambient conditions (Adapt filter)	1. 1. 1.
		APP.FILT. Application filter	1. 1. 2.
		STAB.RNG. Stability range	1. 1. 3.
		ST.DEL. Stability delay	1. 1. 4.
		TARING Taring	1. 1. 5
		AUTOZER. Auto zero	1. 1. 6
		WT.UNIT Basic weight unit	1. 1. 7.
		DISPLAY Display accuracy	1. 1. 8.
		CAL./ADJ. Function of the (Cal) key	1. 1. 9.
		CAL.ROUTINE	1. 1.10.
		CAL.UNIT Weight unit for calibration	1. 1.11.
		ZERO RNG. Zero range	1. 1.12.
		ZERO.ON Zero at Power On	1. 1.13.
		ON.TARE Tare/zero at power:	1. 1.14.
	INTERF. Interface	BAUD Baudrate	1. 5. 1.
		PARITY Parity	1. 5. 2.
		STOP BIT Number of stop bits	1. 5. 3.
		HANDSHK. Handshake mode	1. 5. 4.
		DATA BIT Number of data bits	1. 5. 5.
		DAT.PROT. SBI (ASCII) or printout	1. 5. 6.
	DAT.REC. (Print)	PRINT (manual/automatic)	1. 6. 1.
		STOP automatic printing	1. 6. 2.
		AUT.CYCL. Time-dependent autom. printing	1. 6. 3.
		TAR./PRT. Tare bal./scale after ind. print	1. 6. 4.
		PRT.INIT. Printout of appl. parameters	1. 6. 5.
		FORMAT Line format for printout	1. 6. 6.
		GLP ISO/GLP-compliant printout	1. 6. 7.
		TIME 12h/24h	1. 6. 8.
		DATE format	1. 6. 9.
	EXTRAS (Additional functions)	MENU Can Edit / Can change settings	1. 8. 1.
		HORN Acoustic Signal	1. 8. 2.
		KEYS (Keypad)	1. 8. 3.
		EXT.KEY External switch function	1. 8. 4.
		ON MODE Power-on mode	1. 8. 5.
		BACKLIT Display backlighting	1. 8. 6.
	RESET	MENU Factory settings	1. 9. 1.
APPLIC. Application programs	WEIGH		2. 1.
	UNIT Toggle	DISPLAY Display accuracy	2. 2. 2.
	COUNTING	RESOLUT.	2. 3. 1.
		REF.UPDT. Auto reference updating	2. 3. 2.
	PERCENT weighing	DEC.PLCS Decimal places	2. 4. 1.
	NET.TOT. Net total	COMP.PRT. Printout of components	2. 5. 1.
	TOTAL Totalizing	COMP.PRT. Printout of components	2. 6. 1.
	ANIMALW. Animal weighing	ACTIVTY. Animal activity	2. 7. 1.
		START	2. 7. 2.
	CALC. Calculation	METHOD (Operator)	2. 8. 1.
		DEC.PLCS Decimal places	2. 8. 2.
	DENSITY determination	DEC.PLCS Decimal places	2. 9. 1.
INPUT Input	ID NO.	ID input; max. 7 characters	3. 1.
INFO Information	VERSION, SER.NO., MODEL	Displays software vers., serial no., model	4. 1./.2./.3.
LANGUAGE (LANGUAG.)	ENGLISH (factory setting)		5. 1.
	DEUTSCH (German)		5. 2.
	FRANC. (French)		5. 3.
	ITAL. (Italian)		5. 4.
	ESPANOL (Spanish)		5. 5.
	PYCCK (Russian)		5. 6.
	POLSKI (Polish)		5. 7.
	CODES Menu shows codes (not texts)		5. 8.

Parameter settings: Overview

o = Factory setting; √ = User-defined setting

Level 1 [•]	Level 2 [••]	Level 3 [•••]		Level 4 [••••]	Code
1.) SETUP	BAL.SCAL Weigh cell functions	AMBIENT conditions (Filter adaptation)		V.STABLE Very stable conditions	1. 1. 1. 1
			o	STABLE Stable conditions	1. 1. 1. 2
				UNSTABL Stable conditions	1. 1. 1. 3
				V.UNSTBL. Very unstable conditions	1. 1. 1. 4
		APP.FILT. Application filter	o	FINAL.RD. Final readout mode	1. 1. 2. 1
				FILLING Filling mode	1. 1. 2. 2
		STAB.RNG. Stability range		1/4 DIG. (digit)	1. 1. 3. 1
				1/2 DIG. (digit)	1. 1. 3. 2
				1 DIG. (digit)	1. 1. 3. 3
				2-DIG. (digit)	1. 1. 3. 4
				4 DIG. (digit)	1. 1. 3. 5
			o	8 DIG. (digit)	1. 1. 3. 6
		STAB. delay		No delay	1. 1. 4. 1
			o	Short delay	1. 1. 4. 2
				Medium delay	1. 1. 4. 3
				Long delay	1. 1. 4. 4
		TARING Taring		W/O STB W/o stability	1. 1. 5. 1
			o	W/ STAB After stability	1. 1. 5. 2
		AUT.ZERO Auto zero		OFF	1. 1. 6. 1
			o	ON	1. 1. 6. 2
		WT.UNIT Basic Weight unit		For list of units, Gram to Newton	1. 1. 7. 1 to 1. 1. 7.23
		DISPLAY Basic accuracy	o	ALL	1. 1. 8. 1
				MINUS 1 One level lower	1. 1. 8. 2
				Increment of the measured values one level lower	1. 1. 8. 3
				Increment of the measured values two levels lower	1. 1. 8. 4
				Increment of the measured values three levels lower	1. 1. 8. 5
				INCRM. 1 Last digit single increment	1. 1. 8. 6
				resolution by a factor of 10	1. 1. 8. 8
		CAL./ADJ. Function of the (Cal) key	o	CAL.EXT. Adjustment/calibration with factory-set weight	1. 1. 9. 1
			o	E.CAL.USR. External calibration/adjustment with user-defined weights (factory-set on WZA25-NC)	1. 1. 9. 3
				CAL.INT. Internal calibration/adjustment only on models WZA...-NC	1. 1. 9. 4
				LIN.EXT. Linearization with factory-set weights	1. 1. 9. 6
				LIN.E.USR. Linearization with user-def. weights	1. 1. 9. 7
				STR.PREL. Store preload	1. 1. 9. 8
				CLR.PRELOAD Clear preload	1. 1. 9. 9
				BLOCKED (Cal) Blocked	1. 1. 9. 11
		CAL.ROUTINE	o	ADJ. one sequence	1. 1. 10. 1
				CAL./ADJ. as required	1. 1. 10. 2
		CAL.UNIT Weight unit for calibration	o	GRAMS	1. 1. 11. 1
				KILOGR. Kilograms	1. 1. 11. 2
				POUNDS	1. 1. 11. 3
		ZERO RNG. Zero range		DEFAULT. (factory-set)	1. 1. 12. 1
			o	2 PERC.ent	1. 1. 12. 2
				5 PERC.ent	1. 1. 12. 3
				10 PERC.ent	1. 1. 12. 4
		INT.ZERO Power On		Zero at power-on default (factory-set)	1. 1. 13. 1
				Initial zero 2%/max. cap	1. 1. 13. 2
			o	Initial zero 5%/max. cap	1. 1. 13. 3
				Initial zero 10%/max. cap	1. 1. 13. 4
				Initial zero 20%/max. cap	1. 1. 13. 5
				Initial zero 50%/max. cap	1. 1. 13. 6
				Initial zero 100%/max. cap	1. 1. 13. 7
		ON.TARE (Tare/Zero at Power/Zero-setting range)	o	ON	1. 1. 14. 1
				OFF	1. 1. 14. 2

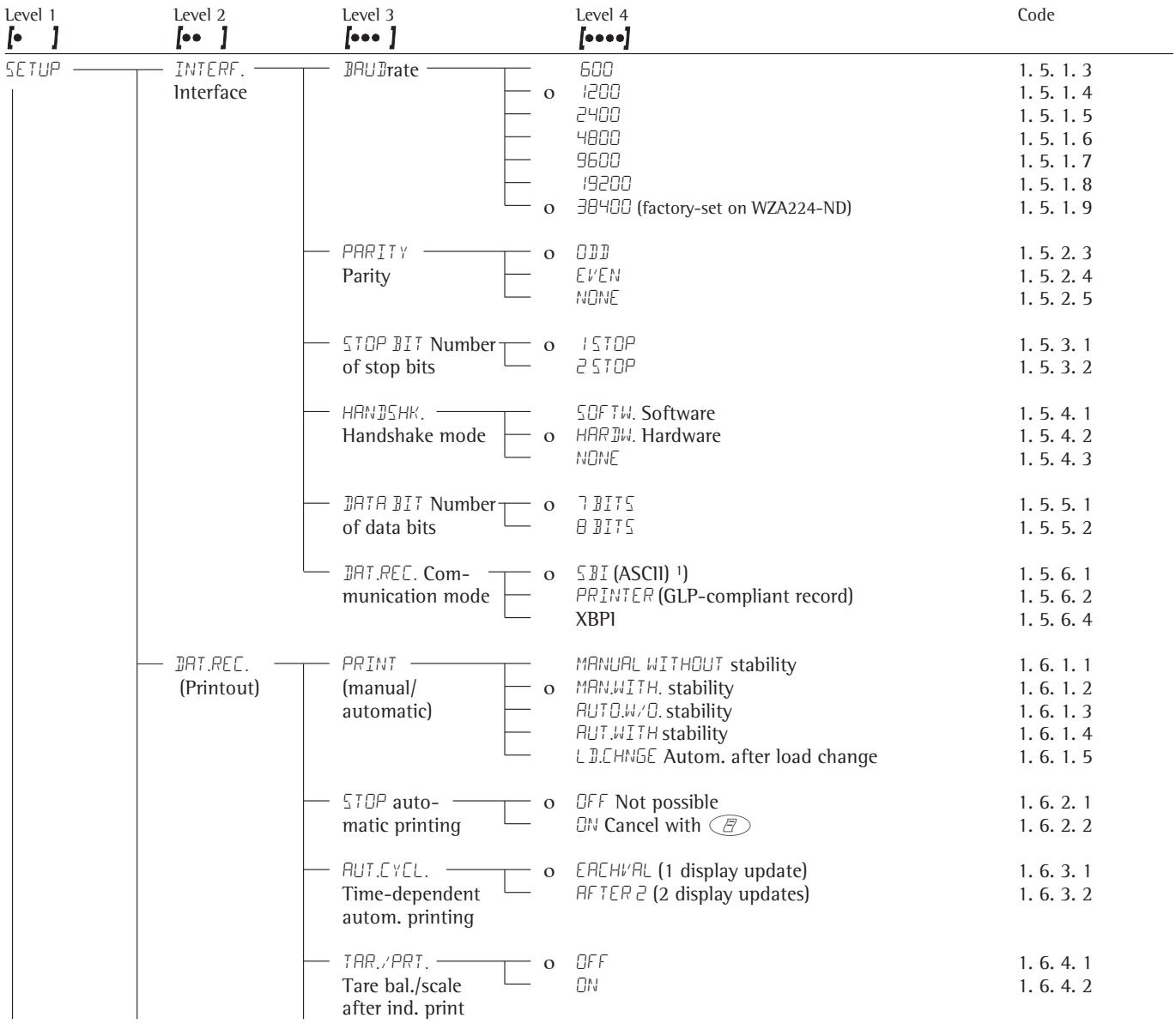

1) Note concerning verified balances/scales as legal measuring instruments in the EU*:
In the setting "SBI", the non-verified display digit is not automatically identified.
Please take the corresponding measures or adjust the settings on the peripheral device.

Level 1 [•]	Level 2 [••]	Level 3 [•••]		Level 4 [••••]	Code
SETUP	BAT.REC. (Printout)	PRT.INIT. Printing application parameters	o	OFF	1. 6. 5. 1
				ALL All parameters	1. 6. 5. 2
				MAINPAR. Main parameters	1. 6. 5. 3
		FORMAT Line format for printout	o	16.CHAR. 16 characters (w/o ID)	1. 6. 6. 1
				22.CHAR. 22 characters (w/ ID)	1. 6. 6. 2
				2NDLINE with date/time	1. 6. 6. 3
		GLP ISO/GLP-compliant printout	o	OFF	1. 6. 7. 1
				CAL.-ADJ. Only for calib./adj.	1. 6. 7. 2
				ALWAYS on	1. 6. 7. 3
		TIME	o	24 H 24-hour format	1. 6. 8. 1
				12 H 12-hour format “AM/PM”	1. 6. 8. 2
		DATE	o	DD.MMM.YY Day/month/year	1. 6. 9. 1
				MMM.DD.YY Month/day/year	1. 6. 9. 2
	EXTRAS (Additional functions)	MENU	o	CANEDIT	1. 8. 1. 1
				RD.ONLY Read only	1. 8. 1. 2
		HORN Acoustic Signal		OFF	1. 8. 2. 1
			o	ON	1. 8. 2. 2
		KEYS (Keypad)	o	FREE	1. 8. 3. 1
				LOCKED	1. 8. 3. 2
		EXT.KEY. Function of the external switch	o	PRINT key (🖶)	1. 8. 4. 1
				Z/TARE (Tare)	1. 8. 4. 2
				CAL. (Cal)	1. 8. 4. 3
				SELECT (Select Menu)	1. 8. 4. 4
				CF (CF)	1. 8. 4. 5
				ENTER (Enter)	1. 8. 4. 6
				LOCKED Key locked	1. 8. 4. 9
		ON MODE Power-on mode		OFF/ON Off/on/standby	1. 8. 5. 1
				STANDBY On/standby	1. 8. 5. 2
			o	AUTO ON Auto on	1. 8. 5. 3
		BACKLIT Display backlighting		OFF	1. 8. 6. 1
			o	ON	1. 8. 6. 2
	RESET Reset menu	MENU Factory settings		YES Restore factory settings	1. 9. 1. 1
			o	NO Do not restore settings	1. 9. 1. 2

D: Distribution of Lab Water and Air

The following pictures provides a visual representation of how lab air and water was controlled for distribution to the apparatus parts.

Figure D.1: *Stand built to house air and water distribution.*

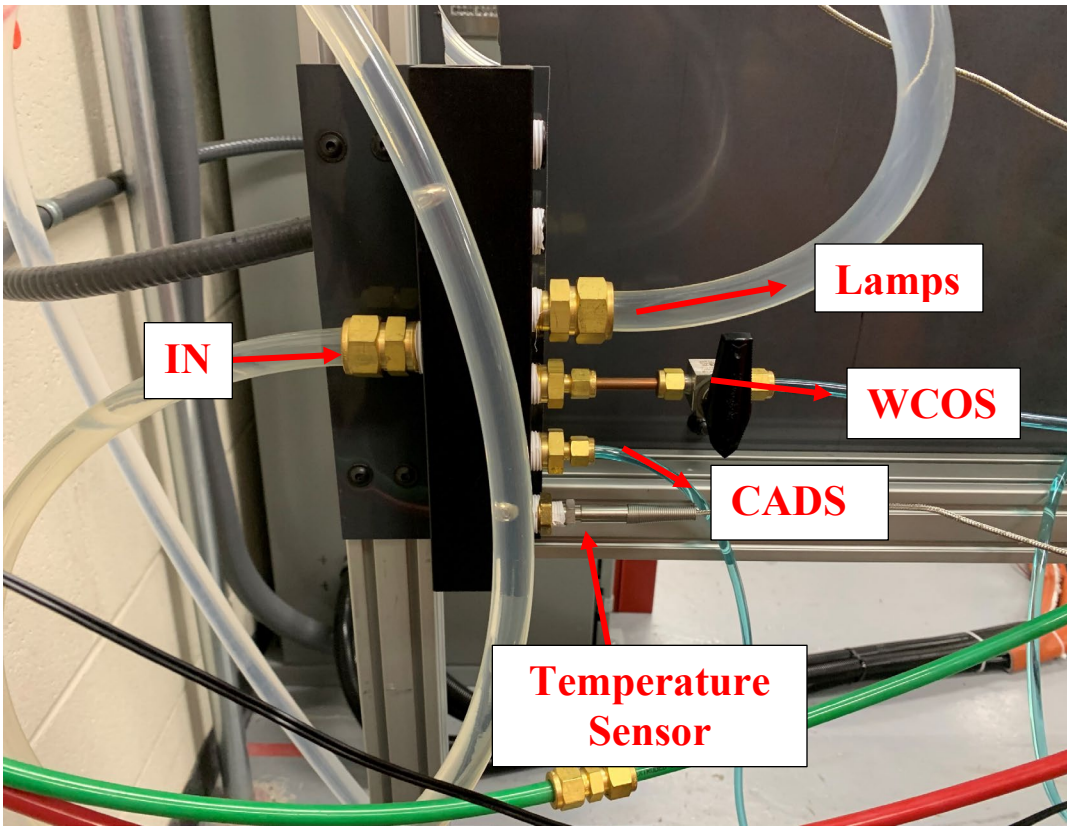

Figure D.2: *Water Distribution.*

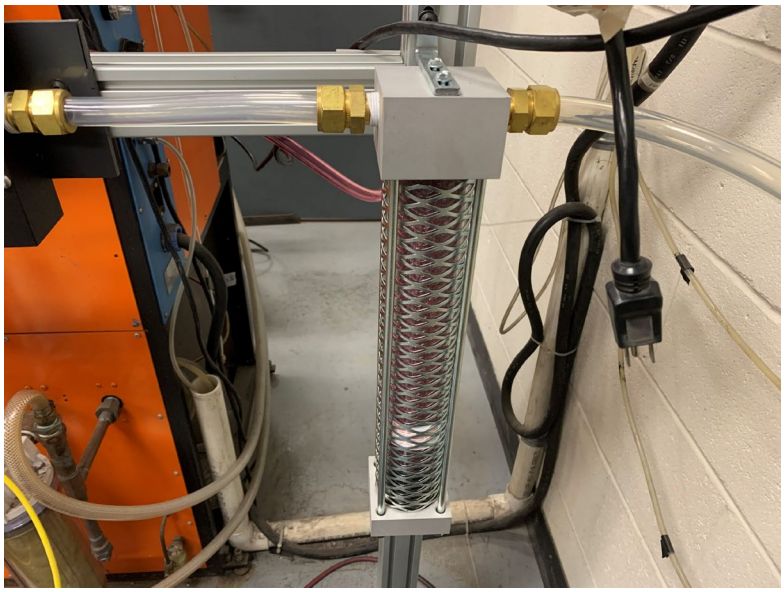

Figure D.3: *Air Dryer and Filter, removes particles up to 5 microns.*

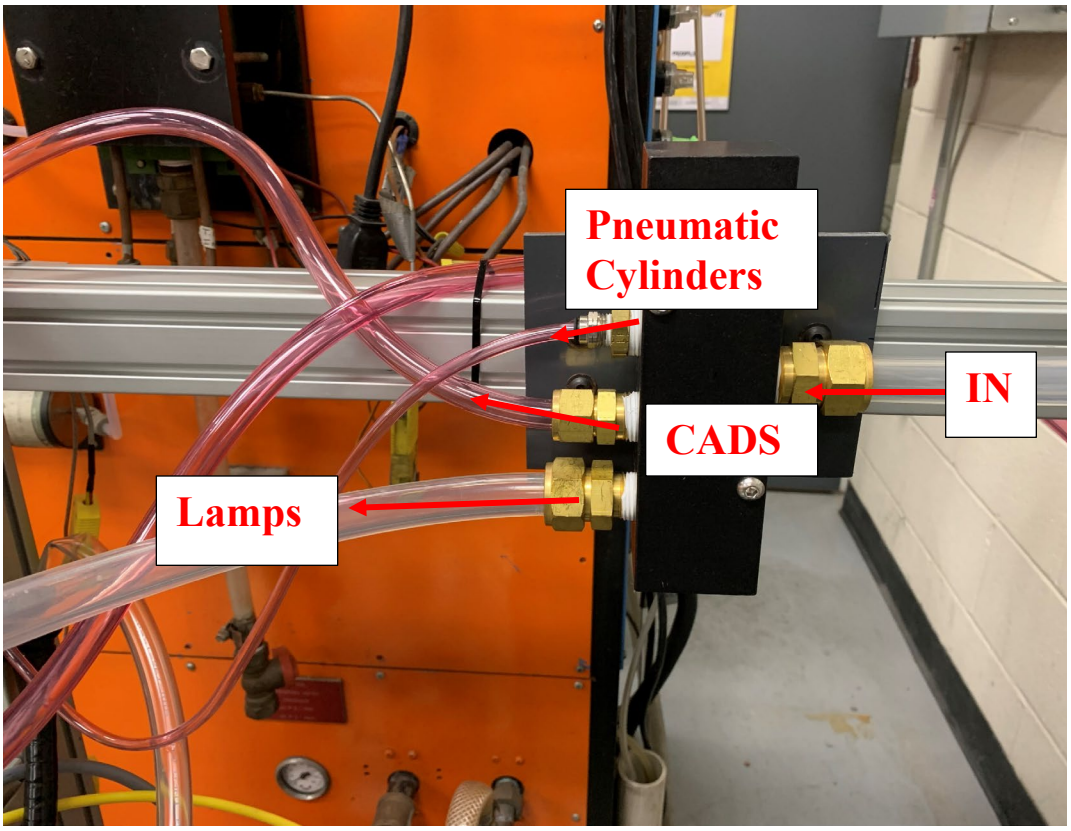

Figure D.4: *Air Distribution.*

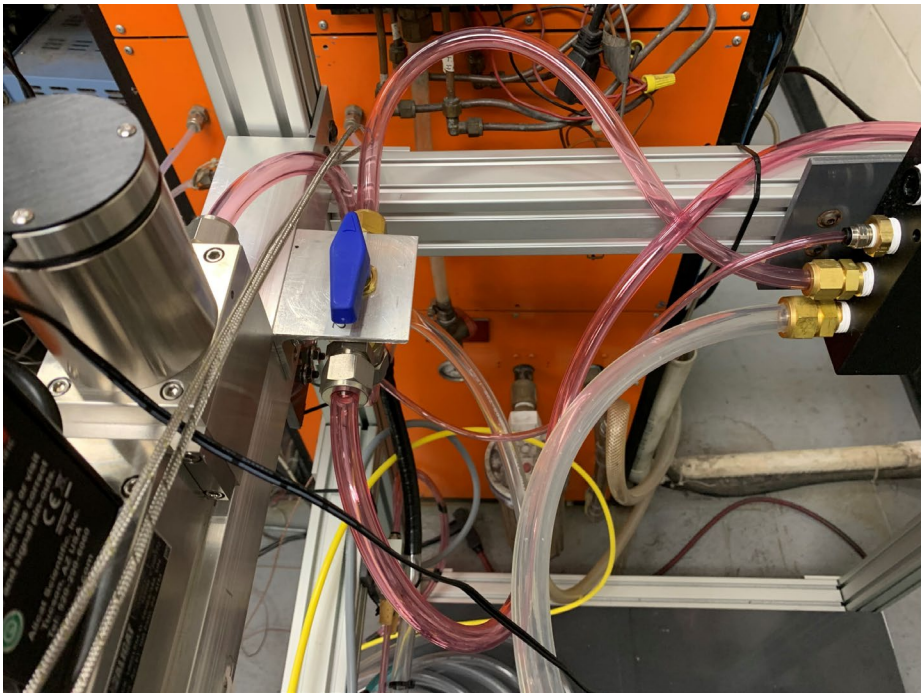

Figure D.4: *Air System*

Bibliography

[1] Halliwell, S. M. (2002). Polymers in Building and Construction. Rapra Technology Ltd.

[2] Papaspyrides, C. D., & Kiliaris, P. (Eds.). (2014). Polymer green flame retardants. Elsevier.

[3] Babrauskas, V. (1984), Development of the cone calorimeter—A bench-scale heat release rate apparatus based on oxygen consumption. Fire Mater., 8: 81-95. https://doi.org/10.1002/fam.810080206

[4] United States. Federal Aviation Administration. Office of Aviation Research. (2005). Polymer flammability : final report. U.S. Dept. of Transportation, Federal Aviation Administration, Office of Aviation Research. https://purl.fdlp.gov/GPO/LPS64543.

[5] Swann, J. D., Ding, Y., McKinnon, M. B., & Stoliarov, S. I. (2017). Controlled atmosphere pyrolysis apparatus II (CAPA II): A new tool for analysis of pyrolysis of charring and intumescent polymers. Fire Safety Journal, 91, 130 – 139. https://doi.org/10.1016/j.firesaf.2017.03.038

[6] Girods P., Bal H., Biteau, H., Rein, G. and Torero, J.L., 2011. Comparison of Pyrolysis Behavior Results between the Cone Calorimeter and the Fire Propagation Apparatus Heat Sources. International Association of Fire Safety Science 10: 889-901. 10.3801/IAFSS.FSS.10-889

[7] Vytenis Babrauskas, The Cone Calorimeter, Hurley, M. J. S. of F.P. Engineers., SFPE Handbook of Fire Protection Engineering, Quincy, Mass., 2016.

[8] ASTM E1354-17, Standard Test Method for Heat and Visible Smoke Release Rates for Materials and Products Using an Oxygen Consumption Calorimeter, ASTM International, West Conshohocken, 2017.

[9] ASTM E2058-19, Standard test method for measurement of material flammability using a fire propagation apparatus, ASTM International, West Conshohocken, 2019.

[10] NFPA 287, Standard Test Method for Measurement of Flammability of Materials in Cleanrooms Using a Fire Propagation Apparatus, Quincy, MA, (2017).

[11] Girods, P., Bal, N., Biteau, H., Rein, G., Torero, J. L., & 10th International Symposium on Fire Safety Science College Park, MD, USA 2011 06 19 - 2011 06 24. (2011). Comparison of pyrolysis behaviour results between the cone

calorimeter and the fire propagation apparatus heat sources. Fire Safety Science, 889-901, 889–901. https://doi.org/10.3801/IAFSS.FSS.10-889

[12] Thomas, J. C., Hadden, R. M., & Simeoni, A. (2017). Experimental investigation of the impact of oxygen flux on the burning dynamics of forest fuel beds. Fire Safety Journal, 91, 855–863. https://doi.org/10.1016/j.firesaf.2017.03.086

[13] Liu, X. (2012). Design and analysis of new gasification apparatus based on the standard cone calorimeter (dissertation). University of Maryland.

[14] Brohez, S. (2005). Uncertainty analysis of heat release rate measurement from oxygen consumption calorimetry. Fire and Materials, 29(6), 383–394. https://doi.org/10.1002/fam.895

[15] Chow, W. K., & Han, S. S. (2011). Heat release rate calculation in oxygen consumption calorimetry. Applied Thermal Engineering, 31(2-3), 304–310. https://doi.org/10.1016/j.applthermaleng.2010.09.010

[16] Pandey, A., Larroche, C., Gnansounou, E., Khanal, S. K., Dussap, C.-G., & Ricke, S. (Eds.). (2019). Biofuels : alternative feedstocks and conversion processes for the production of liquid and gaseous biofuels (Second, Ser. Biomass, biofuels, biochemicals). Academic Press.

[17] Babrauskas, V., Twilley, W. H., Janssens, M., & Yusa, S. (1992). A cone calorimeter for controlled-atmosphere studies. Fire and Materials, 16(1), 37–43. https://doi.org/10.1002/fam.810160106

[18] Leonard, J. E., Bowditch, P. A., & Dowling, V. P. (2000). Development of a controlled-atmosphere cone calorimeter. Fire and Materials, 24(3), 143–150. https://doi.org/10.1002/1099-1018(200005/06)24:3<143::AID-FAM728>3.0.CO;2-L

[19] Hermouet, F., Rogaume, T., Guillaume, E., Richard, F., Marquis, D., & Ponticq, X. (2021). Experimental characterization of the reaction-to-fire of an acrylonitrile-butadiene-styrene (abs) material using controlled atmosphere cone calorimeter. Fire Safety Journal, 121. https://doi.org/10.1016/j.firesaf.2021.103291

[20] Research Inc., IRheaters.com. (2006). General Product Data Sheet http://www.researchinc.com/files/General%20Products%20Data%20Sheet.pdf

[21] ISO 5660-1,Reaction-to-fire tests — Heat release, smoke production and mass loss rate — Part 1: Heat release rate (cone calorimeter method) and smoke production rate (dynamic measurement), Geneva: International Organization for Standardization, 2015.

[22] ISO 12136, Reaction to fire tests — Measurement of material properties using a fire propagation apparatus, Geneva: International Organization for Standardization, 2011.